# EXTRACELLULAR MATRIX MECHANOBIOLOGY OF BREAST TUMOR STROMA

A Dissertation

Presented to the Faculty of the Graduate School

of Cornell University

in Partial Fulfillment of the Requirements for the Degree of

Doctor of Philosophy

by

Karin Chieh Wang

August 2015

# EXTRACELLULAR MATRIX MECHANOBIOLOGY OF BREAST TUMOR STROMA

Karin Chieh Wang, Ph.D.

Cornell University 2015

The extracellular matrix (ECM) is a complex fibrillar structure that provides biochemical and mechanical cues to cells. Fibronectin (Fn) is a fundamental ECM protein implicated in cell signaling and behavior in both physiological and pathological conditions. Fn comprises 3 types of repeating modules (I, II, III), which contain binding sites for cells, ECM components, and growth factors. Its type III repeating modules lack disulfide bonds and under cell traction or ECM strain, extend and unfold to expose cryptic binding sites or disrupt exposed binding sites. Therefore, Fn is considered as a mechanotransducer, in which cell-induced conformational changes alter its biological behavior.

Fn is known to be up-regulated in tumor stroma. However, how Fn is altered and its role in tumorigenesis is unclear. The results herein demonstrate how invasive breast cancer cell secretion activates pre-adipocytes to deposit an initial Fn matrix that is stiffer and more unfolded than its healthy counterpart to mediate an integrin switch in downstream cell attachment. These newly attached cells, in response to the altered ECM, enhance pro-angiogenic secretion.

Furthermore, Fn binds to collagen I (Col I), another major ECM protein. Col I is known to be dependent on previous Fn matrices. Col I is a key proponent in mediating invasive breast cancer, found to be more crosslinked, stiffer, and exhibiting enhanced remodeling to create ECM tracks for increased cell migration. How altered Fn mediates changes in downstream Col I deposition is yet unclear.

The results herein show how invasive breast cancer cell secretion enhances activated pre-adipocytes ability to remodel the initially deposited Fn ECM. This altered Fn ECM, through proteolytic activity, is replaced by a dense, dysregulated Fn-Col ECM. The findings of this dissertation highlight how breast cancer cell secretions alter stromal ECM deposition and remodeling. This work combined physical science tools with biochemical tools to evaluate the importance of tumor stroma. These findings may provide insight into the development of breast tumor therapies to prevent tumor progression into the surrounding stroma for eventual metastasis.

## BIOGRAPHICAL SKETCH

Karin Wang was born and raised in New York. She attended the Bronx High School of Science from 2001 – 2005. Afterwards, she obtained her BE/MS in Biomedical Engineering and BS in Applied Math and Statistics from Stony Brook University in 2010. During her time at Stony Brook University, she worked in Professor Benjamin Hsiao's lab in the Chemistry department. In his research group, she used chemistry and materials science tools to design nanofibrous scaffolds and thermo-sensitive gels for tissue engineering of articular cartilage and controlled release of therapeutic drugs, respectively. Karin went on to pursue her PhD in Biomedical Engineering at Cornell University with Professor Delphine Gourdon. During her doctoral studies, she utilized physical and biochemical tools to study structural changes in the fibrillar protein network of aggressive breast tumor stroma. She has presented at numerous national and international conferences and has won many travel awards to present her doctoral research at these interdisciplinary conferences. After completing her doctoral studies in 2015, Karin will be a postdoctoral fellow in Professor Jeffrey Fredberg's lab at the Harvard School of Public Health, where she will investigate collective cell migration.

For my family: this dream was possible only because of their love and support.
Thank you, from the bottom of my heart!

## ACKNOWLEDGEMENTS

I would like to acknowledge my research advisor, Professor Delphine Gourdon, for seeing my potential and giving me the incredible opportunity to pursue my doctoral degree in her interdisciplinary research group. She has taught me so much during these past 5 years, cultivating in me a passion for mechanobiology and cappuccinos. She has tirelessly supported and encouraged me during my time at Cornell; allowing me to present at numerous national and international conferences, providing feedback during my teaching fellowships, and writing endless letters of recommendations. I am truly grateful for all your mentorship. Thank you.

I would also like to recognize my graduate committee members, Professor Claudia Fischbach and Professor Jan Lammerding. Professor Fischbach introduced me to my advisor when I first arrived at Cornell, and graciously shared her lab resources and expertise with me during my doctoral studies. Professor Lammerding kindly provided constructive feedback and career advice. Thank you for sharing your knowledge, advice, support, and time. I sincerely appreciate your guidance.

Furthermore, I would like to gratefully thank all the Gourdon lab group members for their support during my doctoral studies. Specifically, I would like to acknowledge the following people for all their time in and out of lab: Roberto Andresen Eguiluz, Fei Wu, Rebecca Schur, Shengling Hu, Keli Thurston, Victoria Benson, Marion Quien, Lauren Hsu, Soyoung Min. We have worked through many late nights and weekends together, and persevered through the highs and lows of our research to be great friends and colleagues. To all the other members, though I was not situated in Bard, I truly appreciate your time and support.

Additionally, I would like to thank the Fischbach lab members for taking me in and treating me as an honorary lab member. I am grateful for their friendship, mentorship, and

training. Thank you Young-hye Song, Maureen Lynch, David Infanger, Scott Verbridge, Peter DelNero, Nora Springer, Siyoung Choi, Emily Chandler, Daniel Brooks. I would especially like to thank Bo Ri Seo, who always had time to answer my questions, help me with my research, and take a break for lunch or dinner.

Moreover, I am thankful for Sara Che, Natalie Kelly, and Elizabeth Wayne. You all know I am the epitome of introverted-ness, and yet, you still manage to get me to relax and enjoy life outside of lab. You ladies are the best.

There are many other people that I have gotten to know over the years here at Cornell, and I cannot thank you all enough for your friendship, assistance, and support. Also, my childhood friends from home: we may not have seen each other as much since I started graduate school, but you all try to make time for me when I am home and you are all amazing for that.

And my family, how else could I have come this far without your love and tireless support? My grandmother, my loving parents, my cousins, uncles, aunts, niece, nephews, I hope you are all proud of me.

Lastly, I would like to thank Michael Mitchell. You have helped me grow so much, in life and in my pursuit of a career in academia. You always encourage me to do my best (and be my silly self), and I have come so far because of your support. Thank you for cheering me on and believing in me. They say home is where the heart is. When I am with you, I am home.

## TABLE OF CONTENTS

## LIST OF FIGURES

**Chapter 1**



**Chapter 2**



**Chapter 3**

**Chapter 4**



## LIST OF TABLES

## LIST OF ABBREVIATIONS

| | |
|---|---|
| **c-** | control |
| **CAF** | Cancer-associated fibroblast |
| **Col I** | Collagen I |
| **ECM** | Extracellular matrix |
| **Fn** | Fibronectin |
| **FRET** | Förster resonance energy transfer |
| **MI/** | MMP inhibited |
| **MMP** | Matrix metalloproteinase |
| **SFA** | Surface forces apparatus |
| **TC-** | Tumor-conditioned |
| **TSF** | Tumor soluble factors |
| **VEGF** | Vascular endothelial growth factor |

# CHAPTER 1

# INTRODUCTION

## 1.1. Breast cancer and metastasis

Breast cancer, the second most common type of cancer for females after skin cancer, has the highest national care expenditure in the United States at $16.5 billion (National Cancer Institute, National Expenditures for Cancer Care, 2010 data). Aggressive breast cancer can be malignant and life threatening, as tumor cells are able to spread via blood vessels and lymph nodes to bone, lung, liver, and brain. For those diagnosed with aggressive, metastatic breast cancer, the 5-year survival is only ~26% (National Cancer Institute, SEER Cancer Statistics, 2005-2011 data). Therefore, understanding the mechanism behind aggressive tumor growth and invasion is integral in improving patient prognosis. This dissertation focuses on understanding the contribution of the extracellular matrix (ECM) to facilitating aggressive tumor progression.

## 1.2. The extracellular matrix facilitates tumor growth and metastasis

The ECM is a complex fibrillar network that regulates cellular behavior.[1] The ECM is comprised of a variety of proteins and sugars that not only provide structural (biomechanical) support for cells, but also biochemical signals to assist in maintaining tissue homeostasis.[1,2] Properties such as composition, rigidity, topography, and porosity are physical signals that can either block or facilitate cell migration by influencing cytoskeletal structure.[3,4] The ECM acts as localized reservoirs of biochemical cues such as growth factors or ECM fragments, providing indirect and direct signals for cells to sense and interact with their microenvironment.[5,6] Furthermore, cells sense and react to ECM biomechanical signals via clustering of focal adhesions to exposed cryptic binding sites on mechanotransducer proteins for altered cell

behavior such as cell proliferation and migration.[7,8] All these ECM signals work in synergy to regulate cellular behavior and in turn, stimulate signaling within cells to regulate its microenvironment. The ECM is remarkably dynamic under normal conditions, able to suppress tumor growth. However, when the ECM is dysregulated and changes in the microenvironment accumulate, it can assist and enhance tumor progression and metastasis.[9,10] Breast cancer cells are able to enlist a variety of other cells within the surrounding breast stroma to facilitate ECM dysregulations for: (i) survival via tumor angiogenesis to provide oxygen, nutrient, and waste exchange,[11,12] and (ii) invasion via altered ECM organization and remodeling for enhanced cell migration.[13,14] Cancer associated fibroblasts (CAFs) differentiated from recruited mesenchymal stem cells (MSCs), are implicated as active contributors to tumor stroma ECM dysregulations.[15-18] Consequently, it is critical to elucidate the role of CAFs in mediating dysregulations in stromal ECM.

### 1.3. Tumor stroma components and regulators

The tumor stroma is a heterogeneous microenvironment, composed of stiff tumor ECM and increasingly deformable cells within.[19,20] This altered stroma is composed of abnormal amounts of various ECM components. Fibronectin (Fn) is one of the most common components of the ECM, and contains multiple binding sites for cell, ECM, and growth factor components that may be exposed or disrupted when Fn conformation is altered (Fig. 1.1).[21] Therefore, Fn is an essential signaling molecule in the ECM. This dissertation will demonstrate how Fn mechanobiology affects cell, ECM, and pro-angiogenic signaling. Type I collagen (Col I), a triple α-helical protein, is another common component of the ECM. Col I in stiff tumor stroma are highly cross-linked, linearized, and a major contributor to tumor stiffness.[22,23] Col I

fibrillogenesis is known to depend on initial Fn deposition,[24,25] however, Fn-Col I interactions are poorly understood. Furthermore, ECM dynamics are regulated by matrix metalloproteinases (MMPs), proteolytic enzymes that are able to recognize and digest specific matrix components, as well as activate other MMPs and molecules.[26] Increased MMP activity is associated with tumor angiogenesis and invasion.[27-30] Another molecule, vascular endothelial growth factor (VEGF), is a pro-angiogenic factor that binds Fn.[31] Furthermore, VEGF bioavailability is regulated by MMPs.[32] Therefore, elucidating the mechanisms by which ECM components Fn and Col I, MMPs, and VEGF synergistically alter the tumor stroma for aggressive tumor progression, would provide insight to how tumor grow and metastasize, and also aid in the development of preventative diagnostic tools and therapies.

### 1.4. Research objectives

*I hypothesized that tumor-conditioned preadipocytes, a model of CAFs in the tumor stroma, deposit an initial unfolded and stiffer Fn matrix that dysregulate subsequent Fn-Col I dynamics. I further hypothesize that the development of this tumor-conditioned Fn-Col I network*

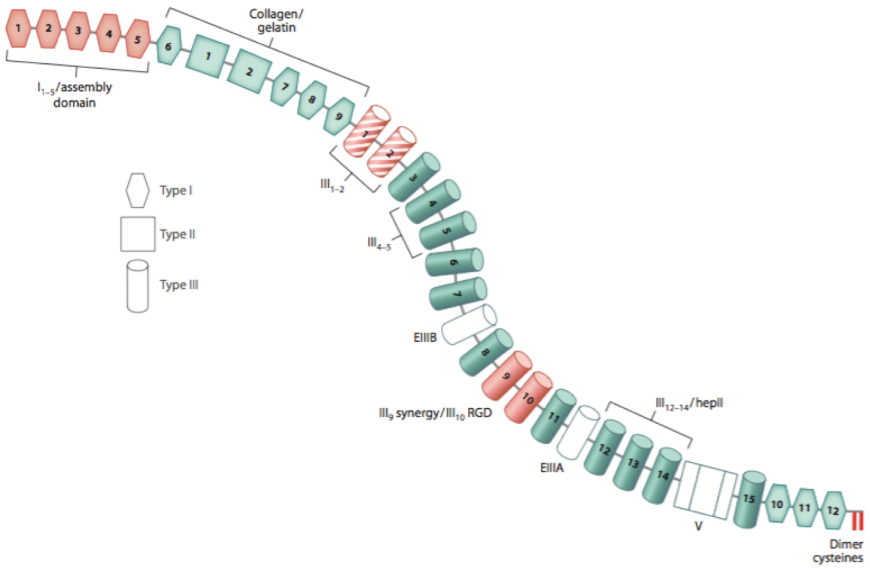


**Figure 1.1. Monomeric subunit of Fn**[33]

*presented a topologically different ECM that altered cellular behavior in regulating MMP and VEGF secretion.*

**Aim 1**. **Characterized tumor-conditioned Fn molecular conformation and its contribution to overall matrix stiffness**

Determined the conformation, composition, and morphology of the initial Fn matrix deposited by 3T3-L1 preadipocytes conditioned with tumor soluble factors derived from MB-MDA-231 breast cancer cells. Correlated molecular-scale Fn conformational changes with changes in bulk (cellular-scale) matrix stiffness, by combining studies utilizing the Förster Resonance Energy Transfer imaging technique and the Surface Forces Apparatus, respectively.

**Aim 2. Characterized the kinetics of tumor-conditioned Fn-Col matrices deposition/remodeling and its associated pro-angiogenic signaling**

Ascertained the contribution of altered Fn conformation over time to dysregulated Col I deposition and Fn-Col I interactions. Investigated contribution of matrix metalloproteinase activity to tumor-conditioned Fn-Col I matrix topology and remodeling. Quantified vascular endothelial growth factor (VEGF) secretion as an indication of tumor angiogenesis for cancer progression.

## 1.5. Fibronectin conformations and the Förster Resonance Energy Transfer (FRET) technique

To investigate dysregulated biochemical ECM signaling, exogenously delivered FRET-labeled Fn[7,34,35] was deposited by tumor-conditioned preadipocytes. As depicted in the

schematic of Fig. 1.2, 4 specific cysteines within Fn dimers are labeled with AlexaFluor 546 (acceptor fluorophores) and 7-9 lysines are randomly labeled with AlexaFluor 488 (donor fluorophores). Non-radiative energy transfer only occurs when excited donor fluorophores are spectrally and spatially close to acceptor fluorophores. Only 10% of exogenous Fn was FRET-labeled to prevent inter-molecular energy transfer. The resulting FRET intensity ratios ($I_A/I_D$) quantified from confocal images provides overall Fn matrix conformations in a field of view; Fig. 1.2 depicts a representative FRET ratio vs. unfolding via chemical denaturant. Areas of high FRET intensity ratios indicate areas in which close-to-compact Fn molecules are present in fibers. Areas of low FRET intensity ratios indicate areas in which Fn fibers are composed of extended and/or unfolded molecules. Local altered Fn conformation in the overall matrix population indicate altered biochemical cues delivered to cells and matrix components.

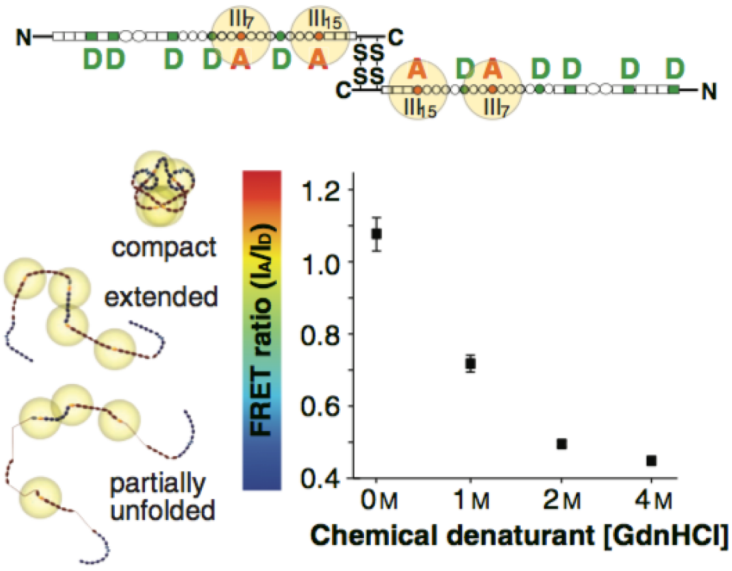


**Figure 1.2. FRET-labeled Fn schematic and unfolding**[36]

### 1.6. Fibronectin mechanics and the Surface forces apparatus (SFA) technique

We used the SFA to measure the compressive stiffness of ECM deposited by tumor-associated preadipocytes cultured *in situ*. The SFA is a light-based tool (Fig. 1.3) that measures a

variety of forces between two molecularly smooth surfaces mounted in a cross-cylindrical configuration to simulate the well-defined sphere-on-flat geometry.[37,38] Matrices were directly cultured on mica surfaces (substrate required for SFA interferometric measurements) and probed with bare mica surfaces to obtain normal forces by measuring the deflection of a double-cantilever of known spring constant. Interference fringes, called fringes of equal chromatic order, were shifted and blunted when in contact with the matrices. The SFA measured stiffness by rebuilding mechanical force-distance profiles and extracting compressive elastic moduli of Fn matrices from a model proposed by Johnson.[39] Altered Fn matrix mechanics measured will reveal links between molecular protein conformations and bulk Fn matrix biomechanics.

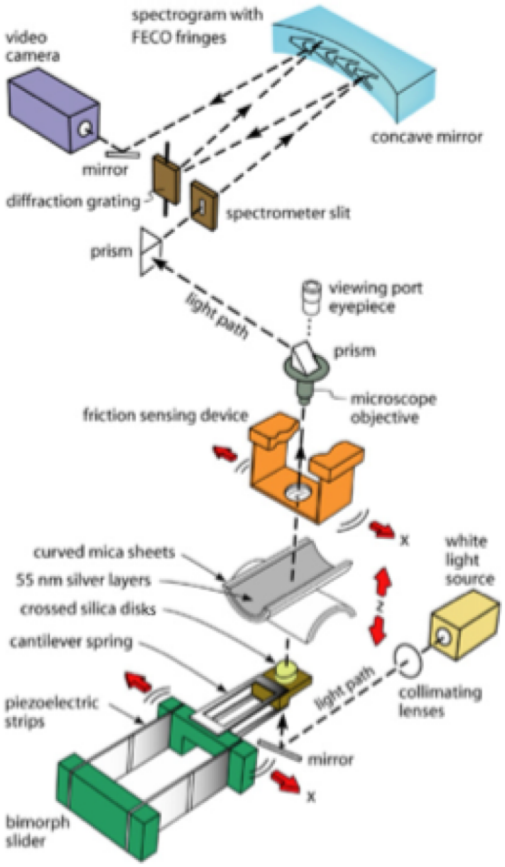


**Figure 1.3. SFA schematic**[37]

**FIBRONECTIN MECHANOBIOLOGY REGULATES TUMORIGENESIS**

*In revision, Cellular and Molecular Bioengineering (2015)*

## 1.7. Contributors

Authors of this manuscript are: Karin Wang, Bo Ri Seo, Claudia Fischbach, Delphine Gourdon

K.W., B.R.S., C.F., and D.G. wrote the paper.

Acknowledgements: Funding by the NSF under award DMR-1352299 (to DG), by the NIH/NCI under award R01 CA185293 (to CF and DG), and by the Cornell Center on the Microenvironment & Metastasis under award NCI U54 CA143876 (to CF).

## 1.8. Abstract

Fibronectin (Fn) is an essential extracellular matrix (ECM) glycoprotein involved in both physiological and pathological processes. The structure-function relationship of Fn has been and is still being studied, as changes in its molecular structure are integral in regulating (or dysregulating) its biological activities via its cell, matrix component, and growth factor binding sites. Fn comprises three types of repeating modules; among them, FnIII modules are mechanically unstable domains that may be extended/unfolded upon cell traction and either uncover cryptic binding sites or disrupt otherwise exposed binding sites. Cells assemble Fn into a fibrillar network; its conformational flexibility implicates Fn as a critical mechanoregulator of the ECM. Fn has been shown to contribute to altered stroma remodeling during tumorigenesis. This review will discuss (i) the significance of the structure-function relationship of Fn at both

the molecular and the matrix scales, (ii) the role of Fn mechanobiology in the regulation of tumorigenesis, and (iii) Fn-related advances in cancer therapy development.

### 1.9. Fn and its significance in cancer

Fibronectin (Fn) is one of the most abundant extracellular matrix proteins (ECM) along with collagen. Fn was first discovered as a high molecular weight fibroblast cell surface protein in the early 1970s,[40,41] and then as an extracellular fibrillar network surrounding fibroblasts through immunofluorescence and scanning electron microscopy.[42] Early isolation of Fn revealed a dimeric glycoprotein with two subunits measuring ~220 kDa[43] held together by disulfide bonds.[44] Most Fn is synthesized by hepatocytes to circulate in the bloodstream as soluble plasma Fn. Various cells also secrete Fn, named cellular Fn, to be directly assembled into an insoluble fibrillar network. Plasma and cellular Fn mediate different biological behaviors; plasma Fn is essential in clots during early wound healing whereas cellular Fn mediates late wound healing, neovascularization, and angiogenesis (Fig. 1.1A).[45,46] Fn is also implicated in other physiological (e.g., embryogenesis[47]) and pathological[48] (e.g., fibrosis, cancer) processes.

Originally Fn was discovered because fibroblast cells lacked a cell surface protein after viral transformation.[41,42] However, the loss of Fn was not a good marker of malignancy, as some anchorage-independent tumorigenic cell lines were still able to assemble a fibrillar Fn network.[49] Further studies assessing the role of Fn in malignancy revealed high concentrations of plasma Fn after mice were inoculated with Ehrlich tumor cells,[50] but plasma Fn fluctuated with clinical events such as chemotherapy.[51,52] Other reports addressed the controversial deposition of Fn in tumors and found that it was absent in tumors but abundant in the

surrounding stroma.[53,54] As such, understanding Fn dynamics, i.e., Fn deposition and remodeling during tumorigenesis, is essential to expanding our knowledge of cancer.

The tumor stroma is a complex microenvironment in which components are recruited or remodeled to facilitate invasive growth and metastasis.[55,56] Therefore, specific focus has been placed on understanding how the surrounding ECM is altered to mediate tumor progression.[57,58] Cancer-associated fibroblasts (CAFs) are major sources of increased ECM deposition and altered remodeling[59] to create tracks for cancer cell invasion.[60] This review will discuss (i) the importance of Fn structure, matrix assembly, and mechanics in invasive tumor growth, and (ii) their relevance to improved therapeutic strategies and diagnostic tools.

### 1.10. Fibronectin mechanoregulation of various cellular activities

Fn is a mechanoregulator of the ECM due to its conformational flexibility[61-64] in both plasma[65] and fibrillar forms.[7,66] Fn comprises 3 repeating modules: FnI, FnII, and FnIII (Fig. 1.1).[67] FnI and FnII are mechanically stable modules as they are secured by disulfide bonds but FnIII lack these disulfide bonds and are sensitive to external mechanical forces.[68] FnIII modules are made up of 7 β strands within 2 anti-parallel β sheets surrounding a hydrophobic core, with $FnIII_{10}$ holding a RGD loop (cell-binding site) between the F ($6^{th}$) and G ($7^{th}$) β strands.[69] The RGD sequence is a ubiquitous cell binding region as it has also been found in other proteins such as fibrinogen.[70] Fn contains two sites that collaboratively confer adhesion,[71] the RGD site on $FnIII_{10}$ and the PHSRN synergy site located on the adjacent $FnIII_9$.[72] Simultaneous engagement to both RGD and PHSRN sites is essential for integrins $\alpha_5\beta_1$[73] resulting in a binding that is highly sensitive to Fn molecular conformation.[74] In contrast, the binding of most other integrins, including $\alpha_v\beta_3$ integrins, requires engagement only

to the RGD loop and is not sensitive to Fn conformation.[75] Briefly, the RGD loop is separated from the PHSRN site by 30-40 Å and a small rotation between $FnIII_9$ and $FnIII_{10}$ orients the two cell binding sites on the same side of the Fn molecule.[76] Therefore, any change either in the orientation (i.e., in the relative angles between the two adjacent modules) or in the conformation (e.g., $FnIII_{10}$ unfolding as shown in Fig. 1.4B), alters the type of transmembrane receptors used by cells to bind to the Fn matrix,[77] and the subsequent downstream signaling. Another important region on Fn essential to mechanoregulation is the $FnIII_{12\text{-}14}$ sequence, which binds various growth factors[78] for sustained, localized signaling. Immobilization of growth factors modulates different downstream signaling.[79] Specifically, Fn-bound vascular endothelial growth factor (VEGF) mediates structured vascularization whereas soluble VEGF directs large, leaky vasculature.[32] Thus, Fn conformational flexibility is able to regulate cell activity via integrin specificity and growth factor binding.

Various cells are able to incorporate plasma Fn into the predominantly cellular Fn based-ECM of any tissue[80,81] Additionally, fibroblasts are able to deposit a Fn matrix by secreting and assembling Fn into fibers at the cell periphery.[82] Cells' integrins $\alpha_5\beta_1$[83,84] and $\alpha_{IIb}\beta_3$[85] binding to Fn were shown to play a role in Fn matrix assembly. This requires mechanical stimulation provided by cellular traction forces, possibly to induce a conformational change in Fn and expose cryptic binding sites to mediate Fn polymerization.[86,87] Recent advances in super-resolution microscopy such as direct stochastic optical reconstruction microscopy provide insight to the ordered structure of Fn within bundled fibers; demonstrating that Fn molecules are aligned within fibers with alternating N-terminal and C-terminal overlapping regions.[88] Fn maturation follows deposition and involves the polymerization of nascent deoxycholate-soluble Fn ultrathin fibrils into mature deoxycholate-insoluble Fn thick fibrils networks.[88,89]

Although multiple Fn conformations coexist simultaneously in the matrix (and in individual fibrils), the average Fn conformation has been reported to evolve during ECM maturation from compact/extended Fn in early fibrils to extended/unfolded Fn in mature fibrils and matrices.[7,35,90] The polymerization of Fn in extended conformations[91] stimulates cell growth[92], a process that may be mediated by interactions with heparin sulfate proteoglycans (another matrix component to which Fn binds).[93,94] Fn networks may also be initiated via self-assembly. Fn molecules contain conformational-dependent[95] binding sites for itself located on $FnI_{1\text{-}5}$, $FnIII_{1\text{-}2}$, $FnIII_{4\text{-}5}$, $FnIII_{12\text{-}14}$,[96-98] possibly mediated by interaction with $FnIII_{10}$.[99] Furthermore, fragments of these binding sites have been shown to inhibit Fn-Fn interactions and Fn fibrillogensis.[100,101] Thus, changes to initial Fn conformations are also crucial in the regulation of Fn binding to other ECM components (including itself), and modulate further ECM deposition and remodeling.

The assembly of an initial Fn network[33] is often a prerequisite for the downstream deposition of collagen.[24,102,103] Reciprocally, the co-deposition of collagen has several effects on the initial Fn matrix: it assists further Fn remodeling by matrix metalloproteinases such as MT1-MMP,[104] it stabilizes the ECM,[24] it promotes cell proliferation and maintenance of microtissue morphology (ECM reorganization),[105] and it facilitates cell migration.[106]. The reported co-localization of both Fn and procollagen within the cell further demonstrates a likely synergistic relationship between these two ECM proteins.[107] Fn contains a large (multimodular) collagen binding site[108] located on modules $FnI_6FnII_{1\text{-}2}FnI_{7\text{-}9}$.[109] Regions within this site[110] collectively confer binding [Katagiri 2003] to the collagen α1(I) chain between residues 757 and 791.[25,111] Collagen binding stabilizes the 90° kink between

$FnI_6FnII_{1\text{-}2}FnI_7$ and $FnI_{8\text{-}9}$,[112] which is believed to assist Fn in maintaining a compact/relaxed conformation in the stroma, further regulating normal tissue homeostasis.

Fn-coated beads restrained by optical traps revealed cells' ability to sense their environment and to respond to increased external resistance[113] due to the strengthening of cytoskeletal tension, as later confirmed by traction force microcopy.[114] Additionally, lysophosphatidic acid (from platelets)[115] mediated Rho-activated stress fiber formation and enhanced Fn matrix assembly,[116] revealing the importance of cellular tension in Fn fibrillogenesis.[117] Briefly, $\alpha_5\beta_1$ integrins translocating along actin cytoskeletal bundles elongate Fn molecules[118] with varying amounts of force,[119] which initiates Fn polymerization and induces cytoskeletal tension.[120] L8, an antibody known to bind Fn and to inhibit Fn fiber assembly,[121] increased its binding to Fn fibers when Fn was mechanically strained (e.g., via Rho-mediated cell tension) and consequently exposed a cryptic binding site.[122] Detailed analysis of Fn matrix assembly and maturation indicated that Fn fibers are highly elastic[123-125] and heterogeneous as they comprise multiple molecular conformations, from compact/relaxed to extended/unfolded.[7,35] The elasticity of Fn fibers can be attributed to the conformational flexibility of FnIII modules (lacking disulfide bonds) that are allowed to extend/unfold upon cellular traction, as suggested by steered molecular dynamics simulations[126] and Fluorescence Resonance Energy Transfer.[7] Fn's cell-induced conformational changes implicate this glycoprotein as a critical mechanotransducer in translating mechanical signals from the external environment into biochemical signals mediated by integrin clustering and cytoskeletal tension.[127,128]

### 1.11. Roles of conformation and mechanics of Fn in tumorigenesis

In fetal tissues and cancers, cellular Fn is larger[129] and alternatively spliced[130] to contain the following sequences: IIICS, ED-A, ED-B, which confer additional conformational changes to Fn.[131-134] Fn ED-A is found at sites of tissue remodeling and during dysregulated signaling, it promotes a fibrotic phenotype[135,136] for tumorigenesis[137] and for neovascularization of metastases.[138] This splice variant was reported to enhance VEGF-C secretion via the PI3K/Akt signaling pathway.[139] Fn ED-A secreted by endothelial cells (isolated from tumors) was also found to induce epithelial-mesenchymal transition of cancer cells by activating the FAK-Src signaling pathway via $\alpha_9\beta_1$.[140,141] Instead, Fn ED-B is found in the tumor stroma[142] and in the tumor vasculature.[143] This splice variant of Fn has been found to enhance cell adhesion and formation of focal adhesions for cell spreading.[144] ECM stiffening, a hallmark of cancer, has been found to enhance ED-B splicing of Fn to propagate a tumorigenic phenotype.[145] Thus, changes in conformation, mechanics, and alternative splicing of Fn synergistically regulate tumorigenesis.

Fn is up-regulated in the tumor stroma.[48] Its up-regulation[146] has been attributed to CAFs, fibroblasts with altered phenotype and function.[147] CAFs are activated by TGF-β[148] or transformed by Fn-tissue transglutaminase contained in microvesicles released from cancer cells.[149] Breast tumor CAFs deposit an initially dense, unfolded[150] and stiff[151] Fn matrix that facilitates an integrin switch (from $\alpha_5\beta_1$ to $\alpha_v\beta_3$),[36,152] resulting in enhanced pro-angiogenic (VEGF) secretion.[151,153] Changes to Fn materials properties can in turn mediate a cascade of signaling events for tumorigenesis (e.g., ECM unfolding, stiffening, tumor angiogenesis, and tumor invasion) (Fig. 1.4B).

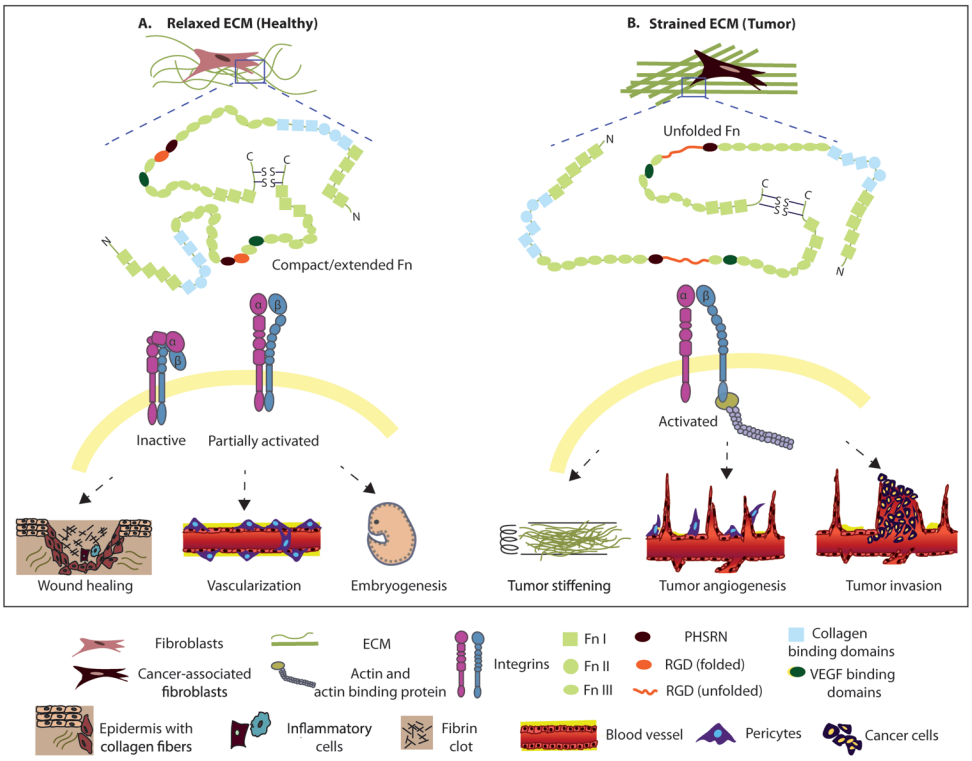


**Figure 1.4. Structure-function relationship of fibronectin in healthy and pathological conditions**

In healthy conditions, the ECM is in balance between relaxed and strained conditions to maintain normal tissue homeostasis. However, the ECM in tumor stroma has lost its integrity and begins to mediate an altered ECM phenotype. The relaxed ECM (A) contains mostly compact/extended fibronectin, whereas in the strained ECM (B), fibronectin undergoes conformational and structural changes to resist cell-mediated traction forces. These changes to fibronectin lead to exposure of soluble factor (i.e. VEGF) binding and cryptic sites. Furthermore, these conformational changes facilitate specific matrix component binding to mediate ECM remodeling, or integrin engagement and activation (i.e., $\alpha_5\beta_1$ vs. $\alpha_v\beta_3$) to consequently modulate cell behaviors. Moreover, unfolded Fn is previously correlated with the enhanced fiber strain and bulk ECM stiffening. Therefore, tumor-conditioned fibronectin assembled in tumor stroma facilitate a cascade of dysregulated downstream signaling for tumor progression.

Under conditions of normal tissue homeostasis, Fn mediates strong cellular adhesion. Upon matrix aging during healthy ECM remodeling (e.g., wound healing, vascularization, embryogenesis) (Fig. 1.4A), Fn gradually unfolds while cells become more contractile and develop strong fibrillar adhesions containing $\beta_1$ integrins.[154] $\alpha_5\beta_1$ integrins binding to Fn stimulates myosin II[155] and RhoA-GTPase to form robust peripheral fibrillar adhesions.[156]

These strong adhesive forces between Fn and $\alpha_5\beta_1$ integrins (~93 pN)[157] reduce migration of invasive cells.[158] Changes in Fn conformation are often responsible for a so-called 'integrin switch' as they alter the types of integrins cells may utilize to bind to the surrounding ECM. As mentioned in Section II (1.10), the most abundant Fn integrins, $\alpha_5\beta_1$, require both the synergy and the RGD sites to form complexes with Fn, i.e., strong $\alpha_5\beta_1$-Fn binding is conformation-dependent and occurs only when Fn is in a nearly compact conformation. In contrast, $\alpha_v\beta_3$ integrins require only the RGD site, i.e., weaker $\alpha_v\beta_3$-Fn binding is conformation-independent and will occur even when Fn is unfolded during ECM remodeling.[159] Weak Fn-$\alpha_v\beta_3$ adhesions[160] by cancer cells then lead to greater cytoskeletal reorganization for enhanced migration capacity[161] and resistance against anoikis (Figure 1.4B).[162] Once Fn conformation is permanently altered during tumorigenesis, cell-matrix interactions are dysregulated and changes to downstream signaling take place.

As Fn contains binding sites for cells, growth factors, and matrix components, variations in Fn conformation during tumorigenesis alter all microenvironmental interactions. The up-regulation of Fn combined with the preferred utilization of $\alpha_v\beta_3$ in the tumor stroma mediates the release and activation of matrix metalloproteinase-2 (MMP-2), which favors tumor invasion and metastasis.[163,164] This remodeled altered Fn, may in turn bind with altered affinity[165] to collagen ECM, which may lead to the formation of dysregulated, crosslinked, and stiff Col I[23] tracks for enhanced invasion by cancer cells.[166,167] Although the deposition of collagen usually requires the presence of provisional Fn, the enhanced secretion of TGF-β does lead to collagen fibrillogenesis and fibrotic ECM remodeling even in the absence of Fn.[168]

As mentioned previously, ECM stiffness is also a regulator of tumorigenesis.[10,23,169] ECM stiffening not only promotes Fn ED-B splicing and Fn unfolding for a pro-angiogenic

integrin switch, but also contributes to TGF-β activity,[170] a phenomenon that can influence myofibroblast differentiation[171,172] or epithelial to mesenchymal transition (EMT) for tumor progression.[173] Invasive cells preferentially migrate towards stiffer ECM (durotaxis).[174,175] Durotaxis is mediated by both the recruitment of $\alpha_v\beta_3$ integrins that re-organize and reinforce the cytoskeleton[161,176] at the leading edge of cells[177] and the extensions of filopodia.[178] This rigidity response has been attributed to activation of p130Cas via Fyn recruitment by receptor-like protein tyrosine phosphatase alpha (RPTPα) at the leading edge of these cells.[179] As altered Fn was also shown to be stiffer, it likely directs cancer cell invasion into the surrounding stroma for eventual metastasis.

Finally, Fn binding to cell surfaces via integrins also mediates clustering of growth factor receptors.[180] Enhanced levels of VEGF[181] are secreted by breast cancer cells (and/or fibroblasts subjected to paracrine signaling by breast cancer cells[182]) for tumor angiogenesis.[183,184] An isoform of VEGF, $VEGF_{165}$, increases breast cancer and endothelial cell migration in presence of Fn (and heparin).[185] Specifically, Fn forms a complex with VEGF-receptor-2 and $\alpha_5\beta_1$[186] to bind VEGF[31] on the heparin II binding domain located on $FnIII_{13\text{-}14}$.[187] Furthermore, ECM components such as heparin or heparan sulfate facilitate an extended conformation of Fn to enhance VEGF binding[188] and more-so in acidic conditions.[189] Overall, the Fn matrix is not only a mechanotransducing network, but also a chemical reservoir of signaling molecules for cells as Fn-bound VEGF facilitates organized vascular sprouting and branching[32] via enhanced activation of MAPK through $\beta_1$ mediated clustering of VEGFR2.[5]

### 1.12. Development of Fn-based cancer therapy

During tumorigenesis, primary structure, conformation, and mechanics of Fn are altered, which clearly affects its multiple biological functions. As the ECM stiffens, alternative splicing of Fn increases,[145] which leads to additional conformational changes (in an already highly strained and stiff tumor-associated matrix[151]) and promotes dysregulated downstream cell-matrix interactions for tumor progression. Targeting this altered Fn during tumorigenesis is therefore extremely desirable. Using phage antibody technology, molecular probes were successfully developed to distinguish between different unfolded (strained) states of Fn.[190] Additionally, CGS-1 and CGS-2 human antibody fragments were isolated and found to directly target Fn containing ED-B in human tissues as well as in other species.[191] Another antibody fragment specific for ED-B, scFv(L19), was fused to domains of interleukin-12 (IL-12) to enhance cellular immunity, which led to slower tumor growth and reduced metastasis[192] while injection of a radioactive-homodimer form of the fusion protein, $^{123}$I-L19(scFv)$_2$, in cancer patients demonstrated the potential to image primary and metastatic tumors noninvasively.[193] Using *E. coli* expressing bacterial thioredoxin, therapeutic vaccines specific against ED-A and ED-B were also developed and found to stimulate anti-ED-A and anti-ED-B antibodies to reduce tumor growth.[194,195] Additionally, biologically active fragments of Fn were also utilized.[101,196] Among them, a fragment derived from the first type III repeat in Fn, FnIII$_{1C}$ (named anastellin),[197] was reported to inhibit tumor growth, angiogenesis, and metastasis.[198] Anastellin was found to bind Fn and induce a conformational loss of a Fn epitope containing ED-A, which then activated MAPK and filopodia to stimulate Fn remodeling.[199] However, it was recently reported that it also mediated an inflammatory and pro-angiogenic phenotype of stromal cells within tumors.[200] Finally, Fn-derived N-terminal and C-terminal heparin-binding domains, respectively named heparin I and heparin II domains,

were also found to inhibit cancer cell adhesion and invasion by reducing $\alpha_v\beta_3$ expression and MMP-9 activity.[201] As advances are made in our knowledge of Fn nanostructure (e.g., splice variants), assembly (e.g., fibrillogenesis, molecular arrangement in fibers, strain-induced conformational changes, remodeling), and mechanics (e.g., contributions of both elastic and viscoelastic properties of Fn to direct cell behavior) during tumorigenesis, the development of therapeutic strategies and diagnostic tools will continue to improve to mitigate tumorigenesis.

### 1.13. Conclusions and future perspectives

Fn is able to trigger a wide range of cellular activities and is extremely dynamic, constantly undergoing remodeling processes where one or more of its essential properties are modified. Modulation of Fn dynamics is likely a strategy for tumor stromal cells to respond to microenvironmental changes (in particular, paracrine signaling from cancer cells) and contribute actively to tumorigenesis. However, because of the reciprocal nature of cell-Fn interactions, it is still unclear whether early Fn alterations in the tumor microenvironment are a cause or a consequence of the disease.

Numerous Fn-linked tumorigenesis mechanisms thus still need to be unraveled. As both plasma and cellular Fn play an inextricable role in mediating different biological functions, delineating their respective contributions during tumorigenesis must be addressed. Neither the mechanisms responsible for Fn assembly into fibers nor the detailed molecular structure of fibers are well understood, which would certainly help in defining the full range of parameters that regulate the Fn structure-function relationship. Although it is now well accepted that Fn assembly is dysregulated during tumorigenesis and leads to altered materials properties of the entire Fn network, it is likely that other microenvironmental conditions, such as altered MMP

activity, additionally drive changes in Fn remodeling to predispose the altered ECM for tumor progression. Hence, understanding the means by which early Fn alterations occur during tumorigenesis may pave the way for the development of diagnostic tools to catch cancer growth at early stages and of therapeutics to prevent invasive cancer growth.

More specifically to Fn mechanobiology research in the context of cancer, it would be desirable to deconvolute the diverse materials properties of the dysregulated tumor Fn, i.e., to distinguish physical (matrix topology, molecular conformation), biochemical (binding affinity, sequestration), and biomechanical (elasticity, viscoelasticity) alterations during disease progression. For example, aging- and/or disease- induced Fn conformational changes occurring at the molecular scale (e.g., unfolding) dictate the binding of specific types of growth factors, integrins, and matrix components, which has deep implications in driving tumorigenesis. However, these molecular conformational changes are usually accompanied by concurrent topological and mechanical changes at a larger scale, which makes it difficult to unravel specific mechanisms and their chronology.

### 1.14. Dissertation Overview

This dissertation aimed to understand ECM mechanobiology in developing breast tumor stroma, as breast cancer cells must recruit surrounding cells to remodel the stromal ECM into a network that assists breast cancer cells to escape and invade into the body, and endothelial cells to migrate into the tumor and create vasculature to mediate tumor survival during its growth. The introduction of this work includes a review paper currently in revision at the Journal of Cellular and Molecular Bioengineering titled, “Fibronectin mechanobiology regulates tumorigenesis.” This review highlights the importance of understanding the structure-function relationship of Fn

in maintaining normal tissue homeostasis, or when the structure of Fn is altered, mediate a dysregulated signaling cascade for tumor progression.

The 2nd chapter of this dissertation investigated early alterations in the materials properties of the breast tumor-conditioned stromal ECM assembled and how cells sense and respond to these changes. Specifically, I collaborated with others to understand the changes in molecular Fn conformation assembled by tumor-conditioned pre-adipocytes, an *in vitro* model of cancer-associated fibroblasts, and correlated how bulk elastic properties of this Fn ECM correspondingly changes. This chapter revealed how tumor-conditioned Fn ECM networks were unfolded and stiff, and how these altered materials properties of Fn lead to newly seeded cells to utilize $\alpha_v\beta_3$ instead of $\alpha_5\beta_1$ to enhance pro-angiogenic secretion.

The 3rd chapter of this dissertation investigated the development of breast tumor-conditioned stromal ECM. Specifically, my team of undergraduates and I studied the kinetics of ECM deposition and remodeling by tumor-conditioned pre-adipocytes, and how matrix metalloproteinases contributed to the altered tumor-conditioned ECM. This chapter divulged how initially thin, strained, unfolded, viscoelastic tumor-conditioned Fn was rapidly remodeled by matrix metalloproteinases. Furthermore, this rapid remodeling lead to the enhanced and altered deposition of thick and strained Col I fibers. This dense tumor-conditioned Fn-Col I network with altered materials properties mediated by matrix metalloproteinase activity, lead to a changes in pro-angiogenic secretion.

The 4th chapter contains lesson plans developed with K-12 local science school teachers as part of the Cornell Learning Initiative in Medicine and Bioengineering (CLIMB) program designed to expand STEM concepts within the classroom. One academic year was spent with an 8th grade physical science teacher and his classes, and the lesson developed was aimed towards

enhancing the optics module. We worked towards enhancing this module because my dissertation work involves understanding the electromagnetic spectrum and optics, and allowed us to show real-life "science" examples to the students in the context of understanding how I studied breast cancer. During the following academic year, I worked with a 9$^{th}$ grade earth science teacher, and the lesson developed was aimed towards enhancing the rocks and minerals module. We worked towards enhancing this module because of the overlap between my use of microscopes and geologists using microscopes to identify rocks. Additionally, this module was developed with very loose protocols so as to give them experience in developing their own lab procedure to identify an unknown rock and give them a better understanding of how scientists such as myself, approach unknown problems, collect data, analyze said data, and come to a conclusion. The two years spent with the CLIMB program were not just about enhancing STEM concepts in the classroom for the benefit of the young students, but were a means for me to develop skills in teaching scientific concepts for my future career goal of being a faculty member at a top-tier research institution.

The conclusions and future directions chapter describes how my dissertation work contributes to the global health issue of breast cancer. Specifically, I summarize how understanding the materials properties of tumor-conditioned stromal ECM would aid in understanding how breast cancer grows and invades the surrounding breast stroma to eventually metastasize to different organs and lead to poor patient prognosis. I also discuss some future experimental studies to expand on what this dissertation has shown, and some of the limitations of the studies herein.

Finally, the appendix details some of the collaborative work I have been involved in during the course of my dissertation work. Specifically, during my summer immersion at Weill

Cornell Medical College, I worked with a breast cancer pathologist and fellow to understand correlations between radiographic, needle core biopsy, and surgical data. Specifically, if patients with radiographic calcifications are diagnosed as lobular carcinoma in situ (LCIS) via needle core biopsies, and when undergoing subsequent surgeries, show pathological upgrade. Another collaboration involved the development of a tunable 3D scaffold that allowed for the control of protein conformation as determined by adsorbed FRET-labeled Fn. Another final collaboration, involved understanding how changes in the materials properties (including molecular conformation) of obesity-associated myofibroblasts promote tumorigenesis.

The dissertation work herein details my understanding of breast tumorigenesis in the context of materials property changes in stromal ECM mechanobiology and my contribution to this field. This work also details my endeavors in promoting STEM education in K-12 classrooms, as we need more researchers to study global healthcare issues, such as aggressive breast cancer progression. Finally, this work also highlights some of my inter-disciplinary collaborative work with pathologists, materials scientists, and biomedical engineers with different specialties.

# CHAPTER 2

# STIFFENING AND UNFOLDING OF EARLY DEPOSITED FIBRONECTIN INCREASE PROANGIOGENIC SECRETION BY BREAST CANCER-ASSOCIATED STROMAL CELLS

*Published in Biomaterials (2015)*

## 2.1. Contributors

Authors of this manuscript are: Karin Wang, Roberto C. Andresen Eguiluz, Fei Wu, Bo Ri Seo, Claudia Fischbach, Delphine Gourdon

K.W., R.C.A.E., C.F. and D.G. designed research; K.W., R.C.A.E., and F.W. performed research; K.W., R.C.A.E., F.W. and B.R.S. contributed new reagents/analytic tools; K.W., R.C.A.E. and D.G. analyzed data; and K.W., R.C.A.E., C.F., and D.G. wrote the paper.

Acknowledgements: Victoria Benson & Cory Brown for aid in image analysis and Juan Carlos Andresen & Shengling Hu for help in coding. Funding by NSF under award DMR-1352299 (to DG), NIH/NCI under award R01 CA185293 (to CF and DG) and U54 CA143876 (to CF), CONACYT (to RCAE), and the Cornell Center for Materials Research through Award Number (NSF DMR-1120296).

## 2.2. Abstract

Fibronectin (Fn) forms a fibrillar network that controls cell behaviors in both physiological and diseased conditions including cancer. Indeed, breast cancer-associated stromal cells not only increase the quantity of deposited Fn but also modify its conformation. However, (i) the interplay between mechanical and conformational properties of early tumor-associated Fn networks and (ii) its effect on tumor vascularization remain unclear. Here, we first used the Surface Forces Apparatus to reveal that 3T3-L1 preadipocytes exposed to tumor-secreted factors generate a stiffer Fn matrix relative to control cells. We then show that this early matrix stiffening correlates with increased molecular unfolding in Fn fibers, as determined by Förster Resonance Energy Transfer. Finally, we assessed the resulting changes in adhesion and proangiogenic factor (VEGF) secretion of newly seeded 3T3-L1s, and we examined altered integrin specificity as a potential mechanism of modified cell-matrix interactions through integrin blockers. Our data indicate that tumor-conditioned Fn decreases adhesion while enhancing VEGF secretion by preadipocytes, and that an integrin switch is responsible for such changes. Collectively, our findings suggest that simultaneous stiffening and unfolding of initially deposited tumor-conditioned Fn alters both adhesion and proangiogenic behavior of surrounding stromal cells, likely promoting vascularization and growth of the breast tumor. This work enhances our knowledge of cell – Fn matrix interactions that may be exploited for other biomaterials-based applications, including advanced tissue engineering approaches.

## 2.3. Introduction

Varied physicochemical properties of the extracellular matrix (ECM), a dynamic and complex fibrillar network, modulate cellular behavior. In tumors, the ECM is primarily generated by cancer-associated cells (e.g. fibroblasts and adipogenic precursors) and contributes

to sustained tumor growth and survival [1,15-18,202-204]. It exhibits numerous altered materials properties relative to normal ECM including variations in protein composition, structure, and rigidity. In fact, analysis of tumorous ECMs revealed differences in collagen I deposition relative to normal ECMs as suggested by elevated quantities, reorganization, crosslinking, and stiffness of collagen [14,18,22,23,166,205]. Moreover, fibronectin (Fn) might be responsible for additional ECM structural alterations, as indicated by the presence of highly stretched and unfolded Fn fibers in tumor-associated matrices [150,206]. It is important to recognize that tumor-associated Fn and collagen alterations are functionally linked since Fn (i) is essential for the deposition of collagen I in ECMs [18,24,207,208] and (ii) is also used as an indicator for increased tumor aggressiveness [162]. Nevertheless, a clear correlation between structural, conformational, and mechanical properties of the tumorous ECM network and the role of Fn in this process has not been established. This correlation has been hindered partly by the intrinsic complex composition of the ECM, and by the lack of analytical tools that permit simultaneous assessment of ECM materials properties from the matrix/cellular to the molecular scale. Indeed, both collagen and Fn fibers are present in mature ECM and likely synergize to modulate the bulk properties of the tumor ECM [24,209]. Additionally, there is a lack of materials science tools to separately assess morphology and mechanics of native (uncrosslinked) ECM at both matrix/cellular and molecular scales under physiologically relevant conditions.

Altered materials properties of the tumor ECM are clinically relevant as they promote tumor malignancy via direct effects on tumor cells [204] and indirectly by enhancing the formation of new blood vessels (angiogenesis) [14,18,22,23,166,205]. In fact, altered ECM can enhance angiogenesis either by increasing the activity of surrounding endothelial cells [150,206] or by stimulating the secretion of pro-angiogenic factors (e.g. vascular endothelial growth factor

[VEGF]) from cancer-associated fibroblasts [18,24,207,208]. However, the specific ECM properties and associated mechanisms responsible for the pro-angiogenic capability of tumor-associated cells remain unclear.

Here, we integrated a set of physical sciences tools with cancer biology to: (i) characterize the mechanics, conformation, and topology of tumor-associated Fn matrices at both the matrix and molecular scales, and (ii) correlate these materials properties with adhesion and pro-angiogenic factor (VEGF) secretion of adipose stromal cells. Our results revealed that tumor-conditioned Fn matrices were stiffer and more unfolded than control matrices, and that these dysregulated matrices contributed to enhanced VEGF secretion by stromal cells.

## 2.4. Materials and Methods

### *2.4.1. Cell Culture*

As an *in vitro* model of cancer-associated stromal cells, we utilized tumor-associated 3T3-L1 preadipocytes (ATCC, VA). Tumor soluble factors (TSF) from an aggressive metastatic breast cancer line, MDA-MB231 cells (ATCC, VA), were collected to mimic paracrine signaling between a tumor and its surrounding microenvironment. After exposing 3T3-L1s to TSF for 3 days, the preconditioned cells were detached and cultured on mica substrates for 24 hr. Afterwards, culture systems were decellularized [210] and the resulting cell-free matrices were used for parallel mechanical, topological, and conformational characterization.

### *2.4.2. Cell seeding and ECM decellularization*

3T3-L1 (ATCC, VA) preadipocytes (passages 4-10) were preconditioned for 3 days in either α-MEM culture medium (Control) or α-MEM medium containing normalized TSF. After

this preconditioning period, cells were trypsinized and used for parallel SFA and FRET experiments.

Both flat mica sections (culture area: 64-81 $mm^2$/well) and curved mica surfaces (mounted on SFA discs, culture area: 80 $mm^2$/disc) in PDMS chambers were first incubated with human plasma Fn (Life Technologies, NY) at a concentration of 30 μg/mL in phosphate buffered saline (PBS) for 60 min at room temperature to facilitate cell adhesion. After rinsing 3 times with PBS, a concentrated cell solution comprised of $2x10^4$ preconditioned 3T3-L1s (Control or Tumor) was seeded on the mica substrates. After 20 min of cell adhesion, 400 μL of exogenous Fn (50 μg/mL) low serum (1% fetal bovine serum (FBS)) was added. For FRET experiments, the exogenous Fn consisted of 90% unlabeled Fn (unFN) and 10% FRET-labeled Fn to prevent intermolecular FRET. For SFA experiments, only unFN was used.

After culturing at 37°C and 5% $CO_2$ for 24 hr, cultures were decellularized via a modified Cukierman protocol [210] that included deoxycholic acid incubation and extra wash steps, and left unfixed in PBS. Further samples were fixed for 1 hr at 4°C, and washed three times with PBS for further immunostaining and morphology studies.

*2.4.3. SFA*

The Surface Forces Apparatus (SFA) (SurForce LLC, CA) is an interferometry-based technique that uses fringes of equal chromatic order (FECO) to quantify the absolute surface separation between two reflecting surfaces, with nm resolution, while both normal (adhesion) and lateral (friction) forces can be measured. This technique is extensively described in [211,212]. Briefly, in our study, the lower surface was mounted on a double cantilever spring of known elastic constant while the upper surface was connected to a step motor to apply normal

load on the lower surface. A white light source was directed through two SFA surfaces (silica discs) previously glued with semi-reflective silvered mica, building an optical interferometer. The resulting interference FECO were directed towards the entrance slit of a photo-spectrometer (Princeton Instruments, NJ) and recorded with a CCD camera (Princeton Instruments, NJ) for further FECO analysis. The acquisition software used was LightField v4.0 (Princeton Instruments, NJ).

Muscovite mica (S&J Trading, Australia) is a negatively charged, hydrophilic aluminosilicate that is used as preliminary substrate in all SFA experiments. To obtain transparent, uniform, and atomically smooth mica surfaces, we cleaved mica into 1 $cm^2$ sections of 2 to 5 μm in thickness and metallized them with 55 nm of silver to make them semi-reflective. The mica sections (silver side facing down) were then glued with UV curing glue ($E$ = 1.034 GPa, product 61) (Norland, NJ) onto semi-cylindrical silica discs of 10 mm in diameter and 20 mm of curvature radius (ESCO Products, NJ). All preparation steps were performed in a laminar flow cabinet to minimize particulate contamination. Each SFA experiment requires a pair of discs glued with mica sections cut from the same sheet to ensure equal mica thicknesses on both upper and lower discs. Customized PDMS chambers containing cell culture media were used to house the lower discs during the 24 hr matrix deposition process while the upper discs (bare mica), used as indenters during force measurements, were kept clean and stored in a desiccator until needed.

Upper and lower SFA cylindrical discs were mounted in a crossed axis configuration to ensure a well-defined circular contact junction. The lower disc holding the ECM was mounted on a 980 N/m spring and the upper disc (bare mica) was used to indent ECM, as depicted in Fig. 2.1*A*. The SFA stainless steel chamber was filled with 75 mL of warm (37°C) PBS to keep the

ECM in physiological conditions during mechanical characterization, and the entire system was allowed to equilibrate at 37°C for 1 hr. Each ECM was then probed at 4 different locations (approximately 500 μm apart) and each location was indented 3 consecutive times. The system was allowed to equilibrate for 30 min between each indentation and 15 min between locations. Approach (In) and retraction (Out) measurements (force runs) were performed in quasi-static conditions (at a constant speed of 0.5 μm/min) to minimize viscous effects. During force runs, FECO were acquired at a rate of 3 frames per second and post-processed with Matlab R2012b (MathWorks, MA) to yield force-distance profiles. These profiles were further analyzed to extract the compressive elastic moduli using Hertzian contact mechanics between a sphere and an elastic half-space proposed by Johnson [39].

Samples were prepared and mounted in the SFA as described in the previous section. However, the lower surface was mounted onto a more compliant spring (k = 676 N/m) and the ECM samples were indented instantaneously (rather than quasi-statically) by applying increasing step-loads of approximately 3.7 mN (indentation approximately 5 μm) using the SFA fine micrometer, resulting in forces that correspond to $F_1 = F_1' = 3.7$ mN, $F_2 = F_2' = 7.4$ mN, and $F_3' =$ 11.1 mN. Changes in ECM indentation depth (creep) were then monitored over 1800 s by following the shift of the FECO fringes.

*2.4.4. FRET*

Alexa Fluor 488 succinimydyl ester (donor fluorophores) and Alexa Fluor 546 maleimide (acceptor fluorophores) (Invitrogen, CA) were used to label Fn for intramolecular Förster Resonance Energy Transfer (FRET) as previously described by Baneyx *et al.* [90] and Smith *et al.* [7]. Fn concentrations and labeling ratios between donors and acceptors were determined

using a DU®730 UV Vis spectrophotometer (Beckman, IN) at 280 nm, 495 nm, and 556 nm. FRET calibration of labeled Fn was first carried out in denaturant solution by varying guanidine hydrochloride concentrations between 0 and 4M to obtain acceptor/donor intensity ratios ($I_A/I_D$), termed FRET ratios, as a function of protein denaturation. Additional FRET calibration of Fn embedded in fibers was performed via a custom-made strain device and used to correlate Fn fiber FRET ratios with fiber uniaxial strain, as described in [124,213].

Samples were imaged with a Zeiss 710 confocal microscope (Zeiss, Munich, Germany) using the C-apochromat water-immersion 40x/1.2 objective, a pinhole of 2 AU, a 488 nm laser set at 10% power, and a pixel dwell time of 6.3 μs to acquire 16-bit z-stack images spaced 2 μm apart. FRET-Fn fluorescence was simultaneously collected for the donor fluorophores in the PMT1 channel (514 - 526 nm) and for the acceptor fluorophores in the PMT2 channel (566-578 nm), in addition of brightfield imaging. Donor and acceptor z-stack images were analyzed pixel by pixel with a customized Matlab code to generate false color FRET ratio ($I_A/I_D$) images and FRET histograms for each image. Individual FRET z-stack images were stacked in ImageJ (NIH) and reconstructed in Volocity (PerkinElmer, Inc., MA) [7,154,214].

*2.4.5. Immunostaining*

ECMs were decellularized and fixed as previously described [21]. The ECMs were washed with 0.05% Triton X-100 (Thermo Scientific, IL) in PBS (PBS-X) for 5 min, then blocked for non-specific binding with PBS-X containing 1% SuperBlock (Thermo Scientific, IL). After washing twice with PBS-X, the samples were immunostained overnight at 4°C for: Fn using either rabbit or mouse (when co-staining collagen I) antibodies (Sigma-Aldrich, MO), rabbit anti-mouse collagen I (Millipore, MA), mouse anti-talin (Millipore, MA), or rabbit

phosphorylated focal adhesion kinase [pY379] (pFAK) (Invitrogen, CA). After overnight incubation, the samples were washed twice with PBS-X for 5 min each, and incubated for 1 hr at room temperature in a PBS-X/1% Super Block solution of the following formulations: DAPI (Life Technologies, NY) (1:5000), Alexa Fluor 568 Phalloidin (1:250), goat anti-rabbit Alexa Fluor 488 (1:100) or goat anti-mouse Alexa Fluor 488 (1:100), goat anti-mouse Alexa Fluor 647 (1:100) (All Alexa Fluorophores were obtained from Life Technologies, NY). After the secondary antibody incubation, samples were washed twice with PBS-X for 5 min, and kept in PBS for confocal microscopy imaging.

*2.4.6. Image analysis*

Fn fiber diameters and matrix pore sizes were obtained from immunostained confocal microscope images and analyzed using ImageJ (NIH). To this end, 7 z-stack slices were orthogonally projected. Measurements were taken from random locations (including both central and peripheral sample areas). Pore size was analyzed by measuring the average size of the empty spaces with fibers within the projection (as depicted in Fig. 3*B*).

*2.4.7. Pro-angiogenic quantification*

Preconditioned preadipocytes were seeded on Fn coated flat mica surfaces for 24 hr as previously described. To compare between VEGF secretion and matrix sequestration, media was collected and cultures were decellularized and scraped, respectively. To understand how Fn matrix binding affects VEGF secretion, samples were decellularized, blocked for non-specific binding with PBS containing 1% bovine serum albumin for 20 min, sterilized with penicillin-streptomycin overnight, and washed twice with PBS. Untreated preadipocytes were trypsinized

and suspended in serum free media with various integrin-blocking antibodies (3 μg/mL) on a shaker at 37°C for 30 min. Cells were either left untreated, treated with only a rat anti-mouse integrin αv blocker (CD51) (Millipore, MA), treated with only a rat anti-mouse β1 blocker (CD29) (BD Biosciences, CA), or treated with both integrin blockers simultaneously. Cells were then allowed to attach in serum free media at 37°C for 1 hr, before switching to low serum media (1% FBS). After 3 hr (total 4hr), the media were collected to quantify VEGF secretion with a Quantikine ELISA kit (R & D Systems, MN) and samples either extracted for DNA in Caron's buffer or fixed, immunostained, and imaged as previously described. VEGF secretion was normalized by μg of DNA for each corresponding sample and represented as a ratio relative to normalized VEGF secretion by untreated cells on control ECMs.

*2.4.8. Statistics*

Data were statistically analyzed in GraphPad Prism (GraphPad Software, Inc., CA). Student's t-tests or ANOVAs with Tukey's post-hoc tests were performed and statistical significance was determined at $p < 0.05$.

## 2.5. Results

*2.5.1. Tumor-Conditioned Cells Promote Matrix Stiffening through Early Altered Fn Assembly*

To evaluate if tumor cell-secreted factors alter ECM deposition by adipose stromal cells, a major cell type in the mammary microenvironment, we first used the Surface Forces Apparatus (SFA) to assess the overall rigidity of matrices deposited by tumor-associated and control 3T3-L1 preadipocytes (See Fig. 2.1). The SFA allows one to run compressive tests by determining the

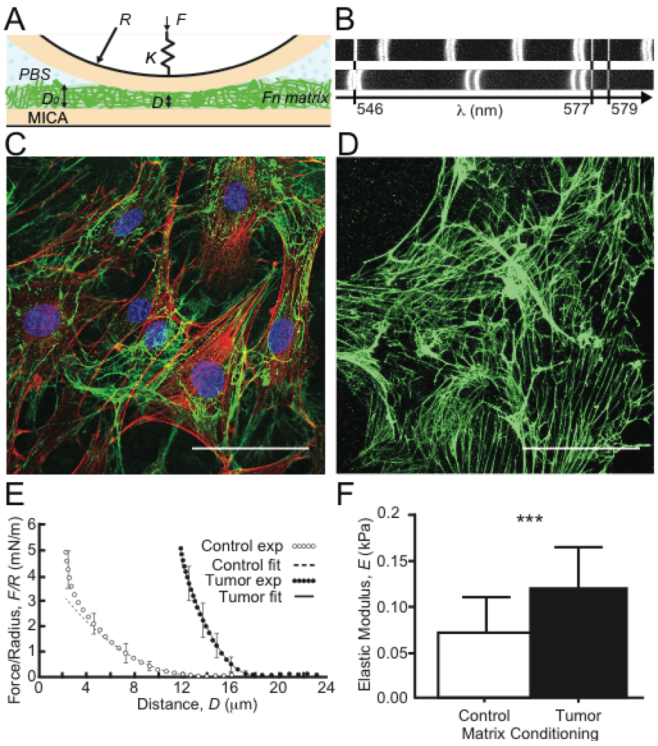


**Figure 2.1. Tumor-associated Fn matrices are stiffer.** (A) Schematics of the Surface Forces Apparatus (SFA) mica surfaces and setup used for mechanical characterization of the matrices at 37°C. (B) Interference fringes measured with the SFA when shining white light through the confining surfaces at large (uncompressed matrix) and small (compressed matrix) separations. (C) Immunostaining of tumor-conditioned stromal cells embedded in their ECM after 24 hr of culture onto SFA mica surfaces (green, Fn; red, F-actin; and blue, nuclei). (D) Same as (C) after decellularization (cell extraction) showing the Fn matrix left behind. Scale bars = 50 μm. (E) To determine Fn matrix stiffness, compressive force-distance profiles were acquired in quasi-static conditions in control (○) and tumor-associated (●) conditions and fitted using a Hertzian model. (F) Mean tumor-associated matrix elastic moduli (n=18) were ~60% higher than those of control matrices (n=20).

absolute distance *D* between two semi-reflecting smooth mica surfaces mounted on silica discs (Fig. 2.1*A*) using interferometric fringes patterns (Fig. 2.1*B*) while applying normal forces *F* via a double cantilever spring[211,212]. Briefly, tumor-associated and control 3T3-L1 cells were seeded onto the lower SFA mica disk in Fn-containing medium for 24 hr (Fig. 2.1*C*) and later removed with decellularization buffer leaving behind a cell-free fibrillar ECM comprising Fn fibers (Fig. 2.1*D*, Fig. 2.2*A*). Compressive measurements were then performed in the quasi-static regime via the upper SFA (bare) mica disk and force-distance profiles were acquired (Fig. 2.1*E*).

Data were further analyzed to extract elastic moduli using Johnson contact mechanics[39], in which the indentation of the matrix under compression $\delta$ is related to the normal force $F$ by the following equation:

$$\frac{F}{R} = \pi E \frac{\delta^2}{D_0}$$

where $R$ is the radius of curvature of the discs, $D_0$ is the matrix thickness at rest, and $E$ the resulting Young modulus. Elastic moduli were calculated over a 25% strain range (Fig. 2.1*F*) and force normalized by radius of curvature ($F/R$) plotted as a function of thickness parameter $\delta^2/D_0$ was used as control for the fit quality (Fig. 2.2*B*). We found that the mean elastic moduli of unfixed/native tumor-associated ECM were significantly higher than those of control matrices ($E$ = 0.12 ± 0.04 vs. 0.07 ± 0.03 kPa, $p < 0.001$).

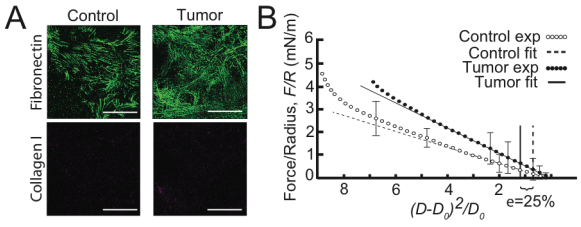


**Figure 2.2.** ECM composition and linearization of force-distance profiles. (A) Cell-derived ECMs were immunostained simultaneously for fibronectin and collagen, showing that early tumor-associated ECMs were comprised exclusively of Fn. Scale bars = 50 μm. (B) Linearization of the representative compressive force-distance profiles for control ECMs (experimental ○, fit - - -) and for tumor ECMs (experimental ●, fit —) shown in Fig. 1*E*. Tumor-associated ECMs show a larger linear regime as compared to the control ECMs.

We have also tested the effect of *in situ* chemical fixation of the matrices (with neutral buffered formalin) on their rigidity and found it increased the stiffness of both tumor-associated and control matrices by 22% and 19%, respectively ($E$ = 0.14 ± 0.06 vs. 0.09 ± 0.05 kPa, $p <$ 0.002) (Fig. 2.3), while the overall stiffening of tumor-associated matrices was maintained.

These data indicate how essential it is to assess mechanical properties of cell-derived materials in their native state instead of using fixatives, which promotes extra stiffening (here by ~20%).

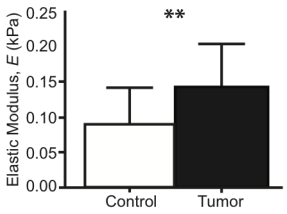


**Figure 2.3.** Chemical crosslinking increases stiffness. Tumor-associated ECMs (n=20) were 60% stiffer than control ECMs (n=30). ($p < 0.05$).

Since the ECM is a viscoelastic material, we next analyzed its creep response by applying instantaneous force and recording changes in ECM indentation depth ($\Delta\delta$) over time (Fig. 2.4*A*). Our results indicate two time-dependent regimes that could be well fitted by a double exponential decay:

$$\Delta\delta(\mathrm{t}) = A_1 e^{\frac{-t}{\tau_1}} + A_2 e^{\frac{-t}{\tau_2}}$$

where $\Delta\delta$ (t) is the matrix thickness decay, $\tau_1$ and $\tau_2$ are the fast and slow characteristic decay times, respectively, and $A_1$ and $A_2$ are the decay amplitudes used as fitting parameters. Tumor-conditioned matrices indicated longer decay times than control matrices in both the fast [$\tau_1$ = 125 ± 30 vs. 47 ± 25 s] and the slow [$\tau_2$ = 1048 ± 152 vs. 701 ± 107 s] regimes, suggesting a trend of overall slower responses of tumor-associated Fn matrices to external forces (Fig. 2.4B).

Collectively, these data indicate that, besides being stiffer, tumor-conditioned matrices may also be more viscous than their control counterpart, which is likely able to dysregulate mechanosignaling to surrounding cells. Although we could not find any previous report of tumor

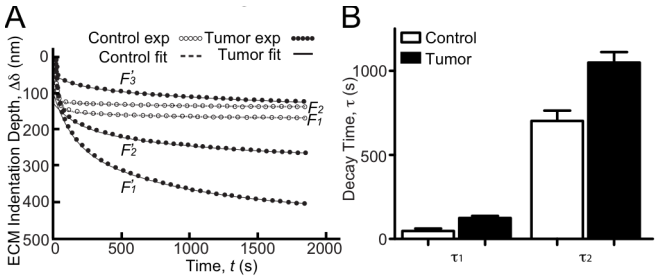


**Figure 2.4.** ECM creep tests. (A) The viscoelastic behavior of both control (○) and tumor-associated (●) Fn matrices was next quantified through creep experiments by monitoring change in matrix indentation depth after rapid (instantaneous) force application. Instantaneous forces correspond to $F_1 = F_1' = 3.7$ mN, $F_2 = F_2' = 7.4$ mN, and $F_3' = 11.1$ mN. All creep data were well fitted using a double exponential decay to extract fast ($\tau_1$) and slow ($\tau_2$) characteristic times. (B) There was an overall slower response (hence higher viscosity) of tumor-conditioned matrices (n=3) compared to that of control matrices (n=2).

ECM viscoelasticity, our matrix creep data are in agreement with the enhanced viscosity detected in breast cancer [215] and prostate cancer [216] tissues. The relative poroelastic and viscoelastic contributions to the matrix characteristic decay times reported here are discussed later.

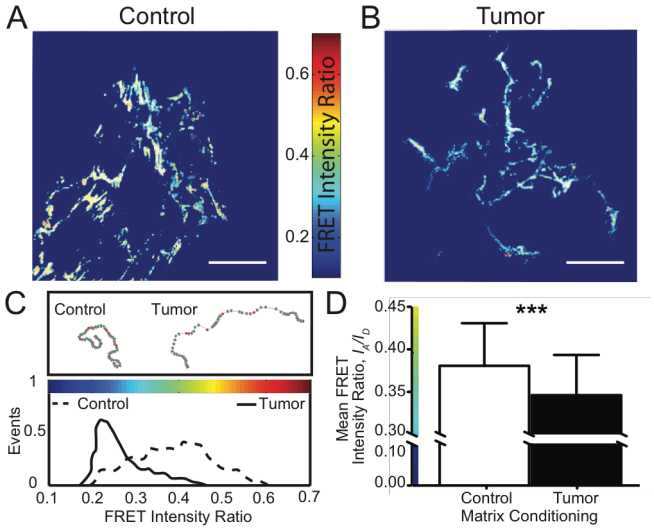


**Figure 2.5. Tumor-associated Fn matrices are more unfolded.** (A, B) FRET-Fn maps showed lower FRET intensity ratios, $I_A/I_D$, in tumor matrices (blue Fn fibers) than in their control counterpart (green/yellow Fn fibers). Scale bars = 50 μm. (C) Corresponding FRET intensity ratios histograms confirmed that tumor-associated Fn matrices comprised mainly stretched/unfolded Fn fibers (low FRET, narrow distribution) while control matrices contained a broader population of Fn conformations (higher FRET, larger distribution). (D) Mean FRET intensity ratios, $I_A/I_D$, of tumor-associated Fn matrices (n=171) were lower than that of control matrices (n=245), indicating that tumor conditions increased unfolding by ~10% with respect to control. Mean ± SD.

*2.5.2. Early Tumor-Conditioned Matrices Comprise Highly Stretched and Unfolded Fn Fibers*

We next combined FRET and confocal microscopy to monitor the incorporation of FRET-labeled Fn into newly developed fibrils over 24 hr, as previously described in [7] and calibrated in detail in [150] (Fig. 2.5). Our *in situ* FRET mapping shows that control cells (Fig. 2.5*A*) deposited high and medium FRET Fn fibers (yellow and green pixels) indicative of the coexistence of close-to-compact and extended Fn conformations. In contrast, tumor-associated cells (Fig. 2.5*B*) generated mostly stretched and unfolded Fn fibers, as indicated by low FRET fibrillar sections (blue pixels). Overall, tumor-associated matrices displayed both a more homogenous Fn population (narrower FRET histogram in Fig. 2.5*C*) and more stretched Fn fibers than control matrices (mean FRET intensity ratio = 0.35 ± 0.047 vs. 0.38 ± 0.05, $p < 0.0001$) (Fig. 2.5*D*). This trend is in agreement with previously published results [150]. Collectively, our data suggest that tumor-conditioned cells deposit Fn fibers with altered conformations that might alter Fn signaling either by exposing new binding sites to cells or by disrupting strain-sensitive binding motives such as the PHSRN synergy site and the RGD loop sequence responsible for $\alpha_5\beta_1$ integrins binding [67,70].

When testing the effect of Fn matrix chemical fixation on FRET, we found it increased the FRET ratio of control matrices (Fig. 2.6*A*) but had no effect on the FRET of tumor-conditioned (Fig. 2.6*B*) matrices, relative to unfixed conditions, denoting an overall strain relaxation and enhancing the differences between tumor-associated and control matrices (mean FRET intensity ratio = 0.35 ± 0.06 vs. 0.45 ± 0.05) (Fig. 2.8*C, D*).

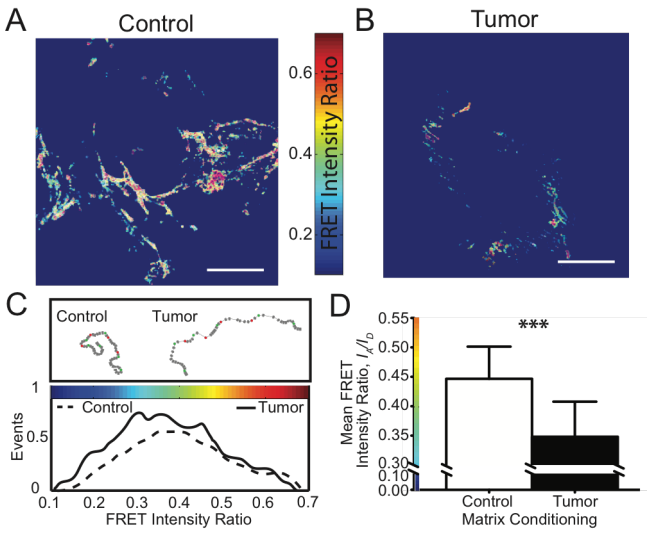


**Figure 2.6. Chemical crosslinking relaxes conformation.** (A) Crosslinked control Fn ECMs comprised close-to-compact/relaxed Fn fibers (high FRET, red/yellow pixels). (B) Crosslinked tumor-associated Fn ECMs comprised stretched/unfolded Fn fibers (low FRET, blue pixels). (C) Representative histograms of FRET ratios displayed. (D) Mean FRET intensity ratios of tumor-associated Fn ECMs (n=14) were significantly lower than that of control Fn ECMs (n=18). Scale bars = 50 μm.

*2.5.3. Early Tumor-Conditioned Fn Matrices are Thicker, Denser, and Comprise Thicker Fibers*

We next investigated the topology of the Fn matrices. We first used the SFA to assess ECM thickness (Fig. 2.7A) and show that tumor-conditioned cells generated a 37% thicker matrix than control cells ($D_0$ = 18.9 ± 1.7 vs. 13.7 ± 0.8 μm, $p < 0.03$). Next, z-projections of 3D reconstructed confocal image stacks (Fig. 2.7B) were used to quantify pore sizes and fiber diameters using ImageJ (NIH). We found that tumor-associated matrices were also denser, as indicated by smaller pores than in control matrices (73.3 ± 96.5 vs. 131.8 ± 179.8 $\mu m^2$) (Fig. 2.7C) and displayed Fn fibers with larger diameters ($Ø_{Tumor}$ = 1.10 ± 0.42 μm) than control matrices ($Ø_{Control}$ = 0.89 ± 0.31 μm) (Fig. 2.3D). Collectively, our data show that the topology of tumor-associated matrices is also altered: indeed, narrower pores and thicker Fn fibers likely contribute to enhanced matrix rigidity as well as altered cell binding and migration.

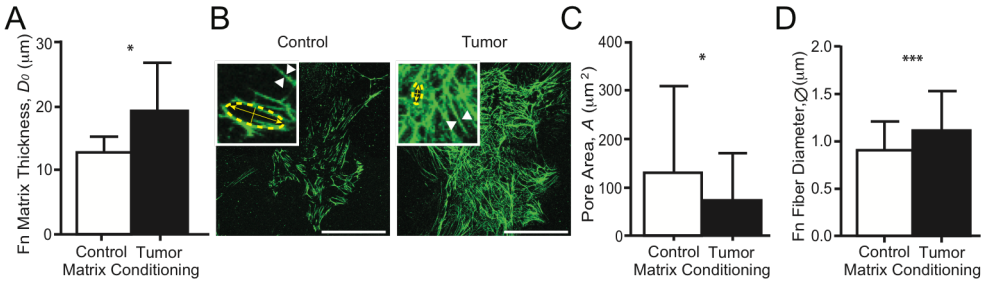


**Figure 2.7. Tumor-associated Fn matrices are thicker, denser, and comprised of thicker fibers.** (A) Tumor-associated Fn matrices (n=21) measured by the SFA were thicker than control matrices (n=17). (B) Z-projections of immunostained control and tumor-associated Fn matrices. Scale bars = 50 μm. Insets: 300% zooms used to determine the pore size and fiber diameter shown in panels (C) and (D), respectively. (C) Pores measured within tumor associated Fn matrices (n=72) were significantly smaller than those measured within control matrices (n=72) ( $p < 0.0001$). (D) Tumor-associated Fn fibers (n=120) possessed larger diameters than those of control Fn fibers (n=120) ($p < 0.05$). Mean ± SD.

*2.5.4. Early Tumor-Conditioned Fn Matrices Rapidly Increase Stromal Cell Proangiogenic Factor Secretion*

To determine the relevance of our results in tumor angiogenesis, we next assessed the proangiogenic capability of fresh 3T3-L1s after their seeding onto the Fn matrices via quantification of vascular endothelial growth factor (VEGF) secretion after 4 hrs. This approach allowed us to ascertain cellular response to a matrix primarily consisting of Fn that has not yet been remodeled. Interestingly, our data indicate that tumor-conditioned Fn matrices inhibited adhesion (40%) relative to control (data not shown), while VEGF secretion was significantly enhanced in the tumor-conditioned ECMs compared to their control counterparts (34%, 1.338 ± 0.472 relative to control vs. 1 ± 0.318) (Fig. 2.8A). We attributed different levels of VEGF to altered secretion (1.326 ± 0.026 relative to control vs. 1 ± 0.105) rather than altered matrix sequestration after we analyzed Fn-matrix lysates indicating negligible amounts of Fn matrix-bound VEGF (approximately 9% of VEGF measured in the media) with no significant differences between tumor and control matrix conditions (0.086 ± 0.002 relative to control vs.

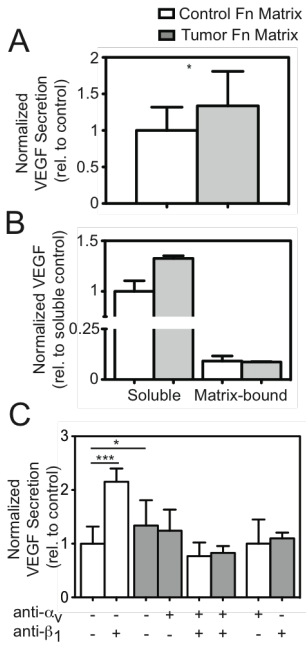


**Figure 2.8. Cells adhere to tumor-associated Fn preferentially through $\alpha_v$ integrins with associated increased VEGF secretion.** (A) After 4 hr, new (untreated) cells secreted significantly higher levels of VEGF when seeded onto tumor-associated Fn (1.338 ± 0.472 relative to control, n = 13) than those seeded onto control Fn (1 ± 0.318, n = 14) ($p < 0.05$). (B) There were differences in VEGF secretion (1.326 ± 0.026 relative to control vs. 1 ± 0.105) but not in matrix sequestration from the same samples after 24hr cultures (0.086 ± 0.002 relative to control vs. 0.091 ± 0.018). n = 2/group. (C) After 4 hr, cells treated with $\beta_1$-integrin blockers and seeded onto control ECMs secreted significantly higher levels of VEGF than untreated cells (2.153 ± 0.246 relative to control, n = 6 vs. 1 ± 0.318, n = 14) ($p < 0.0001$). When cells treated with $\alpha_v$-integrin blockers were seeded onto control ECMs, no change in VEGF secretion was detected compared to untreated cells (1 ± 0.449, n = 4). Cells treated with $\alpha_v$-integrin blockers and seeded onto tumor ECMs secreted slightly lower levels of VEGF than untreated cells (1.242 ± 0.392 relative to control, n = 6 vs. 1.338 ± 0.472, n = 13). For cells treated with $\beta_1$-integrin blockers on tumor ECMs, there was an insignificant decrease in VEGF secretion compared to untreated cells (1.098 ± 0.108, n = 4). As a control, cells treated with both integrin blockers secreted lower levels of VEGF on both control (0.767 ± 0.253, n = 6) and tumor ECMs (0.828 ± 0.126, n = 6). Mean ± SD.

0.091 ± 0.018) (Fig. 2.8*B*). Because Fn conformational changes were previously shown to modulate the binding specificity of integrins [74,153,155,217,218], we also examined altered integrin specificity as a potential mechanism of tumor-induced modified signaling. We initially tested whether introducing integrin blockers would alter VEGF secretion by exposing unconditioned 3T3-L1s to $\alpha_v$ blockers on control matrices and $\beta_1$ blockers on tumor matrices. We detected no significant difference in VEGF secretion on control and tumor matrices, respectively

(Fig. 2.8*C*, +/- white bar and -/+ gray bar). We first tested the role of $\alpha_5\beta_1$ integrins in regulating VEGF secretion by exposing fresh cells to $\beta_1$ blockers prior to seeding. Our data indicate that blockade of $\beta_1$ dramatically increased VEGF secretion relative to the untreated-control condition (Fig. 2.8*C*, -/- and -/+ white bars) indicating that $\alpha_5\beta_1$-mediated interactions with control Fn, may contribute to low VEGF secretion levels by stromal cells. This effect was inhibited by simultaneous addition of an $\alpha_v$ function-blocking antibody (Fig. 2.8*C*, +/+ white bars), suggesting that $\alpha_v\beta_3$ may play a role in this process. We next tested the contribution of $\alpha_v\beta_3$ to increased VEGF secretion of cells interacting with tumor Fn. However, exposure of cells to $\alpha_v$ blockers prior to seeding led to a slight decrease in VEGF secretion (Fig. 2.8*C*, -/- and +/- gray bars), while concomitant blockade of both $\alpha_v$ and $\beta_1$ subunits further lowered VEGF secretion (Fig. 2.8*C*, +/+ gray bars), suggesting Fn-mediated complex integrin compensatory mechanisms.[219] Collectively, our data indicate that the presence of unfolded and stiff Fn fibers in tumor-conditioned matrices enhances 3T3-L1 secretion of VEGF by altering their use of $\alpha_v\beta_3$ over $\alpha_5\beta_1$ integrins. These results are discussed later and are in agreement with previous work by others showing a direct link between $\alpha_v\beta_3$ engagement and increased VEGF secretion.[184]

Because cells respond to altered matrices by modulating their adhesive linkages, we further investigated cell adhesions by monitoring the recruitment of two focal adhesion proteins. Our data reveal differences in both talin and phosphorylated focal adhesion kinase (pFAK [pY397]) distribution among cells reseeded on control or tumor-associated matrices (Fig. 2.9). On control Fn, untreated cells recruited both talin and pFAK to develop fibrillar adhesions (insets: double arrows); instead, cells treated with $\beta_1$ blockers grew adhesive ECM clusters comprising mainly talin (Fig. 2.9, control). On tumor-conditioned Fn, untreated cells developed focal contacts comprising both talin and pFAK (insets: arrowheads) while cells treated with $\alpha_v$

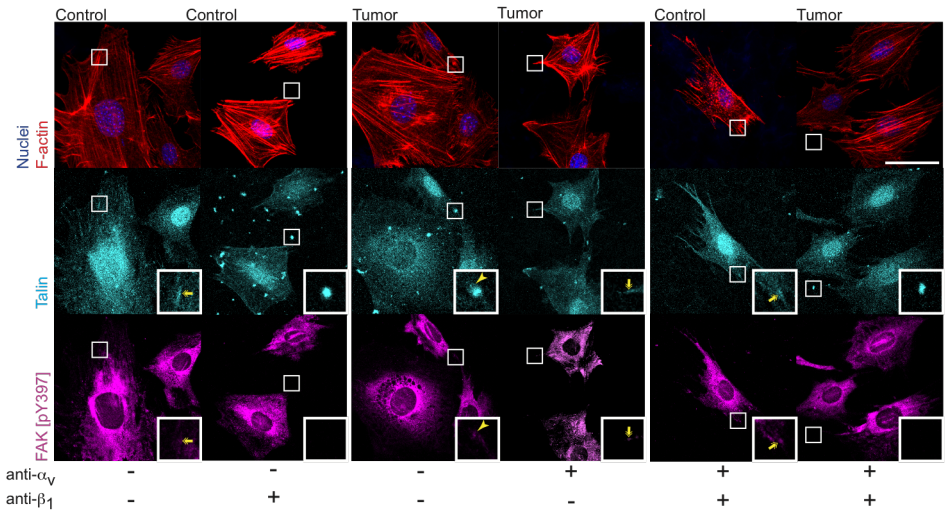


**Figure 2.9.** Focal adhesion protein recruitment on tumor-associated Fn ECMs associated with development of focal contacts. After 4 hr, untreated cells seeded onto control ECMs developed fibrillar adhesions comprising both talin and pFAK (insets: double arrows) while cells treated with $\beta_1$-integrin blockers showed large adhesive clusters (focal contacts consisting of talin only) left behind by cells in the surrounding matrix (insets: ECM cluster). In contrast, untreated cells seeded onto tumor ECMs developed focal contacts comprising both talin and pFAK (insets: large arrowheads), whereas cells treated with $\alpha_v$-integrin blockers were able to develop fibrillar adhesions (insets: double arrows). Cells treated with both integrin blockers were able to develop fibrillar adhesions when seeded onto control ECMs (insets: double arrows) and to generate focal contacts (clusters) when seeded onto tumor ECMs (insets: ECM cluster). Scale bar = 50 μm.

blockers began developing fibrillar adhesion located mainly at the cell periphery (insets: double arrows) (Fig. 2.9, tumor). Interestingly, cells treated with both integrin blockers developed peripheral fibrillar adhesions on control Fn, and left behind ECM clusters on tumor-associated Fn.

Our findings are in agreement with previous work showing that focal contacts comprise primarily $\alpha_v\beta_3$ integrins whereas fibrillar (or mature) adhesions contain principally $\alpha_5\beta_1$ integrins.[220] These different adhesions are activated through different mechanisms: while $\alpha_5\beta_1$ integrins cluster and recruit adhesion proteins in a contractility-independent manner [160], $\alpha_v\beta_3$ integrins require cell contractility to develop nascent adhesions via talin [221], which regulates $\alpha_v\beta_3$ activation via a conformational change of $\beta_3$ reinforcing nascent focal contacts.[222-224]

Our findings indicate that cells forced to utilize $\alpha_v\beta_3$ integrins on stiff and unfolded tumor-associated matrices recruit higher levels of talin to form large focal contacts, which may also modulate proangiogenic behavior.

**2.6. Discussion**

The experiments presented herein suggest that breast cancer cell-secreted factors deregulate early Fn matrix assembly by stromal cells. Increased levels of Fn had been previously detected in tumors, [53] and plasma Fn is implicated in tumor growth.[225] Our findings additionally indicate that the mechanical and the structural/conformational properties of Fn may be different in tumors vs. controls as matrices deposited by stromal cells in response to tumor-secreted factors exhibited increased overall stiffness, fiber stretching, and molecular unfolding. Moreover, these Fn alterations were linked to enhanced proangiogenic capability of the stromal cells with potential implications for tumor angiogenesis.

More specifically, tumor-conditioned matrices are mechanically different from control matrices as they exhibit increased stiffness. Our work also suggests that tumor-conditioned matrices have slower changes in indentation depth, indicative of both elastic and time-dependent (viscous) modifications. Furthermore, these matrices are structurally (and conformationally) altered across multiple length scales as they are overall thicker, denser, and composed of thicker fibers that comprise more unfolded Fn molecules. By combining the SFA with FRET mapping, our study provides a detailed picture of the early deposited Fn matrix from the matrix/cellular level to the molecular level. Our results are in accordance with work of previous investigators but also include new observations with direct implications on Fn-mediated tumor-stroma progression.

At the single fiber level, previous FRET work had shown that strain application to *manually-extruded* Fn fibers led to stiffening and unfolding (above 150% strain) in these fibers [7]. At the matrix level, another FRET study [150] estimated the average strain in *cell-derived* Fn fibers based on a FRET vs. strain calibration (performed on single *manually-extruded* fibers) and anticipated matrix stiffening although no direct measurement of matrix stiffness was performed. To our knowledge, this study reports the first quantitative and direct correlation between overall Fn matrix stiffness and topology at the matrix/cellular scale with Fn conformations at the molecular scale.

Our findings also underline how dramatic the effect of fixatives (commonly used in laboratories) can be on both the mechanical and structural properties of compliant (0.1 kPa range) and porous materials. Indeed, although the general trends of stiffening and unfolding were maintained for tumor-conditioned relative to control matrices, formalin increased rigidity and decreased strain (as indicated by a FRET increase), particularly in control Fn matrices where the random crosslinking of lysines likely resulted in the pinning of dangling/relaxed Fn fibers in the network.

Our stiffness data indicate lower values for tumor-conditioned Fn matrices than for both macroscopic tumors in vivo [226] and single Fn fibers [124]. These difference can be attributed to (i) the higher porosity of cell-free Fn networks (with enhanced fluid transport) relative to the denser tumor tissue, (ii) the presence of both Fn and collagen in mature tumor tissues, and (iii) the different regime of deformations in individual fibers relative to ECM networks, where the deformation (here compression) is distributed over a mesh of disordered and connected fibers that respond collectively to stress by initially aligning/ordering along the compressive surface before being further indented. Moreover our creep data indicate a trend of slower responses of

tumor-conditioned matrices with respect to their control counterparts, with characteristic decay times of the order of $10^2$ and $10^3$ s for ($\tau_1$) and ($\tau_2$), comparable to the time of observation in our experiments. A simple calculation of the characteristic time for solvent molecules to be diffused through the Fn matrix, i.e., so-called poroelastic time $\tau_p$, assuming a typical radius of contact between SFA surfaces of 10 μm and a diffusion constant for cells and tissues of 10 – 100 $\mu m^2/s$ [227,228] leads to $\tau_p$ = 1 – 10 s, i.e., 10 to 100 times faster than the measured ($\tau_1$) and ($\tau_2$), Hence our results suggest that although poroelastic processes contribute to the biphasic system (Fn network + solvent) relaxation at shorter timescales, the longer decay times we report here are mainly due to viscoelasticity, i.e., conformational/structural changes in the Fn network rather than to solvent redistribution through the matrix pores.

Additionally, to obtain cell-derived Fn matrices, we used a well established protocol [210] comprising a mild detergent and multiple washing steps. Decellularizing matrices has previously been shown to (i) relax matrix networks by ~20% [35], and (ii) alter the ratio of DOC soluble (nascent) to DOC insoluble (crosslinked) Fn characterized herein [89], as DOC soluble Fn will have most likely been washed away. Although these effects should not alter our results, which report *relative* differences between control and tumor-conditioned decellularized matrices, future studies will be required to delineate the potential contribution of both relaxation and loss of fibrillar heterogeneity on these matrices, in particular by developing new (less invasive) decellularization protocols.

Matrix topology (denser network and thicker fibers) together with molecular unfolding of the initial Fn matrix may also influence indirectly the overall tumor- conditioned matrix mechanics. Additionally, on one hand, Fn unfolding has been shown to lead to the subsequent deposition of a more unfolded Fn matrix [154]. On the other hand, altered Fn characteristics

might modulate tumor stiffness by altering the deposition of subsequent ECM components. For example, Fn fibers act as templates for the deposition of collagen [106]. In particular, the specific binding of collagen I α1 chain to the gelatin-binding domain of Fn (located on $FnI_6$, $FnII_{1-2}$, and Fn $III_{7-9}$) is necessary for the initial co-deposition of collagen [102]. Because the interaction of Fn with collagen is likely conformation dependent, the unfolded/highly strained Fn fibers initially generated by 3T3-L1s may dramatically affect collagen fibrillogenesis, either by disrupting the exposed binding site for collagen I or by exposing cryptic sites with enzymatic activity such as Fn type IV Col-ase, which is a matrix metalloprotease in the collagen binding domain of Fn capable of digesting collagen [229]. Consequently, Fn unfolding may also indirectly regulate the mechanosignaling of tumor-associated collagen I that ultimately contributes to tumorigenesis [22,23,166].

In this study, we also report that new (untreated) stromal cells seeded onto tumor-associated matrices exhibit decreased adhesion and enhanced VEGF secretion. Because tumor-conditioned Fn matrices exhibit topological, conformational, and mechanical alterations known to alter cell-matrix interactions, we hypothesized that Fn alterations might serve as a mechanosensor and "integrin switch". Tumor-conditioned Fn ECMs were characterized to be dense matrices comprising thick fibers. Thicker fibers may alter ligand density, which in turn, would alter stable focal adhesion formation and downstream cellular behavior [230-233]. As increased ligand density might be another mechanism behind altered cell-Fn matrix interactions in tumors, future studies are needed to probe how antagonizing RGD binding sites could alleviate (in a dose-dependent manner) subsequent cell behavior in tumors. Our results indicate that the cells responsible for enhanced VEGF secretion detected on tumor-associated matrices (comprising mainly stretched/unfolded Fn fibers) tend to favor the use of $\alpha_v\beta_3$ over $\alpha_5\beta_1$ integrins

to interact with Fn. This finding can be explained by differential engagement of either strain-sensitive (e.g., $\alpha_5\beta_1$) or strain-insensitive (e.g., $\alpha_v\beta_3$) integrins with the surrounding matrix. Indeed, the integrin binding FnIII9-III10 sequence of Fn is extremely sensitive to conformational changes resulting from enhanced tension exerted by cells. Earlier reports suggested that the distance between the "synergy" PHSRN site in $FnIII_9$ and the RGD site in $FnIII_{10}$ is critical for engagement and activation of integrin $\alpha_5\beta_1$ [71,72] but has little effect on engagement of integrin $\alpha_v\beta_3$. Therefore the "integrin switch" measured here on tumor-conditioned matrices may be in part explained by strain-induced increased spatial separation between $FnIII_9$ and $FnIII_{10}$ [74], which inhibits the binding of $\alpha_5\beta_1$ to both sites simultaneously [70] and forces cells to utilize more $\alpha_v\beta_3$ to compensate [217]. Our results are in agreement with previous work showing that higher engagement of $\alpha_v\beta_3$ increases VEGF secretion [153,184]. Moreover, we see that $\beta_1$ blockade of cells seeded on control (relaxed) Fn had a greater effect on VEGF secretion than $\alpha_v$ blockade of cells on tumor-conditioned (stretched) Fn. This functional difference may be attributed to VEGF receptor availability, as VEGF is immobilized to Fn through a $\alpha_5\beta_1$/VEGF-receptor [31]. This immobilization inhibits the accessibility of $\alpha_5\beta_1$, leading to VEGF release. Another explanation of the functional difference could be that $\alpha_5\beta_1$ has higher binding affinity (4 nM) to Fn [234] than $\alpha_v\beta_3$ (1.3 μM) [235]. Nevertheless, the measured increase in VEGF secretion may be further modulated by the physicochemical complexity of the tumor-conditioned ECM. This complexity not only entails differences in Fn stiffness and conformation (including different spatial distribution of ligands at the fiber surface), but also varied quantity and composition (e.g. proteoglycans), which can all regulate the observed integrin(s) switching effect. Though the difference in VEGF secretion is small, it is significant, and comparable to our

previous studies in which similarly small differences in VEGF secretion on dense and mature ECM networks significantly affected endothelial cell behavior [153].

Collectively, our results contribute to an improved understanding of the role of early Fn matrix assembly in modulating proangiogenic factor secretion of breast tumor-conditioned stromal cells. Future experiments are needed to further clarify the role of Fn in a 3D tissue-like context. Our studies have been performed on cell-derived Fn-matrix coated mica surfaces, where both substrate rigidity and culture dimensionality can also regulate changes in cell behavior. In particular, the mica substrates used in our studies are stiffer than the tumor tissue, which may affect the mechanics and conformation of the deposited Fn matrix. Similarly, the formation of focal adhesions differs in 2D and 3D cell cultures [236] which also potentially modulates the properties of the Fn matrix. Future studies will (i) validate our integrin-modulated VEGF secretion findings in a physiologically relevant 3D matrix with controlled stiffness and topology, (ii) allow us to discriminate the roles of stiffness and conformation in regulating these processes [237], and (iii) lead to new insights that may improve current anti-VEGF therapies [238].

## 2.7. Conclusions

Our results indicate that, following exposure to breast cancer cell-secreted factors, adipose stromal cells initially deposit in the stroma high amounts of stiff and unfolded Fn with altered topology, which deregulate the behavior of neighboring cells by modifying cell-matrix interactions (altered outside-in signaling). Our work also indicates that such tumor-induced Fn matrix deregulation activates integrin switches in surrounding cells ultimately enhancing VEGF secretion with potential functional consequences on tumor angiogenesis. These findings have important implications for our understanding of tumor growth, as they support the notion of Fn

as a key initiator of mammary tumor angiogenesis. This work also enhances our knowledge of cell – Fn matrix mechanobiological interactions that may be exploited for other biomaterials-based applications, including advanced tissue engineering approaches.

# CHAPTER 3

# BREAST CANCER CELLS INFLUENCE FIBRONECTIN-COLLAGEN SYNERGISTIC DYNAMICS

*In preparation for Advanced Materials (2015)*

## 3.1. Contributors

Authors of this manuscript are: Karin Wang, Bo Ri Seo, Marion Quien, Lauren Hsu, Soyoung Min, Victoria Benson, Claudia Fischbach, Delphine Gourdon

K.W., B.R.S., C.F. and D.G. designed research; K.W., M.Q., L.H., performed research; K.W., and B.R.S. contributed new reagents/analytic tools; K.W., M.Q., L.H., S.M., V.B., and D.G. analyzed data; and K.W., B.R.S., C.F., and D.G. wrote the paper.

Acknowledgements: This work was financially supported by the NSF (DMR-1352299 to DG) and the NIH/NCI (R01 CA185293 to CF and DG). We acknowledge support from the Cornell University NIH-funded Biotechnology Resource Center (BRC) (Grants: 1S10RR025502-01 and 1S10OD010605-01A1). We thank Professor Denise Hocking (University of Rochester) for providing purified plasma fibronectin for FRET-labeling.

## 3.2. Abstract

Breast cancer cells recruit surrounding stromal cells, such as cancer-associated fibroblasts (CAFs), to remodel the extracellular matrix (ECM) for invasive tumor growth. Two major ECM components, fibronectin (Fn) and collagen I (Col I), are known to interact with each other and to regulate cellular behavior. We sought to understand how both Fn and Col I promote invasive tumor growth. Specifically, we assessed how tumor-associated ECM composition, topology, conformation, and fiber kinetics all dynamically evolved. And how these structural ECM changes affected pro-angiogenic secretion by CAFs. Our work suggests that CAFs assembled and reorganized Fn and Col I fibers into thick and dense ECM comprising unfolded and strained fibers with altered viscoelasticity. These microarchitectural changes mediated by matrix metalloproteinases, in turn, modify CAF pro-angiogenic secretion. Collectively, these results highlight the synergistic interplay of Fn and Col I microarchitecture in promoting a dysregulated signaling cascade for invasive breast tumor growth.

## 3.3. Introduction

Particular focus has been placed on studying the altered extracellular matrix (ECM) during tumorigenesis, as it provides biochemical and biomechanical cues that alter cellular functions.[1,8] Characteristic ECM modifications that occur are: ECM topology,[166] stiffness,[239] fiber unfolding,[150] crosslinking,[23] remodeling,[240] and ECM composition.[241-243] Fibronectin (Fn), a major ECM glycoprotein, regulates cell signaling and behavior in both physiological and pathological conditions. Fn is a mechanotransducer protein: cell-induced conformational changes affect cell adhesion and growth factor binding.[7] Cancer cells, unable to assemble their own Fn matrix, up-regulate Fn in the surrounding stroma.[53]

Tumor-secreted factors conditioning (TC) of fibroblasts mediate the assembly of Fn into highly stretched and unfolded fibers,[150] resulting in an overall stiffer and denser ECM responsible for enhanced pro-angiogenic signaling.[151] Collagen I (Col I) deposition is primarily dependent on previously assembled Fn matrices.[24,102,103] And Col I is another prominent ECM protein with many contributions to tumorigenesis.[18,23] Therefore, Fn-Col I interactions during TC are critical for our understanding of tumor stroma modifications.

In this study, we seek to elucidate the dynamics of TC-ECM assembly. Specifically, we (i) assessed composition, topology, and conformation of the composite TC-ECM (Fn and Col I) over time, (ii) evaluated how matrix metalloproteinases (MMPs) contribute to altered TC-ECM evolution, and (iii) assessed associated changes in pro-angiogenic factor secretion.

## 3.4. Materials and methods

### *3.4.1. Cell culture*

3T3-L1 pre-adipocytes and MDA-MB-231 breast cancer cells (ATCC, VA) were cultured in Minimum Essential Medium (α-MEM) with 10% fetal bovine serum (FBS) and 1% penicillin-streptomycin (PS). Tumor soluble factors (TSF) were obtained from MDA-MB-231 cells cultured in α-MEM (1% FBS & 1% PS) for 24 hrs. 3T3-L1s were preconditioned with either control (c-) or normalized TSF (TC-) in α-MEM (1% FBS & 1% PS) for 3 days, before seeding 5 x $10^3$ cells/0.8 $cm^2$ for immunostaining and conformational studies, or 25 x $10^3$ cells/3.8 $cm^2$ for pro-angiogenic studies onto Fn-coated (30 μg/mL) Lab-Tek$^{TM}$ chambered coverglass (Thermo Scientific, MA) or 12-well plates (Corning, MA), respectively. Preconditioned cells were maintained in conditioning medium until 24 hr before a timepoint (Day 1, 5, 9) then switched to α-MEM (1% FBS & 1% PS) with Fn (50 μg/mL: 10% FRET-

labeled for conformational experiments). After 24 hr, samples were fixed for FRET or immunostained imaging.

*3.4.2. Immunostaining*

Nonspecific binding was blocked with PBS/1% SuperBlock (Thermo Scientific, MA) for 1 hr at room temperature before immunostaining for Fn (1:400 anti-mouse antibody) (Sigma-Aldrich, MO) and Col I (1:100 anti-rabbit antibody) (EMD Millipore, MA) overnight at 4°C. After washing with PBS (2x), samples were incubated with Alexa Fluor 647 goat anti-mouse (1:100), Alexa Fluor 488 goat anti-rabbit (1:100), Alexa Fluor 568 Phalloidin (1:250), and DAPI (1:5000) in PBS at room temperature for 1 hr. Afterwards, samples were washed (2x) and kept in PBS at 4°C until confocal imaging with a Zeiss 710 confocal microscope (Zeiss, Munich, Germany). All Alexa Fluor reagents were bought from Life Technologies (Grand Island, NY).

*3.4.3. FRET*

Fn were semi-randomly labeled with Alexa Fluor 546 maleimide and Alexa Fluor 488 succinimidyl ester, as previously described [151]. Samples were confocal imaged with the C-apochromat water-immersion 40x/1.2 objective, a pinhole of 2 AU, a 488 nm laser set at 10% power, and a pixel dwell time of 6.3 μs to acquire 16-bit z-stack images spaced 2 μm apart. FRET-Fn fluorescence were collected to quantify FRET ratios (defined as intensity ratios of acceptor and donor fluorophores = $I_A/I_D$) as previously described [151]. Representative FRET z-stack images were stacked in ImageJ (NIH).

*3.4.4. Spinning disk confocal imaging and fiber viscoelasticity*

Plasma Fn randomly single-labeled with Alexa Fluor 488 succinimidyl ester were provided to cultures 24 hr at Day 1, 5, 8. After 24 hr to allow cells to assemble an Fn ECM containing 488-labeled Fn, cultures were placed in a confined chamber within an Inverted Andor/Olympus IX-83 spinning disk confocal microscope (Olympus Corporation, Tokyo, Japan) and time-lapse z-stack images taken every 10 min at 4 separate locations per sample up to 16 hr past the aforementioned timepoints.

*3.4.5. Matrix metalloproteinase inhibition*

For matrix metalloproteinase inhibition experiments, additional samples were supplemented with 20 μM Batimastat (Millipore, MA). Batimastat, a broad spectrum MMP inhibitor, was shown to prevent metastases as well as tumor growth especially at early stages of tumor development.[244,245]

*3.4.6. Pro-angiogenic quantification*

For pro-angiogenic secretion experiments, media were collected at every timepoint and centrifuged at 13500 rpm for 15 min at 4°C to collect supernatants free of cell-debris. VEGF secretion was normalized to DNA extracted from the same timepoint samples in Caron's buffer. Data were represented as ratios to the average 1d control samples of each experiment.

*3.4.7. Statistical analysis*

Data were statistically analyzed in GraphPad Prism (GraphPad Software, Inc., CA) with student's t-tests or ANOVAs with Tukey's post-hoc tests and statistical significance was determined at $p < 0.05$. Mean ± SEM.

## 3.5. Results and Discussion

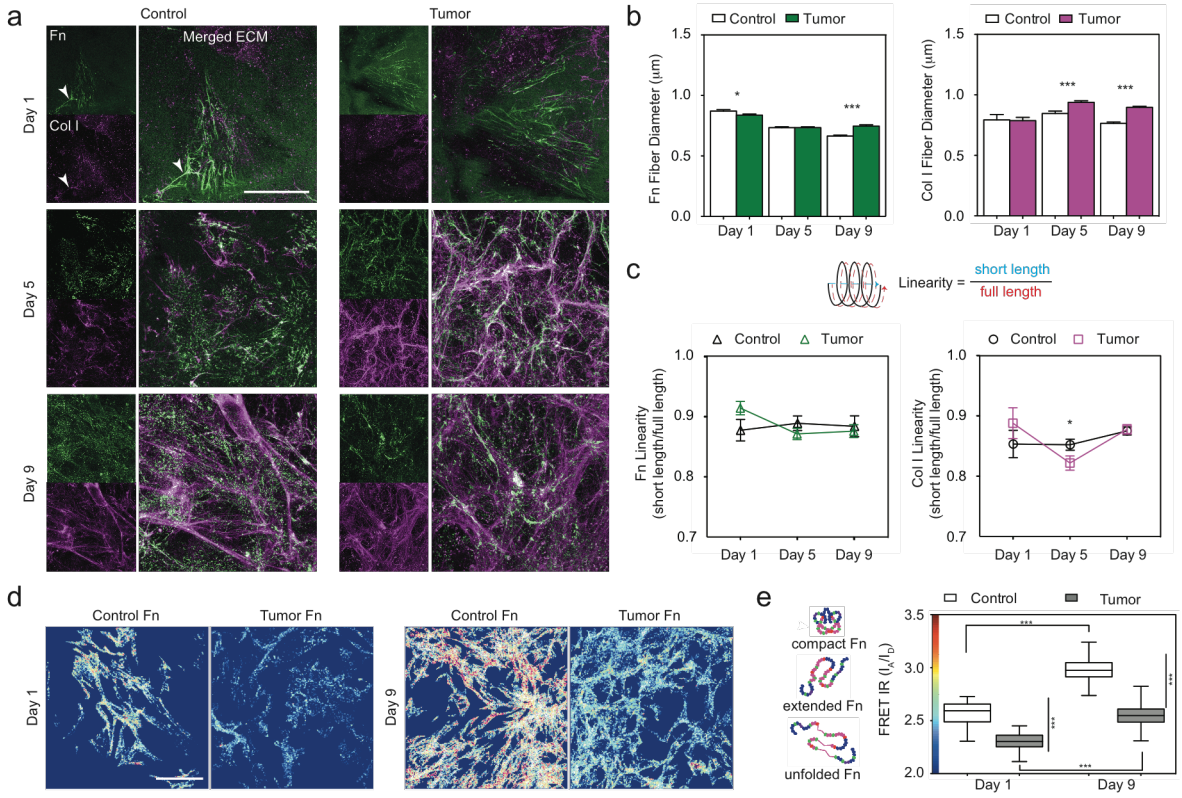


**Figure 3.1. Altered TC-Fn and TC-Col I over time.**
a) Immunofluorescence portraying the evolution of c- and TC-ECMs over 9 days: fibronectin (green) and collagen I (magenta). Overlay of ECM with f-actin and DAPI in SI Fig 1. Fn was present at all timepoints, however most fibrillar Col I was not fully assembled until later time points. b) Initially thin TC-Fn fibers decreased less in diameter once thick TC-Col I fibers were assembled. c) Initially strained TC-Fn and TC-Col I fibers decreased to progress towards control strain values. d) FRET maps show more unfolded Fn (blue) in TC-ECM (right) compared with that of c-ECM (yellow-red). FRET maps also depict a shift in FRET from Day 1 (blue-green) to Day 9 (green-red); Fn conformation relaxes in the presence of Col I. e) Mean FRET ratios ($I_A/I_D$) show significant differences between TC-Fn and c-Fn of early ECM and evolved ECM. Scale bars: 50 μm.

### *3.5.1. Tumor-conditioned matrix topology evolution*

ECM assembled by control (c-) and TC-pre-adipocytes, a model of cancer associated fibroblasts in the peritumoral region, were cultured over 9 days to evaluate the deposition and remodeling of both Fn and Col I over time. Previous studies have shown that these cells initially

deposit a TC-Fn matrix that exhibits altered topology and stiffness.[150,151] We sought to understand how the materials properties of TC-Fn would affect downstream Col I deposition and contribute to stromal changes during tumorigenesis.

Immunofluorescence of c- and TC-ECM portrayed an initial (Day 1) ECM primarily comprising Fn (Fig. 3.1a; Day 1 & SI Figure 1). This early TC-Fn is thin (Fig. 3.1b; **Fn** Day 1: 0.84 ± 0.01 μm, n = 723 vs. 0.87 ± 0.01 μm, n = 640; $p < 0.05$). Thin Fn diameters are likely due to strained (linear) Fn fibers (Fig. 3.1c; **Fn** Day 1: 0.91 ± 0.01, n = 90 vs. 0.88 ± 0.02, n = 49) comprising unfolded Fn molecules (Fig. 3.1d,e; **FRET** Day 1: 2.303 ± 0.011, n = 47 vs. 2.566 ± 0.013, n = 54; $p < 0.0001$). This initial physically altered Fn likely contributes to altered cell-ECM and Fn-Col interactions by exposing/disrupting cryptic binding sites.[64,246,247] An established Fn matrix is generally required for the assembly of other ECM proteins such as fibrillins[248] and collagens.[24] However, one study reports collagen deposition in the absence of Fn through transforming growth factor-β1 (TGF-β1) compensation,[168] which may explain the presence of the few t-Col I fibers found at Day 1 (Fig. 3.1a; **Col I** Day 1: 0.79 ± 0.03 μm, n = 66 vs. 0.79 ± 0.04 μm, n = 54) that were strained (Fig. 3.1c; **Col I** Day 1: 0.89 ± 0.03, n = 34 vs. 0.85 ± 0.02, n = 31), as TGF-β1 is a component of the TC media.[150] Furthermore, Fn and procollagen have been found to co-localize within similar cellular compartments of fibroblasts during secretion,[107] which may contribute to the occasional co-assembly of Fn and Col I in early c-ECMs (Figure 3.1a; Day 1, white arrowheads).

By Day 5 numerous thin, but similar in diameter TC-Fn fibers (Fig. 3.1b; **Fn** Day 5: 0.73 ± 0.01 μm, n = 1862 vs. 0.73 ± 0.01 μm, n = 1226) co-localized with thick bundles of t-Col I fibers (Fig. 3.1a white regions of fibers; **Col I** Day 5: 0.94 ± 0.01 μm, n = 432 vs. 0.84 ± 0.02 μm, n = 338; $p < 0.0001$). However, in c-ECM, only fragmented/digested Fn and thin Col I fibers

were present. By Day 9 more differences arise between c- and TC-ECM (Fig. 3.1a; Day 9). Most TC-Fn was replaced by dense thick TC-Col I fibers (Fig. 3.1b; **Col I** Day 9: 0.9 ± 0.01 μm, n = 1297 vs. 0.76 ± 0.01 μm, n = 647; $p < 0.0001$). The remaining thick TC-Fn fibers (Fig. 3.1b; **Fn** Day 9: 0.75 ± 0.01 μm, n = 1337 vs. 0.66 ± 0.01 μm, n = 1012) were consistently more stretched/unfolded (Fig. 3.1e; **FRET** Day 9: 2.552 ± 0.013, n = 60 vs. 2.975 ± 0.012, n = 76; $p < 0.0001$). Both c- and TC-Fn shifted to higher FRET in the presence of Col I (Fig. 3.1e; Day 9), likely due to Col I binding cooperatively with high affinity for $_{6}$FnI$_{1\text{-}2}$FnII$_{7}$FnI and $_{8\text{-}9}$FnI (gelatin binding domain of Fn) to stabilize the kink between $_{7}$FnI and $_{8}$FnI and maintaining a relaxed conformation.[112] Additionally, mechanical studies of Col I fibers report elastic moduli of 123 MPa,[249] higher than the elastic moduli of ~3.5 MPa measured of 700% strained fibrillar Fn fibers.[124] Col I fibers may be capable of bearing more tension in the ECM to therefore allow unfolded Fn fibers to relax.

Interestingly, initially strained t-Fn and t-Col I fibers then decreased (Fig. 3.1c; **Fn** Day 5: 0.87 ± 0.01, n = 130 vs. 0.89 ± 0.01, n = 79; **Col I** Day 5: 0.82 ± 0.01, n = 169 vs. 0.85 ± 0.01, n = 200; $p < 0.05$) to converge towards control values at Day 9 (Fig. 3.1c; **Fn** Day 9: 0.88 ± 0.01, n = 92 vs. 0.88 ± 0.02, n = 38; **Col I** Day 9: 0.88 ± 0.01, n = 205 vs. 0.88 ± 0.01, n = 220). The converging values suggest that individual fiber strain (and its long range force transmission between cells)[250,251] is inconsequential to the bulk tissue (e.g.: quantity of fibers/bundling or fiber topology). Previous studies have shown that Col I requires the initial assembly of a Fn matrix for subsequent Col I deposition.[24,102] Our data suggests that the initial physical and conformational state of the Fn fibers may regulate how Col I is deposited and altered in tumor stroma. And that once Col I is deposited, its bulk tissue topology may be the driving force of altered tumor stroma mechanotransduction.

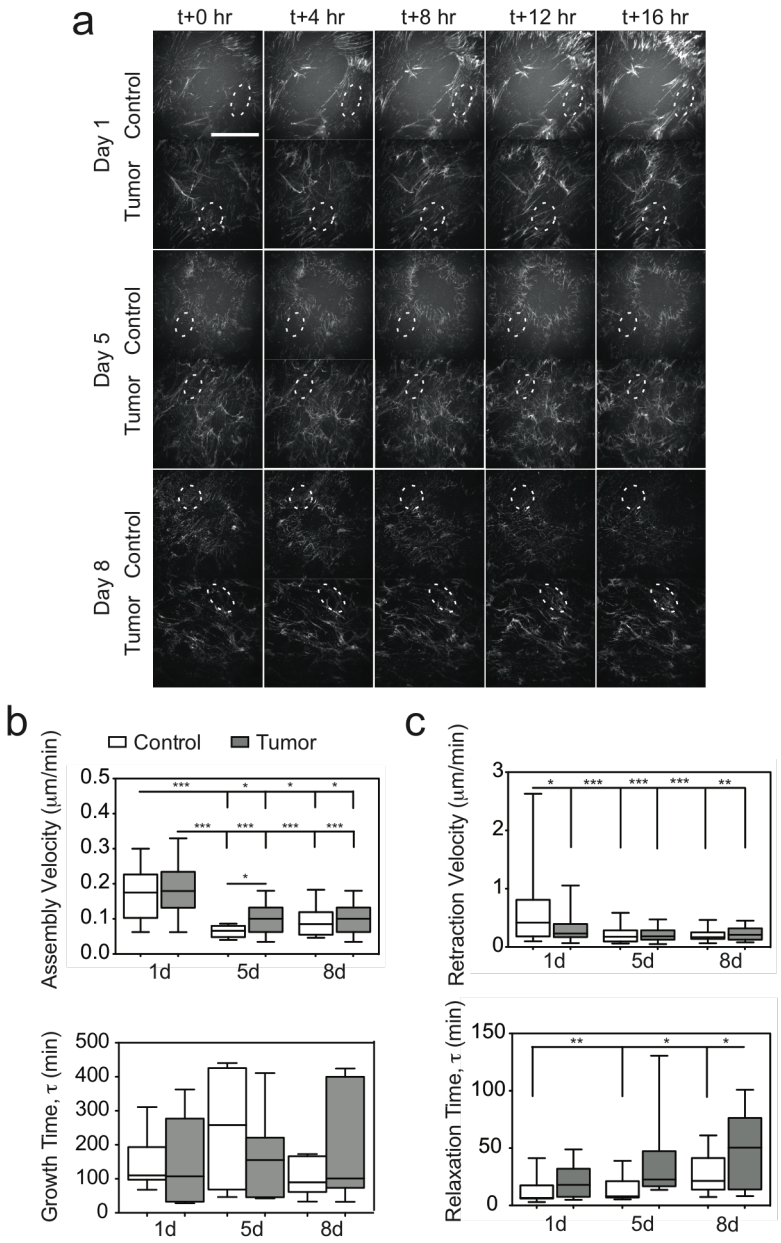


**Figure 3.2. Fiber dynamics.**
a) Time-lapse spinning disk confocal imaging of 488-labeled Fn 16 hr after 1, 5, and 8d timepoints. b) Initial c- and TC-fiber assembly was faster than later timepoint fiber assembly when the ECM was denser and Col I present. Further analysis of Fn growth time by fitting a one phase exponential growth to extract τ (min), revealed no trends between t-Fn and control Fn growth. c) Later Fn fiber retraction rates were slower than that of initial (1d) control Fn fiber retraction rates. Further analysis of Fn relaxation time by fitting a one phase exponential decay to extract τ (min), reveal trends in relaxation time: TC-Fn fibers have longer relaxation times that increased at later timepoints compared with control Fn fiber relaxation times. Scale bar = 50 μm. Mean ± SEM.

*3.5.2. Fiber dynamics*

Throughout ECM evolution, the fibrillar network under dynamic strain and relaxation was undergoing reorganization and remodeling (Fig. 3.2). In agreement with other studies of Fn fiber reorganization,[252] globular Fn was translocated to continue Fn fiber extension or digested, as depicted within the dotted regions of the time-lapse images (Fig. 3.2a). We quantified Fn fiber assembly and retraction velocities to assess individual fiber kinetics. Initial TC-Fn fiber assembly velocity was slightly faster than c-Fn assembly (Fig. 3.2b: Day 1 = 0.19 ± 0.02 μm/min, n = 16 vs. 0.17 ± 0.02 μm/min, n = 19). Both c- and TC-Fn initial fiber assembly velocities were significantly faster than that of later timepoints (Fig 3.2b: c-Fn compared to Day 1 c-Fn: Day 5 = 0.06 ± 0.005 μm/min, n = 12; $p < 0.0001$, Day 8 = 0.1 ± 0.01 μm/min, n = 12; $p < 0.05$; TC-Fn compared to Day 1 TC-Fn: Day 5 = 0.1 ± 0.01 μm/min, n = 14; $p < 0.0001$, Day 8 = 0.1 ± 0.01 μm/min, n = 14). Further analysis of Fn growth time by fitting a one phase exponential growth to extract τ (min), revealed no trends between TC-Fn and c-Fn growth times (Fig. 3.2b: Day 1: 148 min ± 53.8 min, n = 6 vs. 141.9 ± 28.7 min, n = 8, Day 5: 157.9 ± 44.1 min, n = 8 vs. 250.6 ± 95.1 min, n = 4; Day 8: 189.5 ± 70 min, n = 6 vs. 109.1 ± 25.7 min, n = 5). With regards to initial Fn fiber retraction (Day 1 control), all c- and TC-Fn fiber retraction velocity (μm/min) slowed at later timepoints (Fig. 3.2c: (TC-Fn: Day 1 = 0.33 ± 0.05 μm/min, n = 26; $p < 0.05$. Day 5 = 0.21 ± 0.02 μm/min, n = 22; $p < 0.0001$. Day 8 = 0.22 ± 0.03, n = 13; $p < 0.001$; c-Fn: Day 5 = 0.2 ± 0.03 μm/min, n = 24; $p < 0.0001$. Day 8 = 0.21 ± 0.02 μm/min, n = 21; $p < 0.0001$) were slower than that of initial (Day 1) control Fn fiber retraction velocity (Fig. 3.2c: 0.57 ± 0.1 μm/min, n = 30). Subsequent exponential decay analysis of individual Fn fiber relaxation kinetics to assess the viscoelastic properties of individual fibers reveal overall longer relaxation time, τ (min), for TC-Fn fibers than c-Fn fibers (Fig. 3.2c: TC-Fn: 1d = 21.8 ± 4.9

min, n = 11. 5d = 38.9 ± 11.7 min, n = 10. 8d = 45.4 ± 16.8 min, n = 5; c-Fn: 1d = 11.5 ± 3.4 min, n = 11; 5d = 14.3 ± 4.6 min, n = 7; 8d = 26.8 ± 4.7 min, n = 12). Additionally, as the ECM evolved to a complex Fn-Col I network, Fn fibers at later timepoints, especially in the case of TC-ECM, displayed longer relation times. The enhanced viscoelasticity of tumor-associated Fn fibers over time may be due the rapid reorganization of these fibers into a deoxycholate-insoluble form,[101] suggesting an inherent change in the crosslinked molecular configuration of Fn molecules within a fiber[151] that would affect Fn molecule re-assembly into its native globular state.[253] Further, the dense tumor-associated ECM network may more efficiently entrap interstitial fluid, which may also affect individual fiber dynamics.[254-256] Variability in Fn fiber relaxation times may be due to mixed population measurements of Fn fibers at the leading edge of cells versus the rear of the cell[257] or heterogeneous local tension in the network[258]. Also, the increased presence of altered Col I fibers[23,259] in the ECM network may provide noncovalent hindrance;[260] co-localized or not, the denser network of thick ECM fibers, with its own viscoelastic properties[249], may interfere with individual Fn fiber relaxation (entanglement).[261]

*3.5.3. Matrix metalloproteinase contribution to matrix topology*

Rapid stromal remodeling during tumorigenesis, has been attributed to enhanced MMP activity.[242,262] Batimastat, a broad spectrum MMP inhibitor, was used to assess the role of MMPs in TC-ECM remodeling. Immunofluorescence of MMP inhibited (MI/) TC-ECM display different Fn and Col I ECM composition and evolution (Fig. 3.3a) compared with that of TC-ECM in Fig. 3.1a. MI/TC-ECM was composed primarily of a dense and aligned Fn network with thicker fibers (Fig. 3.3b; **Fn** Day 1: 0.92 ± 0.01 μm, n = 732; $p < 0.01$ (c-Fn); $p < 0.0001$ (TC-

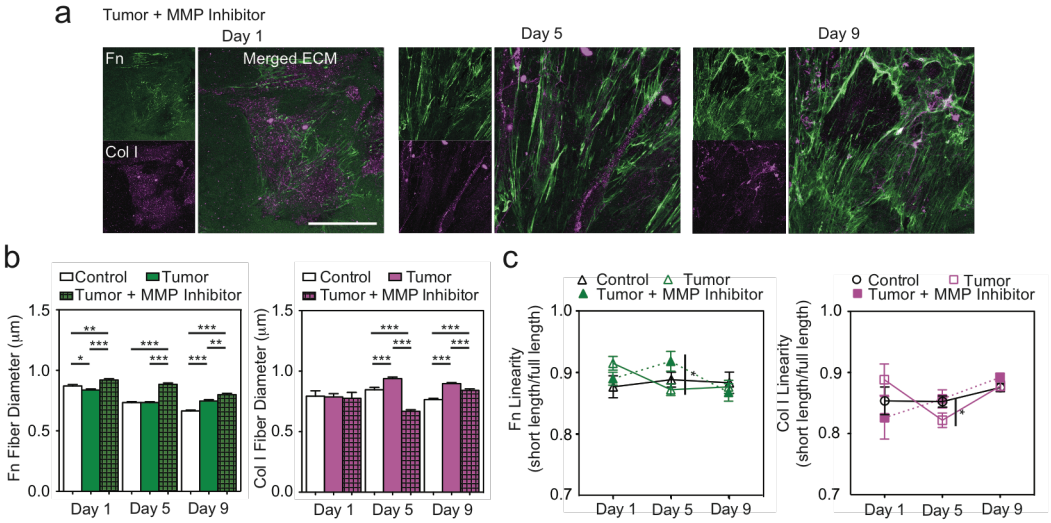


**Figure 3.3. Matrix metalloproteinases contribute to altered evolution of TC-ECM.** a) Immunofluorescence of MI/TC-ECMs reveal few TC-Col I fibers assembled. b) MI/TC-Fn fibers were thicker than c- or TC-Fn fibers. Conversely, MI/TC-Col I fibers were thinner than TC-Col fibers. c) MI/TC-Fn linearity fluctuated with trends similar to that of c-Fn fibers. MI/TC-Col I linearity was initially lower than that of TC-Col I fibers, then increased over time and revealed similar trends to that of c-Col fibers. Scale bar: 50 μm.

Fn), Day 5: 0.88 ± 0.01 μm, n = 811; $p < 0.0001$ (c-Fn & TC-Fn), Day 9: 0.8 ± 0.01 μm, n = 1078; $p < 0.0001$ (c-Fn); $p < 0.01$ (TC-Fn)). These data suggest that when unable to remodel previous ECM networks, TC-cells utilize previously assembled Fn as a framework to continue depositing Fn. These TC-cells perhaps continue depositing Fn in an attempt to create ECM tracks for tumor cell migration[60]. These fibers were under similar strain at Day 1 and 9, but were significantly strained at Day 5 (Fig. 3.3c; **Fn** Day 1: Day 1: 0.89 ± 0.01, n = 94, Day 5: 0.92 ± 0.02, n = 55; $p < 0.05$, Day 9: 0.87 ± 0.01, n = 76). The few MI/TC-Col I fibers deposited were thinner (Fig. 3.3b; **Col I** Day 1: 0.78 ± 0.05 μm, n = 33, Day 5: 0.67 ± 0.01 μm, n = 232; $p < 0.0001$ (c-Fn & TC-Fn), Day 9: 0.84 ± 0.01 μm, n = 383; $p < 0.0001$ (c-Fn); $p < 0.001$ (TC-Fn))). These data suggest that MMP activity is critical for tumor stroma remodeling, as TC-cells are unable to proteolytically degrade and remodel TC-Fn to expose Col I binding sites for downstream TC-Col I deposition. Specifically, MT-MMP1 (MMP 14), a MMP inactivated by

Batimastat, is essential for Fn cleavage[263] and endocytosis,[104] and implicated in collagen turnover during normal tissue homeostasis.[264] These MI/TC-Col I fibers were strained similar to that of c-Col I fibers (Fig. 3.3c; **Col I** Day 1: 0.83 ± 0.03, n = 14, Day 5: 0.86 ± 0.01, n = 90, Day 9: 0.89 ± 0.01, n = 130)). Again, all samples at Day 9 reveal converging linearity, which may be an indication of an ideal individual fiber strain even when inhibited MMP activity suppresses ECM remodeling.

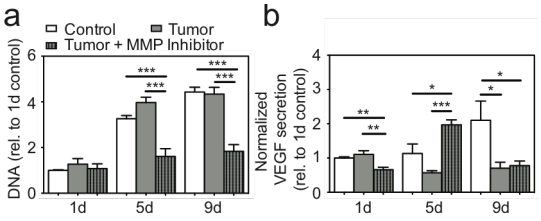


**Figure 3.4. TC-VEGF secretion fluctuates with ECM evolution**
a) At all timepoints, TC-DNA (relative to 1d control) were not significantly different from c-DNA. However, MI/TC-DNA were less than that of TC-DNA. b) Over time, TC-VEGF secretion (normalized to DNA, then Day 1 control) decreased. Initial and late MI/TC-VEGF secretion were low.

*3.5.4. Proangiogenic secretion during matrix evolution*

These inhibition studies reveal the importance of MMPs in remodeling Fn for collagen fibrillogenesis. Furthermore, MMP activity is complex and does not consist only in physical remodeling. MMPs have also been implicated in growth factor bioavailability and activation of vascular endothelial growth factor (VEGF).[265] Next, to understand the effect of these ECMs with different topologies on secretion of proangiogenic factors, VEGF secretion during TC-ECM remodeling was quantified. Altered fiber thickness, strain, and conformation of the TC-ECM may alter cell binding and immobilization/bioavailability of factors such as VEGF. Cell number assessed by DNA quantification, revealed no significant differences between c- and TC-cells (Fig. 3.4a; **DNA** Day 1: 1.27 ± 0.24, n = 6 vs. 1 ± 0.024, n = 6; Day 5: 3.97 ± 0.23, n = 6 vs. 3.26 ± 0.14, n = 6; Day 9: 4.34 ± 0.295, n = 6 vs. 4.43 ± 0.21, n= 5). However, MI/TC-cells measured

less DNA (Fig. 3.4a; **DNA** Day 1: 1.08 ± 0.21, n = 6, Day 5: 1.61 ± 0.34, n = 6; $p < 0.0001$ (TC-ECM & MI/TC-ECM), Day 9: 1.84 ± 0.29, n = 6 vs. 4.34 ± 0.295, n = 6; $p < 0.001$ (TC-ECM & MI/TC-ECM). This decrease is likely due to alterations of Fn as it plays a major role in cell proliferation.[93] Interestingly, TC-VEGF secretion decreased significantly when there are thick Col I fibers present (Fig. 3.4b; **VEGF** Day 1: 1.11 ± 0.11, n = 6 vs. 1 ± 0.035, n = 6, Day 5: 0.57 ± 0.063, n = 6 vs. 1.13 ± 0.28, n = 6, Day 9: 0.70 ± 0.18, n = 6 vs. 2.10 ± 0.56, n = 5; $p < 0.05$). This effect may be due to the immobilization of VEGF to the collagen rich ECM.[5,266,267] Another means by which VEGF secretions decreases could be due to enhanced activity of MMP2, which was previously shown to decrease VEGF secretion[268]. In contrast, initial and late MI/TC-VEGF secretion were low compared to Day 5 (Fig. 3.4b; **VEGF** Day 1: 0.66 ± 0.073, n = 6; $p < 0.01$ (c- & TC-ECM), Day 5: 1.97 ± 0.15, n = 6; $p < 0.05$ (c-ECM); $p < 0.0001$ (TC-ECM)). This change in VEGF secretion suggests that at Day 5, cells are unable to immobilize VEGF to the strained TC-Fn with $\alpha_5\beta_1$ integrins.[31] Interestingly at Day 9, MI/TC-VEGF secretion decreased to levels measured for untreated TC-VEGF secretion, possibly due more VEGF bound to the dense and less strained Fn network (Fig. 3.4b; **VEGF** Day 9: 0.78 ± 0.14, n = 6; $p < 0.05$ (c-ECM)).

### 3.6. Conclusion

Collectively, our findings highlight the effects of breast tumor secreted factors on pre-adipocyte ECM assembly dynamics. Initial thin, strained, and unfolded Fn fibers, more compliant and stretch-sensitive than the subsequent thick Col I fibers deposited during ECM remodeling, conferred altered structure (ligand availability). These alterations in turn, may regulate the bioavailability of VEGF for downstream tumor angiogenesis. The complex and

synergistic interplay of Fn and Col I ECM topology may mediate a dysregulated signaling cascade to facilitate downstream breast tumor invasion into its surrounding stroma.

## 3.7. Supplemental Information

### *3.7.1. SI Figure*

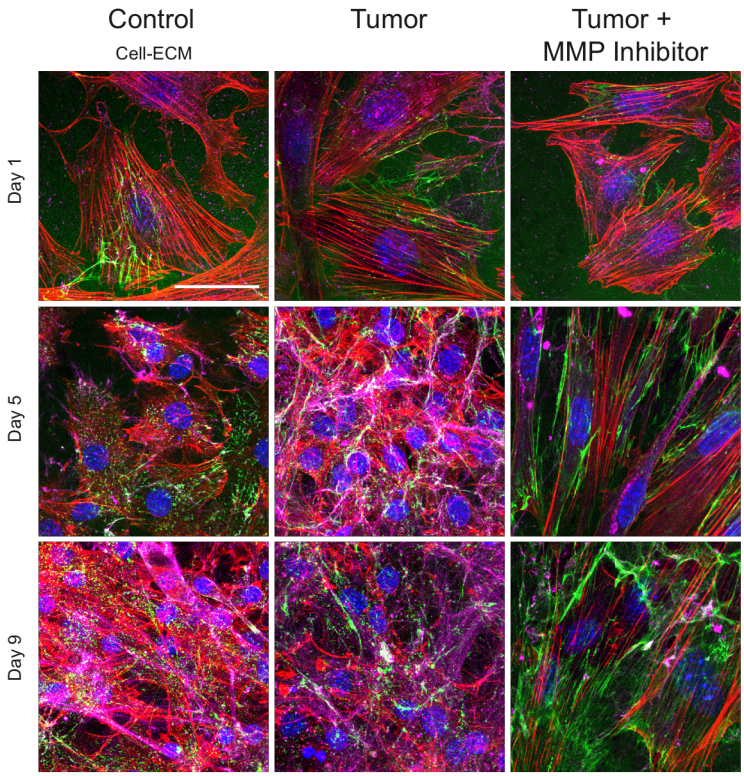


**Figure 3.5. ECM assembly.**
Merged immunostained cell-ECM images of Day 1, 5, 9 control, tumor, and MMP inhibited tumor samples. F-actin (Alexa Fluor 546) and DAPI. Scale bar: 50 μm.

# CHAPTER 4

# NSF CORNELL LEARNING INITIATIVE IN MEDICINE AND BIOENGINEERING

## 4.1. Contributors to: "Development of Inquiry Based Optics Module for Middle School Students"

This details the lesson plans developed as part of an optics module for an 8th grade physical sciences class. During the course of this dissertation work, I developed an understanding of optics through my widespread use of confocal microscopy to obtain FRET and fluorescent images of my samples. Using my past experiences, I developed a module on lights and lenses to not only reach NYS standards in physical sciences, but to show the students how the concepts they learned in this module, applied to current practices by scientists to study global health problems such as breast cancer.

Authors of this manuscript are: Karin Wang, Robert Doran, Shanna Shaked, Shivaun Archer, Claudia Fischbach, and Delphine Gourdon

*Presented at BMES 2013 Annual Meeting*

Acknowledgements: Professor Shivaun Archer and Professor Christopher Schaffer for their guidance of this program. The Cornell Learning Initiative in Medicine and Bioengineering (CLIMB) BME NSF K-12 program funded this work (DGE 0841291). Robert Doran from Newfield Central School and Shanna Shaked of the Education department at Ithaca College

helped develop this curriculum. Assistance was provided by Nevjinder Singhota and Jaimi Doran.

## 4.2. Abstract

*Introduction*

Teaching core concepts to middle school students and maintaining their attention is a daunting task. However, Biomedical Engineering can provide an integrative connection between different disciplines and help students learn about the connections between basic science and health issues. Herein is an inquiry-based optics module designed to provide a better understanding of the properties of lights and lenses, and how they are used in the world around them, especially in biomedical applications. This type of BME-based K-12 curriculum activity provides opportunities for students to experience science, rather than learn an abstract collection of facts.

*Materials and Methods*

The materials for this module are readily accessible from a science class stockroom. Materials: an overhead projector, various prisms, an old cd, spray bottle, convex and concave mirrors, plane mirrors, string, masking tape, beakers, spoons, paper diffraction glasses, lasers, LED photon micro lights of different colors, concave and convex lenses, marbles, spectroscopes, incandescent and compact fluorescent light bulbs and lamps, gas light bulbs and gas bulb power source, flashlights, laptops with lens simulations, portable fluorescent UV light, vials of vegetable oils, fluorescent mineral rocks, tonic water, UV color changing beads, highlighters, magnifying glasses, microscope slides, plastic coverslips, various fibers, strands of human hair, and microscopes.

*Four Day Module*: (i) Day 1 – lecture and handouts on light reflection and refraction, colors of light and pigments, concave and convex mirrors and lenses, and fluorescence and their applications to medicine and BME e.g. microscopy. This was interspersed with demos and YouTube videos; (ii) Day 2 – lab with seven inquiry based optic stations, where students rotated amongst the stations, learning how light refracts with prisms, looking through concave and convex mirrors and increasing understanding with virtual lens simulations, working with light reflection and angles, predicting and observing the sun's spectrum after observing different light bulb spectrums, seeing how different mediums refract light, and examining the fluorescence of objects such as plants and rocks; (iii) Day 3 – short lecture on fluorescent microscopy and completion of lab; (iv) Day 4 – "fun" forensic science inquiry activity to solve the murder of a stuffed owl with lenses and fingerprints found at the crime scene, using a fluorescent blood trail (liquid detergent fluoresces under UV light), hair and fibers found on the body and weapon, and role-playing to interrogate suspects. Though this module was presented in 4 days, each section can be done separately. After the lecture on Day 1, a questionnaire was given out to assess how well the students understood concepts such as focal points, the difference between convex and concave lenses, different energies in the electromagnetic spectrum, fluorescence, lenses in scopes, and their practical applications. The same questionnaire was given out at the end of Day 4 to assess if their understanding of optics had improved. The questionnaire was scored for the purpose of quantitatively evaluating their understanding of optics and paired t-tests were run to test for statistical significance ($p < 0.01$).

*Results and Discussion*

Most students were capable of completing five of the seven stations within the 1.5 periods allotted. All classes were able to correctly identify suspects based on fingerprints, find

the scene of the crime, follow the fluorescent "blood" trail to the hidden body (stuffed owl) and possible weapon (box cutter), and uncover hair and fiber found on the body and weapon. The students also accurately identified the murderer as the guinea pig (the teacher's pet). 70% of the four 8th grade physical science classes were able to complete both the pre- and post-questionnaire. The average score on the assessment questionnaires increased 35% after the students took part in the lab and activity (Fig 4.1).

*Conclusions*

Inquiry-based labs and activities are effective methods by which students are able to retain and apply theoretical concepts taught in lectures to every day life, as well as increase students interest in STEM careers. These students significantly improved their understanding of essential optics concepts and its application to medicine and engineering.

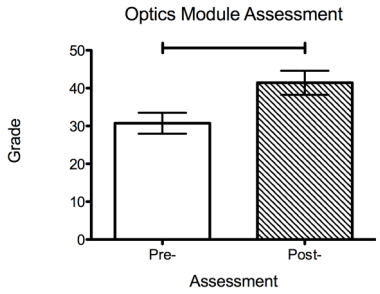


**Figure 4.1. Assessment**
Four 8th grade physical science classes (n = 60) were given the same assessment questionnaire before and after the lab and activity portion of the optics module. 70% of the students completed both pre- and postquestionnaires. Students demonstrated significant ($p<0.01$) improvement in understanding fundamental optics concepts. (Mean ± SEM)

### 4.3. Optics Curriculum with Robert Doran

*Subject*: Optics and Their Biomedical Applications

*Level*: 8th (Middle School)

*Standards*:

Standard 1: Analysis, Inquiry, and Design (Scientific Inquiry)

- S1.1 Formulate questions independently with the aid of reference appropriate for guiding the search for explanations of everyday observations.
- S1.2 Construct explanations independently for natural phenomena, especially by proposing preliminary visual models of phenomena.
- S1.3 Represent, present, and defend their proposed explanations of everyday observations so that they can be understood and assessed by others.
- S1.4 Seek to clarify, to assess critically, and to reconcile with their own thinking the ideas presented by others, including peers, teachers, authors, and scientists.
- S3.1 Design charts, tables, graphs, and other representations of observations in conventional and creative ways to help them address their research question or hypothesis.
- 3.2 Interpret the organized data to answer the research question or hypothesis and to gain insight into the problem.

Standard 4: Process Skills

- General skills (1,2,3,4,7,8,9)

Standard 4: The Living Environment

- 1.1a Living things are composed of cells. Cells provide structure and carry on major functions to sustain life. Cells are usually microscopic in size.

Standard 4: The Physical Setting

- 4.1d Different forms of energy include heat, light, electrical, mechanical, sound, nuclear, and chemical. Energy is transformed in many ways.

- 4.4a Different forms of electromagnetic energy have different wavelengths. Some examples of electromagnetic energy are microwaves, infrared light, visible light, ultraviolet light, X-rays, and gamma rays.
- 4.4b Light passes through some materials, sometimes refracting in the process. Materials absorb and reflect light, and may transmit light. To see an object, light from that object, emitted by or reflected from it, must enter the eye.
- 4.4d Electrical energy can be produced from a variety of energy sources and can be transformed into almost any other form of energy.

Standard 6: Interconnectedness: Connections

- 3.1 Cite examples of how different aspects of natural and designed systems change at different rates with changes in scale.

Standard 7: Interdisciplinary Problem Solving

- 2.1 Students participate in an extended, culminating mathematics, science, and technology project. The project would require students to: working effectively, gathering and processing information, generating and analyzing ideas, common themes, realizing ideas, presenting results

*Schedule*: 4 periods (40 – 50 minutes each)

*Objective:* Herein is an inquiry-based optics module designed to provide a better understanding of the properties of lights and lenses, and how they are used in the world around them, especially in biomedical applications.

*Students will*: complete a 1.5 period long lab consisting of hands-on activities to understand how light, lenses, and mirrors work

- Learn how light refracts with prisms

- Understand and learn how to use concave and convex mirrors
- Increase their understanding of lenses with virtual lens simulations
- Work with light reflection and angles under different conditions
- Predict and observe the sun's spectrum after observing different light bulb spectrums
- Observe and understand how different mediums refract light
- Examine the fluorescence of objects of objects such as plants and rocks

*If time permits*: Solve a forensic crime scene with their knowledge of microscopy and fluorescence

*Vocabulary*:

- Reflection
- Refraction
- Electromagnectic Spectrum
- Light
- Pigment
- Concave
- Convex
- Lenses
- Microscopy
- Focal Point
- Fluorescence

*Materials:*

- Overhead projector
- Various prisms
- Old cd
- Spray bottle
- Convex and concave mirrors
- Plane mirrors
- String
- Masking tape
- Beakers
- Spoons
- Paper diffraction glasses
- Lasers

    - LED photon micro lights of different colors
    - Concave and convex lenses
    - Marbles
    - Spectroscopes
- Incandescent and compact fluorescent light bulbs and lamps
- Gas light bulbs and gas bulb power source
- Flashlights
- Laptops with lens simulations
- Portable fluorescent UV light
- Vials of vegetable oils
- Fluorescent mineral rocks
- Tonic water
- UV color changing beads
- Highlighters
- Magnifying glasses
- Microscope slides
- Plastic coverslips
- Various fibers from clothing
- Strands of human hair
- Microscopes

*Science Content for the Teacher*:

* This module should follow lessons on waves and sound to better understand how energy (electromagnetic vibrations) travels through various mediums, as this module focuses on how our understanding of the properties of visible light allow us to manipulate said properties via lenses and mirrors.

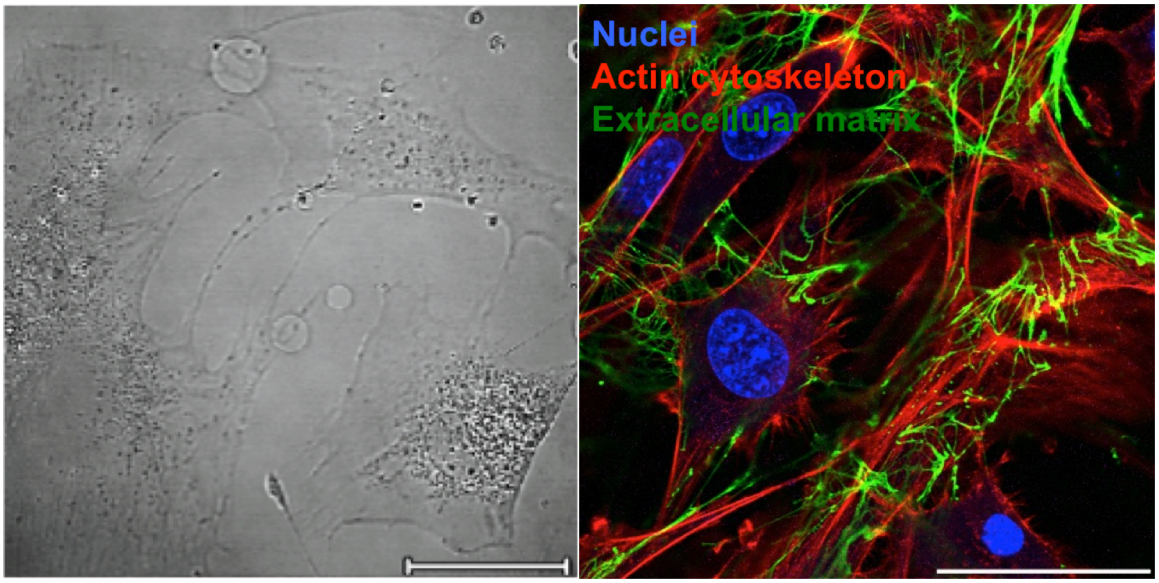


**Figure 4.2. Comparison of regular brightfield image and fluorescent image**
Regular microscopes are able to detect cells and cellular components (left), however, this is nonspecific and does not provide much information. Fluorophores can be attached to specific components (right) to provide more information of biological processes.

Microscopes are very important tools for scientists. Scientists have utilized their understanding of the properties of light, lenses, and mirrors to magnify and study micro-scale samples. Furthermore, through fluorescence microscopy, we are able to detect and observe biological processes within cells (e.g.: nucleus and actin cytoskeleton) and outside cells (extracellular matrix components) with great precision. Specimens are immunostained (fluorophores chemically attached to a specific target) and excited with lasers to view what cannot be observed with regular white light (Fig 4.2). Fluorescence is also very important for crime scene investigations as many biological fluids fluoresce under ultraviolet light. Laundry detergents can be used for fun, hands-on classroom "crime scene" investigations at the end of this optics and fluorescence module. Detergents commonly include brighteners for clothes to appear cleaner, and these brightening agents absorb ultraviolet energy and re-emit in the visible spectrum.

*Preparation:*

- Before beginning this module, we had the students fill out a pre-assessment questionnaire to the best of their ability, and gave the same questionnaire at the completion of this module.
- This module supplemented an existing optics curriculum by Roberto Doran, an 8th grade physical sciences teacher at Newfield Central, NY
    - Introduction to light interspersed with demonstrations
        - Discussed difference between transparent, translucence, and opaque; colors of light vs pigments; regular and diffuse reflection; focal point (real and virtual image)
    - Introduction to lenses and mirrors via light box, lenses, mirrors, and prisms on projector (Scientrific: HL2060-001)
        - Supplemented with brief microscopy and fluorescence lecture

*Classroom Procedure:*

**Optics Lab (1 – 1.5 periods, depending on how rapidly students complete activities)**

**Engage (5 min)**

Students were given lab sheets (Supporting File: Optics Lab) and directions for each lab activity briefly explained.

**Explore (30 – 40 min)**

Students were allowed to work through the lab activities (*in any order), with encouragement and clarification given to struggling students.

**Explain (5 min)**

Students were engaged in a discussion about the properties of light they studied and how these properties of light are used in real life applications such as biomedical research and forensic science.

*Assessment:*

A pre-assessment (Supplemental: Pre and post-assessment Questionnaire) was given to student to understand how well students understood certain concepts.

| | Engage | Explore | Explain | Expand/Synthesis |
|---|---|---|---|---|
| 1 | Student demonstrated interest in lab activities and discussed possible outcomes with lab partner | Student demonstrated interest in completion of lab activities and engaged partner in completing activities | Student was able to accurately explain what was observed during lab activity and hypothesize why said property was observed (e.g.: properties of light, lenses, and mirrors) | Student was interested in how observations during lab activities also occur in every day applications and asked clarifying questions for possible applications not brought up during class discussions |
| 2 | Student demonstrated interest in lab activities | Student demonstrated interest in completion of lab activities | Student was able to accurately explain what was observed during lab activity during discussion | Student understood that properties of light, lenses, and mirrors observed in lab activities are used in everyday applications |
| 3 | Student may not completely understand directions for lab activities; and has little interest in objective of lab | Student may have difficulty completing lab activity and may write down incorrect observations (based on their understanding of lab activity directions) | Student may participate in discussion but with little to no interest | Student may participate in discussion, but with little to no understanding that the properties of light, lenses, and mirrors observed are translatable to everyday application |
| 4 | Student does not understand directions for lab activities and has no interest in objective of lab | Student does not complete lab activities and put little to no effort into writing down observations | Student does not participate in discussion | Student does not participate in discussion |

**Table 1.1. Rubric**
This rubric can be used to assess students during each part of the activity. The term "expectations" here refers to the content, process and attitudinal goals for this activity. Evidence for understanding may be in the form of oral as well as written communication, both with the teacher as well as observed communication with other students.

*Extension Activities*: *If time permits

**Crime Scene Investigation (1 period)**

**Engage (5 min)**

Students were told that a crime may have been committed and that a victim (e.g.: stuffed toy) is missing. They were provided with an activity sheet with possible suspects (e.g.: classmates) and fingerprints "found" where the missing victim was last seen.

**Explore Part I (10 min)**

Students were provided magnifying lenses and given time to narrow down the pool of suspects.

**Explore Part II (20 min)**

Students were provided with portable UV lights and separated into two groups to find the victim and a possible weapon by following the blood trail (e.g.: detergent).

*Supplemental Information***:**

With the introduction of technology into the classroom, there are virtual labs and activities that can be completed by students on a laptop or computer. Within the Supplemental: Optics Lab sheet are links to certain lab activities that allow students to interactively observe properties of light, lenses, and mirrors. Additional resources are available online, one website with interactive java tutorials is the following: http://micro.magnet.fsu.edu/optics/tutorials/index.html.

*Safety:*

1. For activities requiring a light source, students should be cautioned that they should not look directly at the sun.

2. For activities requiring light bulbs, students should be cautioned not to touch the hot bulbs

### 4.4. Contributors to: "Bringing BME Skills into the Classroom: Development of an Inquiry Based Module for Earth Science Students"

This details the lesson plans developed as part of a rocks and minerals module for a 9th grade earth science class. During the course of this dissertation work, I used microscopy to aid in the collection of data. Using my past experiences, I developed a module on using microscopes and thin sections of rocks to not only reach NYS standards in earth science, but to show the students how the brainstorming and data collection/analysis they learned in this module, were used by scientists to study and communicate their findings.

Authors of this manuscript are: Karin Wang, Jennifer Kelly, Shivaun Archer, Claudia Fischbach, and D. Gourdon

*Published in Marcellus Central School District Project*

*Studies Highlighting the Action Research of Educators (SHARE) Monograph (2014).*

Acknowledgements: Professor Shivaun Archer and Professor Christopher Schaffer for their guidance of this program. The Cornell Learning Initiative in Medicine and Bioengineering (CLIMB) BME NSF K-12 program funded this work (DGE 0841291). Jennifer Kelly at Marcellus Central School helped develop this curriculum. Assistance was provided by Nevjinder Singhota.

## 4.5. Abstract

*Introduction*

Current 9th grade students lack certain scientific and technical skills, as it is not required in the State Regents exam. However, core skills utilized by Biomedical Engineers can be introduced, to enhance interest in science, technology, engineering, and medicine (STEM) fields outside of the usual Biology, Chemistry, and Physics classes. Herein is a module in which Earth Science students are able to develop their own lab to characterize and identify thin sections of rocks, learn how to use Excel to compile and analyze data, and use PowerPoint to create posters for a poster symposium. This K-12 curriculum activity provides opportunities for students to experience earth science as scientists, rather than learn an abstract collection of facts, and cultivate strong interest in STEM fields.

*Materials and Methods*

Some materials were obtained from a science class stockroom, others bought from Ward's Science. Materials: Microscopes; clear flexible rulers; metamorphic (slate, hornfels), sedimentary (conglomerate, rock gypsum), and igneous (granite, gabbro) rocks and thin sections; and computer lab with Excel, PowerPoint, and printers. This four day module, comprised of six 40 minute periods, follows a week of an introduction to minerals and a week of an introduction to rocks. Four Day Module: (i) Day 1 – brief lecture to guide students (divided into groups of four or five) in brainstorming on how to develop their lab, "To characterize and identify the thin section of their rock." The students were introduced to the difference between qualitative and quantitative data, and how rock thin sections appear under the microscope. After the students developed a detailed protocol, they worked together to observe and collect data from their thin sections; (ii) Day 2 – The students finished collecting data from their thin sections and a hand-

held rock sample (later provided), and drafted a conclusion as to the type and the name of their sample. Afterwards, students moved to the computer lab for an introduction to Excel and PowerPoint. The students were led through how to input data such as various crystal grain sizes, how to calculate the average grain sizes, how to create a chart, and how to create posters. Afterwards, the students were given time to create their charts and begin developing their 8x11 posters; (iii) Day 3 – The students finished creating their posters; (iv) Day 4 – For the poster symposium, the students were given rubric sheets to grade themselves and other groups (rotating every few minutes). Poster grades were comprised of an average of student-provided points, the teacher's points, and my points. Before the lecture on Day 1, a pre-assessment quiz (which students were told, did not count towards a class grade) was given out to ascertain how well the students understood how percent of mineral content of an igneous rock would lead to its identification, how igneous rocks form, how the foliated arrangement of mineral content within a metamorphic rock could assist in its identification, what was contact metamorphism and how to identify the metamorphic rock formed, the importance of grain size in characterizing sedimentary rocks, and that organic materials can be embedded within sedimentary rocks. The same quiz was given as a post-assessment quiz, after the poster symposium on Day 4. The quizzes were graded and paired t-tests were run to assess for statistical significance ($p < 0.01$). Students were also asked what one positive experience was from the module.

*Results and Discussion*

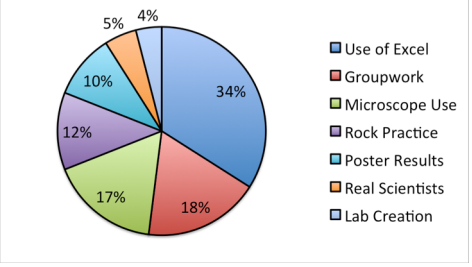


**Figure 4.3. Experience**
Students were asked what they most enjoyed from the module

The students enjoyed this module (Fig 4.3), due to learning how to use excel, working in groups, using microscopes, identifying rocks, creating posters with new ways of showing data, being a scientist, and creating their own lab. The average poster grade was 81%. And there was no significant difference between the pre- and post-assessment quiz grades – though there was a 2% increase (Fig 4.4). This may have been due to students knowing that the assessment quizzes would not count towards their grades and not putting in the effort.

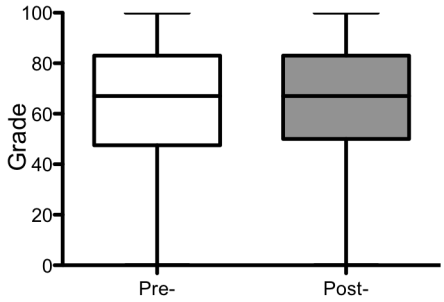


**Figure 4.4. Assessment**
Students completed pre-and post-assessments to determine their understanding of the different types of rocks

*Conclusions*

Inquiry-based activities are effective methods by which students are able to retain and apply theoretical concepts taught in lectures. These students were engaged and improved their understanding of essential mineral and rock concepts. Furthermore, this module teaches

scientific and technical skills, and shows the students that these skills are essential to scientists such as Geologists or Biomedical Engineers.

### 4.6. Geology Curriculum with Jennifer Kelly

*Subject*: Earth Science

*Level*: 9th grade

*Standards*:

Standard 1: Analysis, Inquiry, and Design (Scientific Inquiry)

Students will use mathematical analysis, scientific inquiry, and engineering design, as appropriate, to pose questions, seek answers, and develop solutions.

- Mathematical Analysis – Key Idea 2: Deductive and inductive reasoning are used to reach mathematical conclusions.
- Scientific Inquiry – Key Idea 1: The central purpose of scientific inquiry is to develop explanations of natural phenomena in a continuing, creative process
- Scientific Inquiry – Key Idea 2: Beyond the use of reasoning and consensus, scientific inquiry involves the testing of proposed explanations involving the use of conventional techniques and procedures and usually requiring considerable ingenuity.
- Scientific Inquiry – Key Idea 3: The observations made while testing proposed explanations, when analyzed using conventional and invented methods, provide new insights into phenomena.
- Engineering Design – Key Idea 1: Engineering design is an iterative process involving modeling and optimization (finding the best solution within given constraints); this process is used to develop technological solutions to problems within given constraints

Standard 2: Information Systems

Students will access, generate, process, and transfer information, using appropriate technologies.

- Key Idea 1: Information technology is used to retrieve, process, and communicate information as a tool to enhance learning.

Standard 4: Science Content

Students will understand and apply scientific concepts, principles, and theories pertaining to the physical setting and living environment and recognize the historical development of ideas in science.

- Key Idea 2: Many of the phenomena that we observe on Earth involve interactions among components of air, water, and land.
    - 2.1m Many processes of the rock cycle are consequences of plate dynamics. These include the production of magma (and subsequent igneous rock formation and contact metamorphism) at both subduction and rifting regions, regional metamorphism within subduction zones, and the creation of major depositional basins through down-warping of the crust.
    - 2.1w Sediments of inorganic and organic origin often accumulate in depositional environments. Sedimentary rocks form when sediments are compacted and/or cemented after burial or as the result of chemical precipitation from seawater.
- Key Idea 3: Matter is made up of particles whose properties determine the observable characteristics of matter and its reactivity.
    - 3.1c Rocks are usually composed of one or more minerals.
        - Rocks are classified by their origin, mineral content, and texture.

- Conditions that existed when a rock formed can be inferred from the rock's mineral content and texture.
- The properties of rocks determine how they are used and also influence land usage by humans.

Standard 6: Interconnectedness: Connections

Students will understand the relationships and common themes that connect mathematics, science, and technology and apply the themes to these and other areas of learning.

- Models – Key Idea 2: Models are simplified representations of objects, structures, or systems used in analysis, explanation, interpretation, or design.
- Magnitude and Scale – Key Idea 3: The grouping of magnitudes of size, time, frequency, and pressures or other units of measurement into a series of relative order provides a useful way to deal with the immense range and the changes in scale that affect the behavior and design of systems.

Standard 7: Interdisciplinary Problem Solving

Students will apply the knowledge and thinking skills of mathematics, science, and technology to address real-life problems and make informed decisions.

- Connections – Key Idea 1: Students will apply the knowledge and thinking skills of mathematics, science, and technology to address real-life problems and make informed decisions.
- Strategies: Solving interdisciplinary problems involves a variety of skills and strategies, including effective work habits; gathering and processing information; generating and analyzing ideas; realizing ideas; making connections among the common themes of mathematics, science, and technology; and presenting results.

*Schedule*: 5 periods (40 minutes)

*Objective*: Characterize and identify thin sections of rocks by utilizing core technical skills

After 2 weeks of instruction on rocks and minerals, students will:

- Develop own lab
- Use microscopes to view unknown thin section sample
- Collect qualitative (e.g.: color) and quantitative (e.g.: grain size) data
- Compile and analyze data in Excel
- Create group posters in PowerPoint for poster symposium

*Vocabulary*:

- Igneous
- Sedimentary
- Metamorphic
- Qualitative Data
- Quantitative Data
- Mineral Content
- Grain Size
- Foliation

*Materials:* For Group of 4-5

- Earth Science Reference Tables booklet
- Thin sections (Ward's Science)
    1. 2 igneous
        - ♦ granite
        - ♦ gabbro
    2. 2 sedimentary
        - ♦ conglomerate
        - ♦ rock gypsum (not a good choice, perhaps calcite would have been better)

3. 2 metamorphic
    - hornfels (not a good choice, perhaps talc would have been better)
    - slate

- Rock specimens (Ward's Science)
    1. 2 igneous
        - granite
        - gabbro
    2. 2 sedimentary
        - conglomerate
        - rock gypsum
    3. 2 metamorphic
        - hornfels
        - slate
- Microscope
- Clear flexible rulers
- Computer Lab with Excel and PowerPoint, and color printers

* Note: in the June 2014 Earth Science Regents, students had to identify the name of a rock based on a microscopic image of a thin section

*Science Content for the Teacher*:

* This module should follow lessons on rocks and minerals to better understand how geologists are able to characterize and identify unknown samples

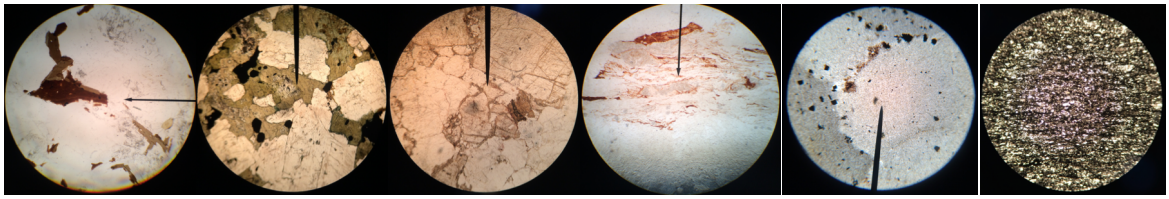

**Figure 4.5. Brightfield microscope view of thin sections**
(L→R) Granite, Gabbro, Conglomerate, Gypsum, Hornfels, Slate

Microscopes, a tool to magnify objects too small to see by eye, are very important in a variety of fields such as Earth Science and Biomedical Engineering. In the case of Earth Science, geologists or more specifically petrologists utilize microscopes (among other tools) to study unknown rock and mineral samples in the laboratory. Petrologists commonly utilize petrographic (polarized) microscopes to assess for properties such as birefringence and pleochroism; most crystalline materials and minerals alter polarizing light directions. Light sources are normally un-polarized, meaning electromagnetic wavelengths of light travel in all directions. However, when these electromagnetic wavelengths of light pass through a polarizing filter, only permitted wavelengths of light pass through – becoming polarized light. When polarized light passes through a rock sample that has birefringence properties, the polarized wavelengths of light split and travel through the sample at different speeds, resulting in different refractive indices. As another example, when polarized light passes through a rock sample that has pleochroism, the absorption of polarized wavelengths of light changes when rotated; simply, the colors vary during rotation. However due to availability issues, this lab was simplified to utilize only observations made from brightfield microscopes to characterize and identify igneous, sedimentary, and metamorphic rocks.

*Preparation*:

- Before beginning this module, we had the students fill out a pre-assessment questionnaire to the best of their ability, and gave the same questionnaire at the completion of this module. Questions were taken from previous regents exams.
- This module supplemented an existing rocks and minerals curriculum by Jennifer Kelly, a 9th grade earth science teacher at Marcellus Central School, NY
    - Introduction to developing a lab procedure
        - Students were guided through a brainstorming session
        - Introduced to the difference between qualitative and quantitative data
        - Introduced to how thin sections of rocks appear under the microscope
    - Introduction to Excel and PowerPoint
        - Students were guided through how to input data, how to create and label charts, and how to create scientific posters through existing templates

*Classroom Procedure*:

**Part 1: Lab Development**

**Engage (Time: 0.5 period)**

Students started off completing a pre-assessment of their current knowledge on rocks and minerals. They were then given blank lab sheets and guided through brainstorming on how to develop a lab to solve the problem provided: to characterize, identify the rock type and name of the thin section. Students were introduced to different types of data: qualitative and quantitative, and also how different rock thin sections appear under the microscope.

**Explore (Time: 1 periods)**

Groups of students worked together to develop a detailed procedure (based on lab materials provided at their desks), to observe their unknown thin section, and to collect both qualitative and quantitative data from the unknown thin sections and rock specimen (provided at the end). Guidance was given to groups to aid in collecting of data and in discussing how the data could lead to identifying the type of rock in the thin section, then the name of the rock. *Groups with rock gypsum and hornfels required a bit more guidance and earlier introduction of rock specimens to use alongside of the rock thin sections.

**Explain (Time: 0.5 period)**

Students were given time to draft a conclusion to the problem they were solving. More guidance was given to struggling groups or groups with rock gypsum and hornfels, which were more difficult to correctly characterize and identify.

**Part 2: Poster Symposium**

**Engage (Time: 0.5 period)**

After all groups were done collecting their data and had drafted a conclusion to their lab, they moved into the computer lab for an introduction to Excel and PowerPoint. The students were led through how to input data such as: various crystal grain sizes, how to calculate the average grain sizes, how to create a labeled chart, and how to create scientific posters.

**Explore (Time: 1.5 periods)**

Groups of students were given time to create charts and their scientific posters (8x11 inches).

**Expand (Time: 0.75 period)**

The groups of students set up a site in the classroom for their scientific posters, alongside microscopes with their thin sections and rock samples. Then they rotated (every few minutes) through the classroom and viewed every thin section, rock sample, and scientific poster. They were also given rubric sheets to grade themselves and other groups. Lab grades were comprised of the average of student provided points added to the Marcellus teacher's points and the Cornell teaching fellow's points.

**Feedback (Time: 0.25 period)**

Students completed a post-assessment of their understanding of rocks and minerals. And also answered the question: what did you find most useful or enjoyable during this activity?

*Assessment*:

Pre- and post-assessments were given to student to understand how well students understood how to characterize and identify igneous, sedimentary, and metamorphic rocks.

*Extension Activities*:

The computer and poster symposium sections of the curriculum were extensional and can be excluded.

*Supplemental Information*:

Polarizing microscopes can also be used in this module, students can collect crystal structure or mineral data via birefringence or pleochroism.

Furthermore, for classrooms without access to microscopes but have access to computers, there is a website, Virtual Microscopes, that has interactive microscope images of thin sections: http://www.virtualmicroscope.org/content/uk-virtual-microscope

| | Engage | Explore | Explain | Expand/Synthesis |
|---|---|---|---|---|
| 1 | Student demonstrated interest in developing their lab activities and scientific posters, while engaging lab partners in discussions on how to collect/show their data | Student enthusiastically developed a detailed lab protocol, collected as much data as possible, and created a comprehensive scientific poster while engaging lab partners | Student was able to accurately determine the type and name of their unknown sample based on the qualitative and quantitative data collected, and present their findings coherently via a scientific poster | Student was interested in what thin sections other groups were observing and how well/accurately other groups determined the type and name of their unknown samples. |
| 2 | Student demonstrated interest in lab activities | Student demonstrated interest in completion of lab activities | Student was able to accurately determine the type and name of their sample, and able to create a poster | Student observed other unknown thin section and rock samples. |
| 3 | Student may not have developed a detailed lab protocol and may not have interest in the objective of lab | Student may have difficulty completing lab activity and may write down incorrect observations | Student may not have correctly determined the type and name of their sample, and may not have created a completed poster | Student may participate in the poster symposium, but with little to no interest other unknown samples |
| 4 | Student does not understand directions for developing a lab protocol and has no interest in objective of lab | Student does not complete lab activities and put little to no effort into writing down observations | Student does not participate in creating a poster | Student does not participate in the poster symposium |

**Table 1.2. Rubric**

The rubric can be used to assess students during each part of the activity. The term "expectations" here refers to the content, process and attitudinal goals for this activity. Evidence for understanding may be in the form of oral as well as written communication, both with the teacher as well as observed communication with other students.

# CHAPTER 5

# CONCLUSIONS

## *5.1. Summary and Limitations*

The work presented herein investigated the paracrine interactions of aggressive breast cancer cells with preadipocytes to model the breast tumor stroma. Understanding how stromal ECM changes during tumorigenesis is critical, as this altered network may provide breast cancer cells a pathway out of the stroma into surrounding organs to metastasize at distant organs. Furthermore, this altered ECM may also assist endothelial cell invasion into the tumor to develop leaky vasculature to transport nutrients in and waste out for tumor growth. This work studied early changes in stromal ECM and how these changes propagated over time to promote tumorigenesis.

Preadipocytes conditioned with tumor factors deposit an initially stiff and unfolded Fn matrix. This dysregulated ECM mediated an integrin switch of newly bound cells to enhance pro-angiogenic signaling. Assessing the evolution of the ECM assembled and remodeled by tumor-conditioned preadipocytes revealed dynamic structural changes in both Fn and Col I. Throughout this MMP-mediated remodeling, initially thin, strained, and unfolded tumor-conditioned Fn fiber topology subtly changed. The altered mechanobiological signaling of Fn likely altered cell binding, growth factor immobilization, and Col I fibrillogenesis to rapidly give rise to a dense, unfolded Fn-Col I ECM that may be conducive for breast tumor growth and invasion into the surrounding stroma. These studies demonstrate the importance of understanding the materials properties of tumor-conditioned ECM and how changes in these properties alter cellular behavior. These studies could aid in understanding which materials properties of the

ECM should be targeted to mitigate tumorigenesis, for example, future work could work towards preventing cells from assembling an unfolded Fn matrix which would prevent cells from switching integrins to bind.

Finally, as with all studies there are limitations to what can be investigated. This work was a simplified model of stromal ECM during tumorigenesis. The breast stroma is composed of a variety of cells and breast cancer cells recruit multiple cell types to facilitate tumor survival and metastasis. Additionally, these studies comprised immortalized cell lines during *in vitro studies*. While immortalized cell lines are useful to grow and study cells indefinitely, these cells have undergone mutations (naturally or induced) to escape cell senescence and therefore may not be physiologically correct cell models. Also, these studies were carried out in 2D substrates (glass/plastic). Cells are known to behave differently on 2D versus 3D substrates, and to respond substrates of different stiffness. A major premise of these studies was to exogenously deliver Fn into the medium for cell uptake, which would be akin to circulating plasma Fn, however, plasma and cellular Fn are known to play different roles during wound healing and most likely also during breast tumorigenesis. Also, the kinetic studies of Fn-Col I included inhibiting a broad spectrum of MMP without characterizing the kinetics and activity of each individual MMP; some MMPs, such as MMP2 and MMP9 have contrasting effects on VEGF secretion. Furthermore, although these studies were at different length scales, more work could be done at the molecular and single fiber level to understand how Fn structure regulates its' mechanobiology to modulate Fn interactions with cells, growth factors, and ECM components. These limitations can be addressed during future studies, some of which are described below.

### *5.2. Future Directions*

*5.2.1. Primary cell and co-culture with other cell types*

This dissertation assessed how 3T3-L1 preadipocytes assembled and remodeled an altered ECM. Future work should involve primary fibroblasts from mice mammary tissue or from patients that are undergoing tumor excision surgery. Additionally, co-culture studies assessing ECM deposition and remodeling should be performed. Example co-culture combinations from cells obtained from mammary tissue, may be breast cancer cells with fibroblasts, tumor-conditioned fibroblasts with endothelial cells, tumor-conditioned fibroblasts with immune cells, and endothelial and immune cells in tumor-conditioned media. These different studies would provide insight to how different cell types synergistically alter ECM deposition and remodeling.

5.2.2. *Downstream ECM interactions*

The techniques and experimental setups described in this work to characterize the structural changes in tumor stroma ECM may further utilized to investigate downstream cell-, growth factor-, or ECM fragment-ECM interactions during tumor invasion and tumor angiogenesis. Before obtaining decellularized tumor-conditioned ECM, specific MMP activity and kinetics should be characterized so as to inhibit particular MMP activity at specific timepoints in an attempt to restore normal ECM materials properties. These decellularized ECM and those assembled by cells treated with or without Batimastat, should be seeded with an aggressive breast cancer cell line such as MDA-MB-231 cells would provide insight to 'optimal' cancer cell-ECM binding dynamics and remodeling kinetics for metastasis. This study could be modified to include FRET-labeled Fn in the decellularized tumor-conditioned ECM to assess changes in ECM conformation during cell binding and migration. If these cells can be transfected to fluorescently label integrins with different fluorophores from the FRET-labeled

Fn, it would be possible to co-localize the dynamics of specific integrin binding to different conformations of Fn. Furthermore, the aforementioned studies may be modified to utilize endothelial cells to quantify eventual angiogenic tube formation/sprouting. Fluorescent labeling of growth factors such as VEGF introduced to the decellularized ECM would provide insight to VEGF-ECM interactions by assessing the co-localization of bound VEGF with the conformation and topology of the ECM network. The addition of endothelial cells to this study would reveal how Fn materials properties and corresponding VEGF binding regulate endothelial cell behavior to form vascular tubes. Also, delivering fluorescently labeled ECM fragments (such as Fn, Col I, heparan sulfate), could provide insight to how Fn conformation affects different ECM component binding kinetics and if there is a corresponding conformational change. Additional experiments could be run with only active MMPs introduced to these decellularized ECM to assess if the ECM is capable of being remodeled without direction by cells, or if MMP activity must work in synergy with cells to remodel the ECM for tumor progression. Lastly, active MMPs should also be introduced to decellularized ECM with bound growth factor or ECM fragments to assess the optimal conditions under which MMPs assist in their bioavailability for tumor progression.

*5.2.3. Moving to 3D platforms*

The studies described here utilize immortalized cell lines and 2D platforms. A continuation of this work into more physiologically and clinically relevant platforms may be obtaining margins of breast stromal tissue of metastatic patients or mice to decellularize and use primary breast cancer and endothelial cells in adhesion and migration studies. Another method by which to translate this work would be to move the studies into 3D gels with varying stiffness (comprising Fn and Col I). Fluorescently labeled cancer cells embedded within the gel and

fluorescently labeled fibroblasts and endothelial cells on the gel would provide insight into the complex dynamics of recruited fibroblasts remodeling the gel and endothelial cells migrating into the gel.

*5.2.4. Types of Fn*

These studies involved exogenous delivery of Fn as a model of plasma Fn in circulation. Future studies should transfect primary cell lines to secrete fluorescent Fn to understand how cellular Fn contributes to the materials properties measured in this work. Additional studies may be carried out to assess the dynamics of cellular and/or plasma (exogenously delivered Fn labeled with another fluorophore). And if possible, also transfect the same primary cell lines to also secrete fluorescent Col I to evaluate the dynamics of Fn and Col I during ECM deposition and Fn-Col I interactions. Finally, as summarized in the introduction, alternate splice variants of Fn also contribute to tumorigenesis. Further studies should be performed in which individual alternative splice variants of Fn are exogenously provided instead, and changes to the molecular conformation and stiffness of the ECM measured.

*5.2.5. Different length scales*

These studies utilized cell-derived Fn matrices to understand how molecular scale conformations and bulk ECM mechanics modulated cell binding for altered pro-angiogenic signaling. Future work should collect and lyophilize these tumor-conditioned Fn matrices in order to reconstitute and use for elastic, viscoelastic, conformational, and binding studies. Individual Fn fibers can be pulled from a concentrated reconstituted Fn solution to assess individual fibers' elastic range, viscoelasticity, and for binding experiments. Individual fibers should be elastically strained at different rates and relaxed to assess how these fibers can return to its initial state under different mechanical stimuli. For viscoelastic measurements, individual

Fn fibers under different strains should be ablated with a laser to assess Fn fiber viscosity by measuring fiber relaxation rates. Further, fibers should be strained until breakage and to measure if and how fibers return to an equilibrium un-strained state. These Fn fiber strain-relaxation experiments should be compared against control Fn fiber measurements. Individual Fn fiber binding experiments could be performed with growth factors, cells, and ECM fragments to determine the optimal 'tumor' binding conditions for each and if there is any corresponding Fn conformation changes. The VEGF-Fn binding experiments should first be run under static conditions, then under dynamic strain conditions (e.g.: increasing strain till breakage, increase and decrease strain at a constant rate, increase and decrease strain at random rates) to assess the conditions in which VEGF without any external factors such as cells, is able to bind and detach from Fn. Finally, these aforementioned studies should be performed with single cells on strained (elastic vs plastic) Fn fibers to investigate how and when VEGF is immobilized or released. These cell-single Fn fiber studies may also be modified to ascertain the effect of specific integrins in immobilizing or releasing VEGF from Fn, by inhibiting or knocking down either $\alpha_5\beta_1$ (facilitates strong fibrillar adhesions and known to aid in immobilizing VEGF) or $\alpha_v\beta_3$ (facilitates weak nascent adhesions and known to be up-regulated during tumor angiogenesis). The studies proposed in this section should also be repeated with alternative splice variants of Fn, as it is known that Fn conformation is altered, which may affect the intrinsic materials properties of pulled Fn fibers (e.g.: elastic and viscoelastic properties, conformation, ability to bind VEGF).

# APPENDIX

## A.1. Pathologic Upgrade Rates on Subsequent Excision When Lobular Carcinoma In Situ Is the Primary Diagnosis in the Needle Core Biopsy With Special Attention to the Radiographic Target

This manuscript was part of my summer immersion at Weill Cornell Medical School to learn more about breast cancer diagnosis and management from a pathologists' point of view. I collected patient data, radiographic data, biopsy slides, and excision slides of patients that had calcifications and/or lobular carcinoma in situ.

Authors of this manuscript are: TM D'Alfonso, K Wang, YL Chiu, SJ Shin

*Published in Archives of Pathology & Laboratory Medicine (2013)*

Abstract

*Context*: Lobular carcinoma in situ (LCIS) as the primary pathologic diagnosis in a needle core biopsy is an infrequent finding, and the management of patients in this setting is controversial.

*Objective*: To determine the rate of pathologic upgrade (defined as the presence of a clinically more-significant lesion in the subsequent excision) in patients with a primary pathologic diagnosis of LCIS in the needle core biopsy.

*Design*: Patients with a primary diagnosis of LCIS in a needle core biopsy who underwent subsequent excision were identified. Core biopsies containing a concurrent high-risk lesion and cases with radiologic-pathologic discordance were excluded. The presence of selected

microscopic features in the needle core biopsy was correlated with pathologic upgrade. Microscopic findings were correlated with the radiographic target in the needle core biopsy.

*Results*: Sixty-one women with primary LCIS in their needle core biopsy showed a 10% pathologic upgrade rate. The percentage of cores involved by LCIS was significantly associated with pathologic upgrade ($P = .04$), whereas the remaining measured parameters were not. When LCIS represented the radiographic target, the pathologic upgrade rate was 18%, whereas when it was an incidental finding, the pathologic upgrade rate was 4%.

*Conclusions*: It may be reasonable for patients with primary, yet incidental, LCIS on needle core biopsy to be managed in a nonsurgical fashion. Larger studies are needed to confirm our findings.

### A.2. 3D Conducting Polymer Platforms for Electrical Control of Protein Conformation and Cellular Functions

This manuscript was part of a collaboration with the Biomedical Engineering and Materials Science departments at Cornell University and the Bioelectronics department at Ecole Nationale Supérieure des Mines. I provided the FRET-labeled Fn that was adsorbed onto the 3D scaffold to determine how changes in Fn protein conformation regulated cell adhesion and pro-angiogenic secretion.

Authors of this manuscript are: AMD Wan, S Inal, T Williams, K Wang, P Leleux, L Estevez, CK Ober, EP Giannelis, C Fischbach, GG Malliaras, D Gourdon

*Published in Journal of Materials Chemistry Part B & C (2015)*

Abstract

We report the fabrication of three dimensional (3D) macroporous scaffolds made from poly(3,4-ethylenedioxythiophene):poly(styrenesulfonate) (PEDOT:PSS) *via* an ice-templating method. The scaffolds offer tunable pore size and morphology, and are electrochemically active. When a potential is applied to the scaffolds, reversible changes take place in their electrical doping state, which in turn enables precise control over the conformation of adsorbed proteins (*e.g.*, fibronectin). Additionally, the scaffolds support the growth of mouse fibroblasts (3T3-L1) for 7 days, and are able to electrically control cell adhesion and pro-angiogenic capability. These 3D matrix-mimicking platforms offer precise control of protein conformation and major cell functions, over large volumes and long cell culture times. As such, they represent a new tool for biological research with many potential applications in bioelectronics, tissue engineering, and regenerative medicine.

## A.3. Obesity-dependent changes of interstitial ECM mechanics and their role in breast tumorigenesis

This manuscript was part of a large collaboration between clinicians, biomedical engineers, and materials scientists to understand how changes in the materials properties of obesity-associated ECM mediated tumorigenesis. I provided the FRET-labeled Fn and assisted in the analysis of confocal FRET images used to determine if Fn molecular conformation was altered when assembled by obesity-associated myofibroblasts.

Authors of this manuscript are: BR Seo, P Bhardwaj, S Choi, J. Gonzalez, RC Andresen Eguiluz, K Wang, S. Mohanan, PG Morris, B Du, XK Zhou, LT Vahdat, A Verma, O Elemento, CA Hudis, RM Williams, D Gourdon, AJ Dannenberg, C Fischbach

*Accepted in Science Translational Medicine (2015)*

Abstract

Obesity and extracellular matrix (ECM) density are considered independent risk and prognostic factors for breast cancer. Whether they are functionally linked is uncertain. Here, we investigated the hypothesis that obesity enhances local myofibroblast content in mammary adipose tissue and that these stromal changes increase malignant potential via enhancing interstitial ECM stiffness. Indeed, mammary fat of both diet- and genetically-induced mouse models of obesity were enriched for myofibroblasts and stiffness-promoting ECM components. These differences were related to varied adipose stromal cell (ASC) characteristics as ASCs isolated from obese mice contained more myofibroblasts and deposited denser and stiffer ECMs relative to ASCs from lean control mice. Accordingly, decellularized matrices from obese ASCs stimulated mechanosignaling and thereby the malignant potential of breast cancer cells. Finally, the clinical relevance and translational potential of our findings were supported by analysis of patient specimens and the observation that caloric restriction in a mouse model reduces myofibroblast content in mammary fat. Collectively, these findings suggest that obesity-induced interstitial fibrosis promotes breast tumorigenesis via altering mammary ECM mechanics with important potential implications for anti-cancer therapies.

## REFERENCES


[1] Lu P, Weaver VM, Werb Z. The extracellular matrix: A dynamic niche in cancer progression. The Journal of Cell Biology 2012;196:395–406.

[2] Cox TR, Erler JT. Remodeling and homeostasis of the extracellular matrix: implications for fibrotic diseases and cancer. Disease Models & Mechanisms 2011;4:165–78.

[3] Ochsner M, Textor M, Vogel V, Smith ML. Dimensionality Controls Cytoskeleton Assembly and Metabolism of Fibroblast Cells in Response to Rigidity and Shape. PLoS ONE 2010;5:e9445.

[4] Orr AW, Helmke BP, Blackman BR, Schwartz MA. Mechanisms of mechanotransduction. Developmental Cell 2006;10:11–20.

[5] Chen TT, Luque A, Lee S, Anderson SM, Segura T, Iruela-Arispe ML. Anchorage of VEGF to the extracellular matrix conveys differential signaling responses to endothelial cells. The Journal of Cell Biology 2010;188:595–609.

[6] Martino MM, Tortelli F, Mochizuki M, Traub S, Ben-David D, Kuhn GA, et al. Engineering the Growth Factor Microenvironment with Fibronectin Domains to Promote Wound and Bone Tissue Healing. Science Translational Medicine 2011;3:100ra89–9.

[7] Smith ML, Gourdon D, Little WC, Kubow KE, Eguiluz RA, Luna-Morris S, et al. Force-Induced Unfolding of Fibronectin in the Extracellular Matrix of Living Cells. Plos Biol 2007;5:e268.

[8] Jaalouk DE, Lammerding J. Mechanotransduction gone awry. Nat Rev Mol Cell Biol 2009;10:63–73.

[9] Bissell MJ, Hines WC. Why don't we get more cancer? A proposed role of the microenvironment in restraining cancer progression. Nature Medicine 2011;17:320–9.

[10] Hanahan D, Weinberg RA. Hallmarks of Cancer: The Next Generation. Cell 2011;144:646–74.

[11] Crawford Y, Kasman I, Yu L, Zhong C, Wu X, Modrusan Z, et al. PDGF-C mediates the angiogenic and tumorigenic properties of fibroblasts associated with tumors refractory to anti-VEGF treatment. Cancer Cell 2009;15:21–34.

[12] Weis SM, Cheresh DA. Tumor angiogenesis: molecular pathways and therapeutic targets. Nature Medicine 2011;17:1359–70.

[13] Goetz JG, Minguet S, Navarro-Lérida I, Lazcano JJ, Samaniego R, Calvo E, et al. Biomechanical remodeling of the microenvironment by stromal caveolin-1 favors tumor invasion and metastasis. Cell 2011;146:148–63.

[14] Calvo F, Ege N, Grande-Garcia A, Hooper S, Jenkins RP, Chaudhry SI, et al. Mechanotransduction and YAP-dependent matrix remodelling is required for the generation and maintenance of cancer-associated fibroblasts. Nature Cell Biology 2013;15:637–46.

[15] Spaeth EL, Dembinski JL, Sasser AK, Watson K, Klopp A, Hall B, et al. Mesenchymal stem cell transition to tumor-associated fibroblasts contributes to fibrovascular network expansion and tumor progression. PLoS ONE 2009;4:e4992.

[16] Mishra PJ, Mishra PJ, Humeniuk R, Medina DJ, Alexe G, Mesirov JP, et al. Carcinoma-associated fibroblast-like differentiation of human mesenchymal stem cells. Cancer Research 2008;68:4331–9.

[17] Karnoub AE, Dash AB, Vo AP, Sullivan A, Brooks MW, Bell GW, et al. Mesenchymal stem cells within tumour stroma promote breast cancer metastasis. Nature 2007;449:557–63.
[18] Chandler EM, Seo BR, Califano JP, Andresen Eguiluz RC, Lee JS, Yoon CJ, et al. Implanted adipose progenitor cells as physicochemical regulators of breast cancer. Proc Natl Acad Sci USa 2012;109:9786–91.
[19] Plodinec M, Loparic M, Monnier CA, Obermann EC, Zanetti-Dallenbach R, Oertle P, et al. The nanomechanical signature of breast cancer. Nature Nanotech 2012;7:757–65.
[20] Byun S, Son S, Amodei D, Cermak N, Shaw J, Kang JH, et al. Characterizing deformability and surface friction of cancer cells. PNAS 2013;110:7580–5.
[21] Akiyama SK, Olden K, Yamada KM. Fibronectin and integrins in invasion and metastasis. Cancer Metastasis Rev 1995;14:173–89.
[22] Provenzano PP, Inman DR, Eliceiri KW, Knittel JG, Yan L, Rueden CT, et al. Collagen density promotes mammary tumor initiation and progression. BMC Med 2008;6:11.
[23] Levental KR, Yu H, Kass L, Lakins JN, Egeblad M, Erler JT, et al. Matrix Crosslinking Forces Tumor Progression by Enhancing Integrin Signaling. Cell 2009;139:891–906.
[24] Sottile J, Hocking DC. Fibronectin Polymerization Regulates the Composition and Stability of Extracellular Matrix Fibrils and Cell-Matrix Adhesions. Molecular Biology of the Cell 2002;13:3546–59.
[25] Dzamba BJ, Wu H, Jaenisch R, Peters DM. Fibronectin binding site in type I collagen regulates fibronectin fibril formation. The Journal of Cell Biology 1993;121:1165–72.
[26] Lauer-Fields JL, Juska D, Fields GB. Matrix metalloproteinases and collagen catabolism. Biopolymers 2002;66:19–32.
[27] Heppner KJ, Matrisian LM, Jensen RA, Rodgers WH. Expression of most matrix metalloproteinase family members in breast cancer represents a tumor-induced host response. AJPA 1996;149:273–82.
[28] Kessenbrock K, Plaks V, Werb Z. Matrix Metalloproteinases: Regulators of the Tumor Microenvironment. Cell 2010;141:52–67.
[29] Sato H, Takino T, Okada Y, Cao J, Shinagawa A, Yamamoto E, et al. A matrix metalloproteinase expressed on the surface of invasive tumour cells. Nature 1994;370:61–5.
[30] Page-McCaw A, Ewald AJ, Werb Z. Matrix metalloproteinases and the regulation of tissue remodelling. Nat Rev Mol Cell Biol 2007;8:221–33.
[31] Wijelath ES, Murray J, Rahman S, Patel Y, Ishida A, Strand K, et al. Novel Vascular Endothelial Growth Factor Binding Domains of Fibronectin Enhance Vascular Endothelial Growth Factor Biological Activity. Circulation Research 2002;91:25–31.
[32] Lee S, Jilani SM, Nikolova GV, Carpizo D, Iruela-Arispe ML. Processing of VEGF-A by matrix metalloproteinases regulates bioavailability and vascular patterning in tumors. The Journal of Cell Biology 2005;169:681–91.
[33] Singh P, Carraher C, Schwarzbauer JE. Assembly of Fibronectin Extracellular Matrix. Annu Rev Cell Dev Biol 2010;26:397–419.
[34] Little WC, Smith ML, Ebneter U, Vogel V. Assay to mechanically tune and optically probe fibrillar fibronectin conformations from fully relaxed to breakage. Matrix Biology 2008;27:451–61.

[35] Kubow KE, Klotzsch E, Smith ML, Gourdon D, Little WC, Vogel V. Crosslinking of cell-derived 3D scaffolds up-regulates the stretching and unfolding of new extracellular matrix assembled by reseeded cells. Integr Biol 2009;1:635–48.
[36] Wan AMD, Schur RM, Ober CK, Fischbach C, Gourdon D, Malliaras GG. Electrical control of protein conformation. Adv Mater Weinheim 2012;24:2501–5.
[37] Israelachvili J, Min Y, Akbulut M, Alig A, Carver G, Greene W, et al. Recent advances in the surface forces apparatus (SFA) technique. Rep Prog Phys 2010;73:036601.
[38] Banquy X, Rabanel J-M, Hildgen P, Giasson S. Direct Measurement of Mechanical and Adhesive Properties of Living Cells Using Surface Forces Apparatus. Aust J Chem 2007;60:638.
[39] Johnson KL. Contact Mechanics. Cambridge University Press; 1985.
[40] Ruoslahti E, Vaheri A, Kuusela P, Linder E. Fibroblast surface antigen: a new serum protein. Biochim Biophys Acta 1973;322:352–8.
[41] Hynes RO. Alteration of Cell-Surface Proteins by Viral Transformation and by Proteolysis. PNAS 1973;70:3170–4.
[42] Wartiovaara J, Linder E, Ruoslahti E, Vaheri A. Distribution of Fibroblast Surface Antigen - Association with Fibrillar Structures of Normal Cells and Loss Upon Viral Transformation. Journal of Experimental Medicine 1974;140:1522–33.
[43] Yamada KM, Weston JA. Isolation of a Major Cell-Surface Glycoprotein From Fibroblasts. PNAS 1974;71:3492–6.
[44] Hynes RO, Destree A. Extensive disulfide bonding at the mammalian cell surface. PNAS 1977;74:2855–9.
[45] To WS, Midwood KS. Plasma and cellular fibronectin: distinct and independent functions during tissue repair. Fibrogenesis & Tissue Repair 2011;4:21.
[46] Grinnell F. Fibronectin and Wound Healing. J Cell Biochem 1984;26:107–16.
[47] Wartiovaara J, Leivo I, Vaheri A. Expression of the cell surface-associated glycoprotein, fibronectin, in the early mouse embryo. Dev Biol 1979;69:247–57.
[48] D'Ardenne AJ, McGee JO. Fibronectin in disease. J Pathol 1984;142:235–51.
[49] Kahn P, Shin SI. Cellular tumorigenicity in nude mice. Test of associations among loss of cell-surface fibronectin, anchorage independence, and tumor-forming ability. The Journal of Cell Biology 1979;82:1–16.
[50] Zardi L, Cecconi C, Barbieri O, Carnemolla B, Picca M, Santi L. Concentration of fibronectin in plasma of tumor-bearing mice and synthesis by Ehrlich ascites tumor cells. Cancer Research 1979;39:3774–9.
[51] Choate JJ, Mosher DF. Fibronectin concentration in plasma of patients with breast cancer, colon cancer, and acute leukemia. Cancer 1983;51:1142–7.
[52] Zerlauth G, Wolf G. Plasma fibronectin as a marker for cancer and other diseases. Am J Med 1984;77:685–9.
[53] Stenman S, Vaheri A. Fibronectin in human solid tumors. Int J Cancer 1981;27:427–35.
[54] Asch BB, Kamat BR, Burstein NA. Interactions of normal, dysplastic, and malignant mammary epithelial cells with fibronectin in vivo and in vitro. Cancer Research 1981;41:2115–25.
[55] Hanahan D, Weinberg RA. The hallmarks of cancer. Cell 2000;100:57–70.
[56] Friedl P, Alexander S. Cancer invasion and the microenvironment: plasticity and

reciprocity. Cell 2011;147:992–1009.
[57] Kass L, Erler JT, Dembo M, Weaver VM. Mammary epithelial cell: Influence of extracellular matrix composition and organization during development and tumorigenesis. The International Journal of Biochemistry & Cell Biology 2007;39:1987–94.
[58] Schedin P, Keely PJ. Mammary Gland ECM Remodeling, Stiffness, and Mechanosignaling in Normal Development and Tumor Progression. Cold Spring Harbor Perspectives in Biology 2011;3:a003228–8.
[59] Malik R, Lelkes PI, Cukierman E. Biomechanical and biochemical remodeling of stromal extracellular matrix in cancer. Trends Biotechnol 2015;33:230–6.
[60] Gaggioli C, Hooper S, Hidalgo-Carcedo C, Grosse R, Marshall JF, Harrington K, et al. Fibroblast-led collective invasion of carcinoma cells with differing roles for RhoGTPases in leading and following cells. Nature Cell Biology 2007;9:1392–400.
[61] Williams EC, Janmey PA, Ferry JD, Mosher DF. Conformational states of fibronectin. J Biol Chem 1982;257:14973–8.
[62] Engel J, Odermatt E, Engel A, Madri JA, Furthmayr H, Rohde H, et al. Shapes, domain organizations and flexibility of laminin and fibronectin, two multifunctional proteins of the extracellular matrix. Journal of Molecular Biology 1981;150:97–120.
[63] Erickson HP, Carrell N, McDonagh J. Fibronectin molecule visualized in electron microscopy: a long, thin, flexible strand. The Journal of Cell Biology 1981;91:673–8.
[64] Bradshaw MJ, Smith ML. Multiscale relationships between fibronectin structure and functional properties. Acta Biomaterialia 2014;10:1524–31.
[65] Alexander SS, Colonna G, Edelhoch H. The structure and stability of human plasma cold-insoluble globulin. J Biol Chem 1979;254:1501–5.
[66] Alexander SS, Colonna G, Yamada KM, Pastan I, Edelhoch H. Molecular properties of a major cell surface protein from chick embryo fibroblasts. J Biol Chem 1978;253:5820–4.
[67] Ruoslahti E. Fibronectin and its receptors. Annu Rev Biochem 1988;57:375–413.
[68] Hynes RO, Yamada KM. Fibronectins: multifunctional modular glycoproteins. The Journal of Cell Biology 1982;95:369–77.
[69] Main AL, Harvey TS, Baron M, Boyd J, Campbell ID. The three-dimensional structure of the tenth type III module of fibronectin: an insight into RGD-mediated interactions. Cell 1992;71:671–8.
[70] Pierschbacher MD, Ruoslahti E. Cell attachment activity of fibronectin can be duplicated by small synthetic fragments of the molecule. Nature 1984;309:30–3.
[71] Obara M, Kang MS, Yamada KM. Site-directed mutagenesis of the cell-binding domain of human fibronectin: separable, synergistic sites mediate adhesive function. Cell 1988;53:649–57.
[72] Aota S, Nagai T, Yamada KM. Characterization of regions of fibronectin besides the arginine-glycine-aspartic acid sequence required for adhesive function of the cell-binding domain using site-directed mutagenesis. J Biol Chem 1991;266:15938–43.
[73] Nagai T, Yamakawa N, Aota S, Yamada SS, Akiyama SK, Olden K, et al. Monoclonal antibody characterization of two distant sites required for function of the central cell-binding domain of fibronectin in cell adhesion, cell migration, and matrix assembly. The Journal of Cell Biology 1991;114:1295–305.
[74] Krammer A, Craig D, Thomas WE, Schulten K, Vogel V. A structural model for force

regulated integrin binding to fibronectin's RGD-synergy site. Matrix Biol 2002;21:139–47.
[75] Kimizuka F, Ohdate Y, Kawase Y, Shimojo T, Taguchi Y, Hashino K, et al. Role of type III homology repeats in cell adhesive function within the cell-binding domain of fibronectin. J Biol Chem 1991;266:3045–51.
[76] Leahy DJ, Aukhil I, Erickson HP. 2.0 A crystal structure of a four-domain segment of human fibronectin encompassing the RGD loop and synergy region. Cell 1996;84:155–64.
[77] Miyamoto S, Katz BZ, Lafrenie RM, Yamada KM. Fibronectin and integrins in cell adhesion, signaling, and morphogenesis. Morphogenesis: Cellular Interactions 1998;857:119–29.
[78] Martino MM, Hubbell JA. The 12th-14th type III repeats of fibronectin function as a highly promiscuous growth factor-binding domain. The FASEB Journal 2010;24:4711–21.
[79] Anderson SM, Chen TT, Iruela-Arispe ML, Segura T. The phosphorylation of vascular endothelial growth factor receptor-2 (VEGFR-2) by engineered surfaces with electrostatically or covalently immobilized VEGF. Biomaterials 2009;30:4618–28.
[80] Oh E, Pierschbacher M, Ruoslahti E. Deposition of plasma fibronectin in tissues. PNAS 1981;78:3218–21.
[81] Deno DC, Saba TM, Lewis EP. Kinetics of endogenously labeled plasma fibronectin: incorporation into tissues. Am J Physiol 1983;245:R564–75.
[82] Steward RL, Cheng C-M, Ye JD, Bellin RM, LeDuc PR. Mechanical stretch and shear flow induced reorganization and recruitment of fibronectin in fibroblasts. Sci Rep 2011;1:147.
[83] Fogerty FJ, Akiyama SK, Yamada KM, Mosher DF. Inhibition of binding of fibronectin to matrix assembly sites by anti-integrin (alpha 5 beta 1) antibodies. The Journal of Cell Biology 1990;111:699–708.
[84] Wu C, Bauer JS, Juliano RL, McDonald JA. The alpha 5 beta 1 integrin fibronectin receptor, but not the alpha 5 cytoplasmic domain, functions in an early and essential step in fibronectin matrix assembly. Journal of Biological Chemistry 1993;268:21883–8.
[85] Wu C, Keivenst VM, O'Toole TE, McDonald JA. Integrin activation and cytoskeletal interaction are essential for the assembly of a fibronectin matrix. Cell 1995.
[86] Lemmon CA, Chen CS, Romer LH. Cell Traction Forces Direct Fibronectin Matrix Assembly. Biophysj 2009;96:729–38.
[87] Carraher CL, Schwarzbauer JE. Regulation of matrix assembly through rigidity-dependent fibronectin conformational changes. Journal of Biological Chemistry 2013;288:14805–14.
[88] Früh SM, Schoen I, Ries J, Vogel V. Molecular architecture of native fibronectin fibrils. Nature Communications 2015;6:7275.
[89] McKeown-Longo PJ, Mosher DF. Binding of plasma fibronectin to cell layers of human skin fibroblasts. The Journal of Cell Biology 1983;97:466–72.
[90] Baneyx G, Baugh L, Vogel V. Coexisting conformations of fibronectin in cell culture imaged using fluorescence resonance energy transfer. PNAS 2001;98:14464–8.
[91] Gildner CD, Roy DC, Farrar CS, Hocking DC. Opposing effects of collagen I and vitronectin on fibronectin fibril structure and function. Matrix Biol 2014;34:33–45.

[92] Sottile J, Hocking DC, Swiatek PJ. Fibronectin matrix assembly enhances adhesion-dependent cell growth. Journal of Cell Biology 1998;111 ( Pt 19):2933–43.
[93] Sottile J, Hocking DC, Langenbach KJ. Fibronectin polymerization stimulates cell growth by RGD-dependent and -independent mechanisms. Journal of Cell Biology 2000;113 Pt 23:4287–99.
[94] Hubbard B, Buczek-Thomas JA, Nugent MA, Smith ML. Heparin-dependent regulation of fibronectin matrix conformation. Matrix Biol 2013.
[95] Hocking DC, Sottile J, McKeown-Longo PJ. Fibronectin's III-1 module contains a conformation-dependent binding site for the amino-terminal region of fibronectin. J Biol Chem 1994;269:19183–7.
[96] Aguirre KM, McCormick RJ, Schwarzbauer JE. Fibronectin self-association is mediated by complementary sites within the amino-terminal one-third of the molecule. J Biol Chem 1994;269:27863–8.
[97] Bultmann H, Santas AJ, Peters DM. Fibronectin fibrillogenesis involves the heparin II binding domain of fibronectin. J Biol Chem 1998;273:2601–9.
[98] Maqueda A, Moyano JV, Hernández Del Cerro M, Peters DM, Garcia-Pardo A. The heparin III-binding domain of fibronectin (III4-5 repeats) binds to fibronectin and inhibits fibronectin matrix assembly. Matrix Biol 2007;26:642–51.
[99] Hocking DC, Smith RK, McKeown-Longo PJ. A novel role for the integrin-binding III-10 module in fibronectin matrix assembly. The Journal of Cell Biology 1996;133:431–44.
[100] Morla A, Ruoslahti E. A fibronectin self-assembly site involved in fibronectin matrix assembly: reconstruction in a synthetic peptide. The Journal of Cell Biology 1992;118:421–9.
[101] McKeown-Longo PJ, Mosher DF. Interaction of the 70,000-mol-wt amino-terminal fragment of fibronectin with the matrix-assembly receptor of fibroblasts. The Journal of Cell Biology 1985;100:364–74.
[102] McDonald JA, Kelley DG, Broekelmann TJ. Role of fibronectin in collagen deposition: Fab' to the gelatin-binding domain of fibronectin inhibits both fibronectin and collagen organization in fibroblast extracellular matrix. The Journal of Cell Biology 1982;92:485–92.
[103] Velling T, Risteli J, Wennerberg K, Mosher DF, Johansson S. Polymerization of type I and III collagens is dependent on fibronectin and enhanced by integrins alpha 11beta 1 and alpha 2beta 1. J Biol Chem 2002;277:37377–81.
[104] Shi F, Sottile J. MT1-MMP regulates the turnover and endocytosis of extracellular matrix fibronectin. Journal of Cell Biology 2011;124:4039–50.
[105] Sevilla CA, Dalecki D, Hocking DC. Regional Fibronectin and Collagen Fibril Co-Assembly Directs Cell Proliferation and Microtissue Morphology. PLoS ONE 2013;8:e77316.
[106] Sottile J, Shi F, Rublyevska I, Chiang HY, Lust J, Chandler J. Fibronectin-dependent collagen I deposition modulates the cell response to fibronectin. AJP: Cell Physiology 2007;293:C1934–46.
[107] Ledger PW, Uchida N, Tanzer ML. Immunocytochemical localization of procollagen and fibronectin in human fibroblasts: effects of the monovalent ionophore, monensin. The Journal of Cell Biology 1980;87:663–71.
[108] Hahn LH, Yamada KM. Identification and isolation of a collagen-binding fragment of

the adhesive glycoprotein fibronectin. PNAS 1979;76:1160–3.
[109] Ingham KC, Brew SA, Migliorini MM. Further localization of the gelatin-binding determinants within fibronectin. Active fragments devoid of type II homologous repeat modules. J Biol Chem 1989;264:16977–80.
[110] Pickford AR, Smith SP, Staunton D, Boyd J, Campbell ID. The hairpin structure of the (6)F1(1)F2(2)F2 fragment from human fibronectin enhances gelatin binding. Embo J 2001;20:1519–29.
[111] Kleinman HK, McGoodwin EB, Martin GR, Klebe RJ, Fietzek PP, Woolley DE. Localization of the binding site for cell attachment in the alpha1(I) chain of collagen. J Biol Chem 1978;253:5642–6.
[112] Erat MC, Sladek B, Campbell ID, Vakonakis I. Structural analysis of collagen type I interactions with human fibronectin reveals a cooperative binding mode. J Biol Chem 2013; 288:17441–17450.
[113] Choquet D, Felsenfeld DP, Sheetz MP. Extracellular Matrix Rigidity Causes Strengthening of Integrin–Cytoskeleton Linkages. Cell 1997;88:39–48.
[114] Wang N, Naruse K, Stamenović D, Fredberg JJ, Mijailovich SM, Tolić-Nørrelykke IM, et al. Mechanical behavior in living cells consistent with the tensegrity model. PNAS 2001;98:7765–70.
[115] Zhang Q, Checovich WJ, Peters DM, Albrecht RM, Mosher DF. Modulation of cell surface fibronectin assembly sites by lysophosphatidic acid. The Journal of Cell Biology 1994;127:1447–59.
[116] Zhang Q, Magnusson MK, Mosher DF. Lysophosphatidic acid and microtubule-destabilizing agents stimulate fibronectin matrix assembly through Rho-dependent actin stress fiber formation and cell contraction. Molecular Biology of the Cell 1997;8:1415–25.
[117] Baneyx G, Baugh L, Vogel V. Fibronectin extension and unfolding within cell matrix fibrils controlled by cytoskeletal tension. PNAS 2002;99:5139–43.
[118] Pankov R, Cukierman E, Katz BZ, Matsumoto K, Lin DC, Lin S, et al. Integrin dynamics and matrix assembly: tensin-dependent translocation of alpha(5)beta(1) integrins promotes early fibronectin fibrillogenesis. The Journal of Cell Biology 2000;148:1075–90.
[119] Oberhauser AF, Badilla-Fernandez C, Carrion-Vazquez M, Fernandez JM. The Mechanical Hierarchies of Fibronectin Observed with Single-molecule AFM. Journal of Molecular Biology 2002;319:433–47.
[120] Hocking DC, Sottile J, Langenbach KJ. Stimulation of integrin-mediated cell contractility by fibronectin polymerization. Journal of Biological Chemistry 2000;275:10673–82.
[121] Chernousov MA, Faerman AI, Frid MG, Printseva OYu, Koteliansky VE. Monoclonal antibody to fibronectin which inhibits extracellular matrix assembly. FEBS Letters 1987;217:124–8.
[122] Zhong C, Chrzanowska-Wodnicka M, Brown J, Shaub A, Belkin AM, Burridge K. Rho-mediated Contractility Exposes a Cryptic Site in Fibronectin and Induces Fibronectin Matrix Assembly. The Journal of Cell Biology 1998;141:539–51.
[123] Ohashi T, Kiehart DP, Erickson HP. Dynamics and elasticity of the fibronectin matrix in living cell culture visualized by fibronectin-green fluorescent protein. PNAS 1999;96:2153–8.

[124] Klotzsch E, Smith ML, Kubow KE, Muntwyler S, Little WC, Beyeler F, et al. Fibronectin forms the most extensible biological fibers displaying switchable force-exposed cryptic binding sites. PNAS 2009;106:18267–72.
[125] Hynes RO. The dynamic dialogue between cells and matrices: implications of fibronectin's elasticity. PNAS 1999;96:2588–90.
[126] Krammer A, Lu H, Isralewitz B, Schulten K, Vogel V. Forced unfolding of the fibronectin type III module reveals a tensile molecular recognition switch. PNAS 1999;96:1351–6.
[127] Vogel V, Thomas WE, Craig DW, Krammer A, Baneyx G. Structural insights into the mechanical regulation of molecular recognition sites. Trends Biotechnol 2001;19:416–23.
[128] Cluzel C, Saltel F, Lussi J, Paulhe F, Imhof BA, Wehrle-Haller B. The mechanisms and dynamics of (alpha)v(beta)3 integrin clustering in living cells. The Journal of Cell Biology 2005;171:383–92.
[129] Matsuura H, Hakomori S. The oncofetal domain of fibronectin defined by monoclonal antibody FDC-6: its presence in fibronectins from fetal and tumor tissues and its absence in those from normal adult tissues and plasma. PNAS 1985;82:6517–21.
[130] Schwarzbauer JE, Paul JI, Hynes RO. On the origin of species of fibronectin. PNAS 1985;82:1424–8.
[131] Carnemolla B, Leprini A, Allemanni G, Saginati M, Zardi L. The inclusion of the type III repeat ED-B in the fibronectin molecule generates conformational modifications that unmask a cryptic sequence. J Biol Chem 1992;267:24689–92.
[132] Balza E, Sassi F, Ventura E, Parodi A, Fossati S, Blalock W, et al. A novel human fibronectin cryptic sequence unmasked by the insertion of the angiogenesis-associated extra type III domain B. Int J Cancer 2009;125:751–8.
[133] Ventura E, Sassi F, Parodi A, Balza E, Borsi L, Castellani P, et al. Alternative splicing of the angiogenesis associated extra-domain B of fibronectin regulates the accessibility of the B-C loop of the type III repeat 8. PLoS ONE 2010;5:e9145.
[134] Fattorusso R, Pellecchia M, Viti F, Neri P, Neri D, Wüthrich K. NMR structure of the human oncofoetal fibronectin ED-B domain, a specific marker for angiogenesis. Structure 1999;7:381–90.
[135] Serini G, Bochaton-Piallat ML, Ropraz P, Geinoz A, Borsi L, Zardi L, et al. The fibronectin domain ED-A is crucial for myofibroblastic phenotype induction by transforming growth factor-beta1. The Journal of Cell Biology 1998;142:873–81.
[136] Shinde AV, Kelsh R, Peters JH, Sekiguchi K, Van De Water L, McKeown-Longo PJ. The α4β1 integrin and the EDA domain of fibronectin regulate a profibrotic phenotype in dermal fibroblasts. Matrix Biology 2014;41:26–35.
[137] Kelsh RM, McKeown-Longo PJ, Clark RAF. EDA Fibronectin in Keloids Create a Vicious Cycle of Fibrotic Tumor Formation. J Investig Dermatol 2015;135:1714–8.
[138] Rybak JN, Roesli C, Kaspar M, Villa A, Neri D. The Extra-domain A of Fibronectin Is a Vascular Marker of Solid Tumors and Metastases. Cancer Research 2007;67:10948–57.
[139] Xiang L, Xie G, Ou J, Wei X, Pan F, Liang H. The extra domain A of fibronectin increases VEGF-C expression in colorectal carcinoma involving the PI3K/AKT signaling pathway. PLoS ONE 2012;7:e35378.
[140] Ou J, Peng Y, Deng J, Miao H, Zhou J, Zha L, et al. Endothelial cell-derived

fibronectin extra domain A promotes colorectal cancer metastasis via inducing epithelial-mesenchymal transition. Carcinogenesis 2014;35:1661–70.
[141] Shinde AV, Bystroff C, Wang C, Vogelezang MG, Vincent PA, Hynes RO, et al. Identification of the peptide sequences within the EIIIA (EDA) segment of fibronectin that mediate integrin alpha9beta1-dependent cellular activities. J Biol Chem 2008;283:2858–70.
[142] Kaczmarek J, Castellani P, Nicolo G, Spina B, Allemanni G, Zardi L. Distribution of oncofetal fibronectin isoforms in normal, hyperplastic and neoplastic human breast tissues. Int J Cancer 1994;59:11–6.
[143] Castellani P, Viale G, Dorcaratto A, Nicolo G, Kaczmarek J, Querze G, et al. The fibronectin isoform containing the ED-B oncofetal domain: a marker of angiogenesis. Int J Cancer 1994;59:612–8.
[144] Hashimoto-Uoshima M, Yan YZ, Schneider G, Aukhil I. The alternatively spliced domains EIIIB and EIIIA of human fibronectin affect cell adhesion and spreading. Journal of Cell Biology 1997;110 ( Pt 18):2271–80.
[145] Bordeleau F, Califano JP, Negrón Abril YL, Mason BN, LaValley DJ, Shin SJ, et al. Tissue stiffness regulates serine/arginine-rich protein-mediated splicing of the extra domain B-fibronectin isoform in tumors. PNAS 2015.
[146] Moro L, Colombi M, Molinari Tosatti MP, Barlati S. Study of fibronectin and mRNA in human laryngeal and ectocervical carcinomas by in situ hybridization and image analysis. Int J Cancer 1992;51:692–7.
[147] Kalluri R, Zeisberg M. Fibroblasts in cancer. Nature Reviews Cancer 2006;6:392–401.
[148] Kojima Y, Acar A, Eaton EN, Mellody KT, Scheel C, Ben-Porath I, et al. Autocrine TGF-beta and stromal cell-derived factor-1 (SDF-1) signaling drives the evolution of tumor-promoting mammary stromal myofibroblasts. PNAS 2010;107:20009–14.
[149] Antonyak MA, Li B, Boroughs LK, al E. Cancer cell-derived microvesicles induce transformation by transferring tissue transglutaminase and fibronectin to recipient cells. PNAS 2011;108.
[150] Chandler EM, Saunders MP, Yoon CJ, Gourdon D, Fischbach C. Adipose progenitor cells increase fibronectin matrix strain and unfolding in breast tumors. Phys Biol 2011;8:015008.
[151] Wang K, Andresen Eguiluz RC, Wu F, Seo BR, Fischbach C, Gourdon D. Stiffening and unfolding of early deposited-fibronectin increase proangiogenic factor secretion by breast cancer-associated stromal cells. Biomaterials 2015;54:63–71.
[152] Elosegui-Artola A, Bazellieres E, Allen MD, Andreu I, Oria R, Sunyer R, et al. Rigidity sensing and adaptation through regulation of integrin types. Nature Materials 2014;13:631–7.
[153] Wan AMD, Chandler EM, Madhavan M, Infanger DW, Ober CK, Gourdon D, et al. Fibronectin conformation regulates the proangiogenic capability of tumor-associated adipogenic stromal cells. Biochim Biophys Acta 2013.
[154] Antia M, Baneyx G, Kubow KE, Vogel V. Fibronectin in aging extracellular matrix fibrils is progressively unfolded by cells and elicits an enhanced rigidity response. Faraday Discuss 2008;139:229.
[155] Friedland JC, Lee MH, Boettiger D. Mechanically activated integrin switch controls alpha5beta1 function. Science 2009;323:642–4.
[156] Danen EHJ, Sonneveld P, Brakebusch C, Fässler R, Sonnenberg A. The fibronectin-

binding integrins alpha5beta1 and alphavbeta3 differentially modulate RhoA-GTP loading, organization of cell matrix adhesions, and fibronectin fibrillogenesis. The Journal of Cell Biology 2002;159:1071–86.
[157] Li F, Redick SD, Erickson HP, Moy VT. Force Measurements of the a5b1 Integrin-Fibronectin Interaction. Biophysj 2003;84:1252–62.
[158] Jia D, Entersz I, Butler C, Foty RA. Fibronectin matrix-mediated cohesion suppresses invasion of prostate cancer cells. BMC Cancer 2012;12:94.
[159] Danen EH, Aota S, van Kraats AA, Yamada KM, Ruiter DJ, van Muijen GN. Requirement for the synergy site for cell adhesion to fibronectin depends on the activation state of integrin alpha 5 beta 1. J Biol Chem 1995;270:21612–8.
[160] Schiller HB, Hermann M-R, Polleux J, Vignaud T, Zanivan S, Friedel CC, et al. β1- and αv-class integrins cooperate to regulate myosin II during rigidity sensing of fibronectin-based microenvironments. Nature Cell Biology 2013;15:625–36.
[161] Balcioglu HE, van Hoorn H, Donato DM, Schmidt T, Danen EHJ. The integrin expression profile modulates orientation and dynamics of force transmission at cell-matrix adhesions. Journal of Cell Biology 2015;128:1316–26.
[162] Zhang Y, Lu H, Dazin P, Kapila Y. Squamous cell carcinoma cell aggregates escape suspension-induced, p53-mediated anoikis: fibronectin and integrin alphav mediate survival signals through focal adhesion kinase. J Biol Chem 2004;279:48342–9.
[163] Saad S, Gottlieb DJ, Bradstock KF, Overall CM, Bendall LJ. Cancer cell-associated fibronectin induces release of matrix metalloproteinase-2 from normal fibroblasts. Cancer Research 2002;62:283–9.
[164] Jiao Y, Feng X, Zhan Y, Wang R, Zheng S, Liu W, et al. Matrix metalloproteinase-2 promotes αvβ3 integrin-mediated adhesion and migration of human melanoma cells by cleaving fibronectin. PLoS ONE 2012;7:e41591.
[165] Erat MC, Slatter DA, Lowe ED, Millard CJ, Farndale RW, Campbell ID, et al. Identification and structural analysis of type I collagen sites in complex with fibronectin fragments. PNAS 2009;106:4195–200.
[166] Provenzano PP, Eliceiri KW, Campbell JM, Inman DR, White JG, Keely PJ. Collagen reorganization at the tumor-stromal interface facilitates local invasion. BMC Med 2006;4:38.
[167] Conklin MW, Eickhoff JC, Riching KM, Pehlke CA, Eliceiri KW, Provenzano PP, et al. Aligned collagen is a prognostic signature for survival in human breast carcinoma. The American Journal of Pathology 2011;178:1221–32.
[168] Moriya K, Bae E, Honda K, Sakai K, Sakaguchi T, Tsujimoto I, et al. A fibronectin-independent mechanism of collagen fibrillogenesis in adult liver remodeling. Gastroenterology 2011;140:1653–63.
[169] Pickup MW, Mouw JK, Weaver VM. The extracellular matrix modulates the hallmarks of cancer. EMBO Reports 2014:e201439246.
[170] Massague J. TGFbeta in Cancer. Cell 2008;134:215–30.
[171] Arora PD, Narani N, McCulloch CA. The compliance of collagen gels regulates transforming growth factor-beta induction of alpha-smooth muscle actin in fibroblasts. AJPA 1999;154:871–82.
[172] Wipff P-J, Rifkin DB, Meister J-J, Hinz B. Myofibroblast contraction activates latent TGF-beta1 from the extracellular matrix. The Journal of Cell Biology 2007;179:1311–23.

[173] Leight JL, Wozniak MA, Chen S, Lynch ML, Chen CS. Matrix rigidity regulates a switch between TGF- 1-induced apoptosis and epithelial-mesenchymal transition. Molecular Biology of the Cell 2012;23:781–91.
[174] Lo CM, Wang HB, Dembo M, Wang YL. Cell movement is guided by the rigidity of the substrate. Biophysj 2000;79:144–52.
[175] Plotnikov SV, Pasapera AM, Sabass B, Waterman CM. Force Fluctuations within Focal Adhesions Mediate ECM-Rigidity Sensing to Guide Directed Cell Migration. Cell 2012;151:1513–27.
[176] Roca-Cusachs P, Gauthier NC, del Rio A, Sheetz MP. Clustering of alpha(5)beta(1) integrins determines adhesion strength whereas alpha(v)beta(3) and talin enable mechanotransduction. PNAS 2009;106:16245–50.
[177] Jiang G, Huang AH, Cai Y, Tanase M, Sheetz MP. Rigidity sensing at the leading edge through αvbβ3 integrins and RPTPα. Biophysj 2006;90:1804–9.
[178] Wong S, Guo W-H, Wang Y-L. Fibroblasts probe substrate rigidity with filopodia extensions before occupying an area. PNAS 2014;111:17176–81.
[179] Kostic A, Sheetz MP. Fibronectin rigidity response through Fyn and p130Cas recruitment to the leading edge. Molecular Biology of the Cell 2006;17:2684–95.
[180] Yamada KM, Even-Ram S. Integrin regulation of growth factor receptors. Nature Cell Biology 2002;4:E75–6.
[181] Ferrara N, Gerber H-P, LeCouter J. The biology of VEGF and its receptors. Nature Medicine 2003;9:669–76.
[182] Hanahan D, Coussens LM. Accessories to the Crime: Functions of Cells Recruited to the Tumor Microenvironment. Cancer Cell 2012;21:309–22.
[183] Goel HL, Mercurio AM. VEGF targets the tumour cell. Nature Reviews Cancer 2013;13:871–82.
[184] De S, Razorenova O, McCabe NP, O'Toole T, Qin J, Byzova TV. VEGF-integrin interplay controls tumor growth and vascularization. PNAS 2005;102:7589–94.
[185] Miralem T, Steinberg R, Price D, Avraham H. VEGF(165) requires extracellular matrix components to induce mitogenic effects and migratory response in breast cancer cells. Oncogene 2001;20:5511–24.
[186] Kim S, Bell K, Mousa SA, Varner JA. Regulation of Angiogenesis in Vivo by Ligation of Integrin α5β1 with the Central Cell-Binding Domain of Fibronectin. The American Journal of Pathology 2000;156:1345–62.
[187] Wijelath ES, Rahman S, Namekata M, Murray J, Nishimura T, Mostafavi-Pour Z, et al. Heparin-II domain of fibronectin is a vascular endothelial growth factor-binding domain: enhancement of VEGF biological activity by a singular growth factor/matrix protein synergism. Circulation Research 2006;99:853–60.
[188] Mitsi M, Hong Z, Costello CE, Nugent MA. Heparin-mediated conformational changes in fibronectin expose vascular endothelial growth factor binding sites. Biochemistry 2006;45:10319–28.
[189] Goerges AL, Nugent MA. pH regulates vascular endothelial growth factor binding to fibronectin: a mechanism for control of extracellular matrix storage and release. J Biol Chem 2004;279:2307–15.
[190] Cao L, Zeller MK, Fiore VF, Strane P, Bermudez H, Barker TH. Phage-based molecular probes that discriminate force-induced structural states of fibronectin in vivo. PNAS 2012;109:7251–6.

[191] Carnemolla B, Neri D, Castellani P, Leprini A, Neri G, Pini A, et al. Phage antibodies with pan-species recognition of the oncofoetal angiogenesis marker fibronectin ED-B domain. Int J Cancer 1996;68:397–405.
[192] Halin C, Rondini S, Nilsson F, Berndt A, Kosmehl H, Zardi L, et al. Enhancement of the antitumor activity of interleukin-12 by targeted delivery to neovasculature. Nat Biotechnol 2002;20:264–9.
[193] Santimaria M, Moscatelli G, Viale GL, Giovannoni L, Neri G, Viti F, et al. Immunoscintigraphic detection of the ED-B domain of fibronectin, a marker of angiogenesis, in patients with cancer. Clin Cancer Res 2003;9:571–9.
[194] Huijbers EJM, Ringvall M, Femel J, Kalamajski S, Lukinius A, Åbrink M, et al. Vaccination against the extra domain-B of fibronectin as a novel tumor therapy. The FASEB Journal 2010;24:4535–44.
[195] Femel J, Huijbers EJM, Saupe F, Cedervall J, Zhang L, Roswall P, et al. Therapeutic vaccination against fibronectin ED-A attenuates progression of metastatic breast cancer. Oncotarget 2014;5:12418–12427–10.
[196] Homandberg GA, Kramer-Bjerke J, Grant D, Christianson G, Eisenstein R. Heparin-binding fragments of fibronectin are potent inhibitors of endothelial cell growth: structure-function correlations. Biochim Biophys Acta 1986;874:327–32.
[197] Morla A, Zhang Z, Ruoslahti E. Superfibronectin is a functionally distinct form of fibronectin. Nature 1994;367:193–6.
[198] Yi M, Ruoslahti E. A fibronectin fragment inhibits tumor growth, angiogenesis, and metastasis. PNAS 2001;98:620–4.
[199] Klein RM, Zheng M, Ambesi A, Van De Water L, McKeown-Longo PJ. Stimulation of extracellular matrix remodeling by the first type III repeat in fibronectin. Journal of Cell Biology 2003;116:4663–74.
[200] Zheng M, Jones DM, Horzempa C, Prasad A, McKeown-Longo PJ. The First Type III Domain of Fibronectin is Associated with the Expression of Cytokines within the Lung Tumor Microenvironment. Journal of Cancer 2011;2:478–83.
[201] Tang N-H, Chen Y-L, Wang X-Q, Li X-J, Wu Y, Zou Q-L, et al. N-terminal and C-terminal heparin-binding domain polypeptides derived from fibronectin reduce adhesion and invasion of liver cancer cells. BMC Cancer 2010;10:552.
[202] Butcher DT, Alliston T, Weaver VM. A tense situation: forcing tumour progression. Nature Reviews Cancer 2009;9:108–22.
[203] Kumar S, Weaver VM. Mechanics, malignancy, and metastasis: The force journey of a tumor cell. Cancer Metastasis Rev 2009;28:113–27.
[204] Paszek MJ, Zahir N, Johnson KR, Lakins JN, Rozenberg GI, Gefen A, et al. Tensional homeostasis and the malignant phenotype. Cancer Cell 2005;8:241–54.
[205] Fischbach C, Kong HJ, Hsiong SX, Evangelista MB, Yuen W, Mooney DJ. Cancer cell angiogenic capability is regulated by 3D culture and integrin engagement. PNAS 2009;106:399–404.
[206] Mammoto A, Connor KM, Mammoto T, Yung CW, Huh D, Aderman CM, et al. A mechanosensitive transcriptional mechanism that controls angiogenesis. Nature 2009;457:1103–8.
[207] Midwood KS, Williams LV, Schwarzbauer JE. Tissue repair and the dynamics of the extracellular matrix. The International Journal of Biochemistry & Cell Biology 2004;36:1031–7.

[208] Anderson JM. Biological responses to materials. Annual Review of Materials Research 2001.
[209] Curran CS, Keely PJ. Matrix Biology. Matrix Biol 2013;32:95–105.
[210] Castelló-Cros R, Cukierman E. Stromagenesis during tumorigenesis: characterization of tumor-associated fibroblasts and stroma-derived 3D matrices. Methods Mol Biol 2009;522:275–305.
[211] Israelachvili JN. Thin film studies using multiple-beam interferometry. Journal of Colloid and Interface Science 1973;44:259–72.
[212] Israelachvili JN, McGuiggan PM. Adhesion and short-range forces between surfaces. Part I: New apparatus for surface force measurements. J Mater Res 1990;5:2223–31.
[213] Little WC, Schwartlander R, Smith ML, Gourdon D, Vogel V. Stretched Extracellular Matrix Proteins Turn Fouling and Are Functionally Rescued by the Chaperones Albumin and Casein. Nano Lett 2009;9:4158–67.
[214] Antia M, Islas LD, Boness DA, Baneyx G, Vogel V. Single molecule fluorescence studies of surface-adsorbed fibronectin. Biomaterials 2006;27:679–90.
[215] Sinkus R, Tanter M, Catheline S, Lorenzen J, Kuhl C, Sondermann E, et al. Imaging anisotropic and viscous properties of breast tissue by magnetic resonance-elastography. Magn Reson Med 2005;53:372–87.
[216] Zhang M, Nigwekar P, Castaneda B, Hoyt K, Joseph JV, di Sant'Agnese A, et al. Quantitative Characterization of Viscoelastic Properties of Human Prostate Correlated with Histology. Ultrasound in Medicine & Biology 2008;34:1033–42.
[217] Petrie TA, Capadona JR, Reyes CD, García AJ. Integrin specificity and enhanced cellular activities associated with surfaces presenting a recombinant fibronectin fragment compared to RGD supports. Biomaterials 2006;27:5459–70.
[218] Seong J, Tajik A, Sun J, Guan J-L, Humphries MJ, Craig SE, et al. Distinct biophysical mechanisms of focal adhesion kinase mechanoactivation by different extracellular matrix proteins. PNAS 2013;110:19372–7.
[219] Hynes RO. A reevaluation of integrins as regulators of angiogenesis. Nature Medicine 2002;8:918–21.
[220] Zamir E, Geiger B. Molecular complexity and dynamics of cell-matrix adhesions. Journal of Cell Biology 2001;114:3583–90.
[221] Jiang G, Giannone G, Critchley DR, Fukumoto E, Sheetz MP. Two-piconewton slip bond between fibronectin and the cytoskeleton depends on talin. Nature 2003;424:334–7.
[222] Wegener KL, Partridge AW, Han J, Pickford AR, Liddington RC, Ginsberg MH, et al. Structural Basis of Integrin Activation by Talin. Cell 2007;128:171–82.
[223] Critchley DR. Biochemical and structural properties of the integrin-associated cytoskeletal protein talin. Annual Review of Biophysics 2009.
[224] Roca-Cusachs P, del Rio A, Puklin-Faucher E, Gauthier NC, Biais N, Sheetz MP. Integrin-dependent force transmission to the extracellular matrix by α-actinin triggers adhesion maturation. PNAS 2013, pp. 1–18.
[225] Au von A, Vasel M, Kraft S, Sens C, Hackl N, Marx A, et al. Circulating fibronectin controls tumor growth. Neoplasia 2013;15:925–38.
[226] Samani A, Zubovits J, Plewes D. Elastic moduli of normal and pathological human breast tissues: an inversion-technique-based investigation of 169 samples. Phys Med Biol 2007;52:1565–76.

[227] Moeendarbary E, Valon L, Fritzsche M, Harris AR, Moulding DA, Thrasher AJ, et al. The cytoplasm of living cells behaves as a poroelastic material. Nature Materials 2013;12:253–61.
[228] Rosenbluth MJ, Crow A, Shaevitz JW, Fletcher DA. Slow stress propagation in adherent cells. Biophysical Journal 2008;95:6052–9.
[229] Schnepel J, Tschesche H. The Proteolytic Activity of the Recombinant Cryptic Human Fibronectin Type IV Collagenase from E. coli Expression. Journal of Protein Chemistry 2000;19:685–92.
[230] Cavalcanti-Adam EA, Volberg T, Micoulet A, Kessler H, Geiger B, Spatz JP. Cell spreading and focal adhesion dynamics are regulated by spacing of integrin ligands. Biophysj 2007;92:2964–74.
[231] Arnold M, Schwieder M, Blümmel J, Cavalcanti-Adam EA, López-Garcia M, Kessler H, et al. Cell interactions with hierarchically structured nano-patterned adhesive surfaces. Soft Matter 2009;5:72–7.
[232] Geiger B, Spatz JP, Bershadsky AD. Environmental sensing through focal adhesions. Nat Rev Mol Cell Biol 2009;10:21–33.
[233] Multiscale relationships between fibronectin structure and functional properties 2013.
[234] Takagi J, Strokovich K, Springer TA, Walz T. Structure of integrin alpha5beta1 in complex with fibronectin. Embo J 2003;22:4607–15.
[235] Liu Y, Pan Y, Xu Y. Binding investigation of integrin alphavbeta3 with its inhibitors by SPR technology and molecular docking simulation. J Biomol Screen 2010;15:131–7.
[236] Fraley SI, Feng Y, Krishnamurthy R, Kim D-H, Celedon A, Longmore GD, et al. A distinctive role for focal adhesion proteins in three-dimensional cell motility. Nature Cell Biology 2010;12:598–604.
[237] Janmey PA, Weitz DA. Dealing with mechanics: mechanisms of force transduction in cells. Trends in Biochemical Sciences 2004;29:364–70.
[238] Cao Y, Langer R. Optimizing the Delivery of Cancer Drugs That Block Angiogenesis. Science Translational Medicine 2010;2:15ps3–15ps3.
[239] Lopez JI, Kang I, You W-K, McDonald DM, Weaver VM. In situ force mapping of mammary gland transformation. Integr Biol 2011;3:910.
[240] Harjanto D, Maffei JS, Zaman MH. Quantitative Analysis of the Effect of Cancer Invasiveness and Collagen Concentration on 3D Matrix Remodeling. PLoS ONE 2011;6:e24891.
[241] Nguyen-Ngoc K-V, Cheung KJ, Brenot A, Shamir ER, Gray RS, Hines WC, et al. ECM microenvironment regulates collective migration and local dissemination in normal and malignant mammary epithelium. PNAS 2012;109:E2595–604.
[242] Oskarsson T. Extracellular matrix components in breast cancer progression and metastasis. The Breast 2013;22:S66–S72.
[243] Naba A, Clauser KR, Lamar JM, Carr SA, Hynes RO, Fuchs E. Extracellular matrix signatures of human mammary carcinoma identify novel metastasis promoters. eLife 2014;3.
[244] Eccles SA, Box GM, Court WJ, Bone EA, Thomas W, Brown PD. Control of lymphatic and hematogenous metastasis of a rat mammary carcinoma by the matrix metalloproteinase inhibitor batimastat (BB-94). Cancer Research 1996;56:2815–22.
[245] Macaulay VM, O'Byrne KJ, Saunders MP, Braybrooke JP, Long L, Gleeson F, et al.

Phase I study of intrapleural batimastat (BB-94), a matrix metalloproteinase inhibitor, in the treatment of malignant pleural effusions. Clin Cancer Res 1999;5:513–20.
[246] Eyckmans J, Boudou T, Yu X, Chen CS. Perspective. Developmental Cell 2011;21:35–47.
[247] Mouw JK, Ou G, Weaver VM. Extracellular matrix assembly: a multiscale deconstruction. Nat Rev Mol Cell Biol 2000;15:771–85.
[248] Dallas SL, Sivakumar P, Jones CJP, Chen Q, Peters DM, Mosher DF, et al. Fibronectin regulates latent transforming growth factor-beta (TGF beta) by controlling matrix assembly of latent TGF beta-binding protein-1. J Biol Chem 2005;280:18871–80.
[249] Shen ZL, Kahn H, Ballarini R, Eppell SJ. Viscoelastic Properties of Isolated Collagen Fibrils. Biophysical Journal 2011;100:3008–15.
[250] Janmey PA, Miller RT. Mechanisms of mechanical signaling in development and disease. Journal of Cell Biology 2011;124:9–18.
[251] Ma X, Schickel ME, Stevenson MD, Sarang-Sieminski AL, Gooch KJ, Ghadiali SN, et al. Fibers in the Extracellular Matrix Enable Long-Range Stress Transmission between Cells. Biophysical Journal 2013;104:1410–8.
[252] Dallas SL, Chen Q, Sivakumar P. Dynamics of assembly and reorganization of extracellular matrix proteins. Curr Top Dev Biol 2006;75:1–24.
[253] Mao Y, Schwarzbauer JE. Fibronectin fibrillogenesis, a cell-mediated matrix assembly process. Matrix Biology 2005;24:389–99.
[254] Barocas VH, Tranquillo RT. Biphasic Theory and In Vitro Assays of Cell-Fibril Mechanical Interactions in Tissue-Equivalent Gels. Cell Mechanics and Cellular Engineering, New York, NY: Springer-Verlag; 1994, pp. 185–209.
[255] Swartz MA, Fleury ME. Interstitial Flow and Its Effects in Soft Tissues. Annu Rev Biomed Eng 2007;9:229–56.
[256] Mak AF. The apparent viscoelastic behavior of articular cartilage--the contributions from the intrinsic matrix viscoelasticity and interstitial fluid flows. J Biomech Eng 1986;108:123–30.
[257] Bloom RJ, George JP, Celedon A, Sun SX, Wirtz D. Mapping Local Matrix Remodeling Induced by a Migrating Tumor Cell Using Three-Dimensional Multiple-Particle Tracking. Biophysical Journal 2008;95:4077–88.
[258] Pedersen JA, Swartz MA. Mechanobiology in the third dimension. Ann Biomed Eng 2005;33:1469–90.
[259] Netti PA, Berk DA, Swartz MA, Grodzinsky AJ, Jain RK. Role of extracellular matrix assembly in interstitial transport in solid tumors. Cancer Research 2000;60:2497–503.
[260] Guidry C, Grinnell F. Contraction of hydrated collagen gels by fibroblasts: Evidence for two mechanisms by which collagen fibrils are stabilized. Collagen and Related Research 1987;6:515–29.
[261] Raeber GP, Lutolf MP, Hubbell JA. Molecularly Engineered PEG Hydrogels: A Novel Model System for Proteolytically Mediated Cell Migration. Biophysical Journal 2005;89:1374–88.
[262] Egeblad M, Werb Z. New functions for the matrix metalloproteinases in cancer progression. Nature Reviews Cancer 2002;2:161–74.
[263] Zhang X, Chen CT, Bhargava M, Torzilli PA. A Comparative Study of Fibronectin Cleavage by MMP-1, -3, -13, and -14. Cartilage 2012;3:267–77.
[264] Manka SW, Carafoli F, Visse R, Bihan D, Raynal N, Farndale RW, et al. Structural

insights into triple-helical collagen cleavage by matrix metalloproteinase 1. PNAS 2012;109:12461–6.
[265] Bergers G, Brekken R, McMahon G, Vu TH, Itoh T, Tamaki K, et al. Matrix metalloproteinase-9 triggers the angiogenic switch during carcinogenesis. Nature Cell Biology 2000;2:737–44.
[266] Park JE, Keller GA, Ferrara N. The vascular endothelial growth factor (VEGF) isoforms: differential deposition into the subepithelial extracellular matrix and bioactivity of extracellular matrix-bound VEGF. Molecular Biology of the Cell 1993;4:1317–26.
[267] Senger DR, Claffey KP, Benes JE, Perruzzi CA, Sergiou AP, Detmar M. Angiogenesis promoted by vascular endothelial growth factor: regulation through alpha1beta1 and alpha2beta1 integrins. PNAS 1997;94:13612–7.
[268] Hollborn M, Stathopoulos C, Steffen A, Wiedemann P, Kohen L, Bringmann A. Positive Feedback Regulation between MMP-9 and VEGF in Human RPE Cells. Invest Ophthalmol Vis Sci 2007;48:4360.